

Archive

USERS' GUIDE FOR
NUMERICAL MODELING OF BUOYANT PLUMES IN A
TURBULENT, STRATIFIED ATMOSPHERE

by

Ralph G. Bennett

and

Michael W. Golay

Energy Laboratory Report MIT-EL 79-004
February, 1979

1

2

3

4

5

6

USERS' GUIDE FOR
NUMERICAL MODELING OF BUOYANT PLUMES IN A
TURBULENT, STRATIFIED ATMOSPHERE

by

Ralph G. Bennett

and

Michael W. Golay

February, 1979

MIT-EL 79-004

Energy Laboratory

and

Department of Nuclear Engineering
Massachusetts Institute of Technology
Cambridge, Massachusetts 02139

Sponsored by

The Consolidated Edison Company of New York, Inc.

Northeast Utilities Service Corporation



NOTICE

The VARR-II User's Guide mentioned in this report is currently available in three volumes from:

U.S. Department of Energy
Technical Information Center
P.O. Box 62
Oak Ridge, Tennessee 37830

The report numbers and current (1979) prices are:

CRBRP-ARD-0106	Vol. I	\$6.75
CRBRP-ARD-0106	Vol. II	\$4.50
CRBRP-ARD-0106	Vol. III	\$6.00

As Limited Distribution Applied Technology Reports, these volumes are available to U.S. Citizens, and "any further distribution by any holder of the documents or of the data therein to third parties representing foreign interests, foreign governments, foreign companies, and foreign subsidiaries or foreign divisions of U.S. companies should be coordinated with the Director, Division of Reactor Development and Demonstration, U.S. Energy Research and Development Administration."

USERS' GUIDE FOR
NUMERICAL MODELING OF BUOYANT PLUMES IN A
TURBULENT, STRATIFIED ATMOSPHERE

by

Ralph G. Bennett

and

Michael W. Golay

ABSTRACT

A widely applicable computational model of buoyant, bent-over plumes in realistic atmospheres is constructed. To do this, the two-dimensional, time-dependent fluid mechanics equations are numerically integrated, while a number of important physical approximations serve to keep the approach at a tractable level. A three-dimensional picture of a steady state plume is constructed from a sequence of time-dependent, two-dimensional plume cross sections--each cross section of the sequence is spaced progressively further downwind as it is advected for a progressively longer time by the prevailing wind. The dynamics of the plume simulations are quite general. The buoyancy sources in the plume include the sensible heat in the plume, the latent heat absorbed or released in plume moisture processes, and the heating of the plume by a radioactive pollutant in the plume. The atmospheric state in the simulations is also quite general. Atmospheric variables are allowed to be functions of height, and the ambient atmospheric turbulence (also a function of height) is included in the simulations.



TABLE OF CONTENTS

	page
ACKNOWLEDGEMENTS	6
PREFACE	7
1. Problem Description and Solution	8
1.1 Introduction	8
1.2 Background and Problem Description	9
1.2.1 Historical Background	9
1.2.2 Characteristics of Bent-Over Buoyant Plumes	10
1.2.3 Overview of Plume Models	11
1.2.4 Scope of Work	14
2. Literature Review	16
2.1 Numerical Plume Models	16
2.1.1 Three-Dimensional Models	17
2.1.2 Two-Dimensional Models	19
2.1.3 Experimental Studies	20
2.2 Numerical Planetary Boundary Layer Modeling	21
3. Hydrodynamic Model Development	23
3.1 Introduction	23
3.2 Model Equation Sets	23
3.2.1 Dry Equations	23
3.2.1.1 Reference State Decomposition	24
3.2.1.2 Reynolds Decomposition and Closure	30
3.2.1.3 Pollutant Transport Equation	37
3.2.1.4 Radioactive Decay Heating	38
3.2.2 Moist Equations	39
3.2.2.1 Reference State Decomposition	40
3.2.2.2 Reynolds Decomposition and Closure	46

	page
3.2.2.3 Equilibrium Cloud Microphysics Model	49
3.2.2.4 Latent Heat Source Term	50
3.3 Model Solution Methodology	53
3.3.1 The VARR-II Fluid Mechanics Algorithm	53
3.3.2 Orientation of the Computer Mesh	54
3.3.3 Downwind Advection of the Mesh	58
3.3.4 Property Data	60
3.3.5 Input Profiles and Boundary Conditions	64
3.3.5.1 Input Profiles	64
3.3.5.2 Boundary Conditions	64
3.3.5.3 Mesh Initialization	67
3.3.6 Mesh Coarsening Capability	69
3.3.7 Statistics Package	72
4. Description of Atmospheric Turbulence	74
4.1 Introduction	74
4.2 Atmospheric Profiles of Wind, Temperature, and Humidity	74
4.3 Turbulence in the Planetary Boundary Layer	77
4.3.1 Introduction	77
4.3.2 Layers in the PBL and Important Processes	78
4.3.3 Prescription of Eddy Viscosity	81
4.3.4 Prescription of Turbulence Kinetic Energy	86
5. Card Input and Sample Problems	90
5.1 Overall Program Support	90
5.2 Card Input Decks	92

	<u>page</u>
5.2.1 The Dry, Buoyant Line-Thermal	92
5.2.2 LAPPES ⁵ Plume of 20 October 1967	92
5.2.3 Moist, Buoyant Line-Thermal	98
5.3 Sample Problem Results	101
5.3.1 The Dry, Buoyant Line-Thermal	101
5.3.2 LAPPES ⁵ Plume of 20 October 1967	101
6. Recommendations for Model Extensions	109
6.1 Calculational Scheme to Include Wind Shear Effects	109
6.2 Calculational Scheme for Time-Dependent Release or Weather	112
6.3 Cloud Microphysics Model	113
 NOMENCLATURE	 116
 LIST OF FIGURES AND TABLES	 121
 REFERENCES	 123
 APPENDIX A. Definitions of Important Variables Added to VARR-II for Simulating Plume Behavior	 128
APPENDIX B. Card Formats for Input Variables	130
APPENDIX C. Statement Number Cross-References	136
APPENDIX D. Computer Code Listing	152

ACKNOWLEDGEMENTS

This research was conducted under the sponsorship of Consolidated Edison and Northeast Utilities Service Corp. The authors gratefully acknowledge their support.

PREFACE

The VARR-II⁴⁰ computer code has been modified for the modeling of buoyant plumes in turbulent, stratified atmospheres. A description of the model and the results and conclusions that have been obtained to date were released in a previous report (MIT-EL 79-002). The purpose of the present report is to serve as a users' guide for the model. The first four chapters of MIT-EL 79-002 have been included in this report to introduce and describe the model; the detailed card input lists and sample problems are found in Chapter 5, and the Appendices. Chapter 6 introduces the model extensions that were considered in the original work.

1. PROBLEM DESCRIPTION AND SOLUTION

1.1 Introduction

With the rapidly increasing burden of air pollution over recent decades, the engineer's ability to analyze the behavior of an ever-widening assortment of effluents has not kept up with the importance of the consequences of the releases. The reason for this is that the "predictive" models of plume behavior that are currently available universally suffer from a lack of extendability. That is, they need to observe the behavior of an ensemble of the releases that they wish to model before they can form an accurate picture of the release. The models are useful only to the extent that an appropriate ensemble of plumes can be created for study, either as full-scale atmospheric releases, or as scaled-down laboratory experiments. Inasmuch as the important turbulent and thermal characteristics of the atmosphere cannot be simulated in the laboratory, and since an ensemble of plumes with catastrophic consequences (e.g., radioactive plumes from nuclear reactor accidents) may be impractical to produce, plume modeling has needed to take a more universal approach.

The purpose of this work is to construct a widely applicable model of plume behavior in realistic atmospheres. To do this, a "first principles" approach is adopted. A

numerical integration of the fluid mechanics equation is undertaken, while a number of important physical approximations to the problem serve to keep the approach at a tractable level. The advantage of the model presented here is the ability to tackle problems outside of the scope of existing models without greatly increasing the resources spent on the analysis.

1.2 Background and Problem Description

1.2.1 Historical Background

Man has produced and observed bent-over buoyant plumes since the discovery of fire. However, the bent-over plume did not have any great impact on society until the advent of large industrial sources near population centers during the industrial revolution. The number of large industrial sources has increased steadily with the industrialization of many countries. In the recent past, the variety of releases from large industrial sources has increased greatly, and now includes the potentially more harmful effluents from chemical refining and combustion processes, nuclear power plants, and large cooling towers. Also, the steady growth of population centers almost always dictates that these new sources will be located in at least moderately populated areas.

Historically, the ability to analyze the effects of large releases and hence to develop technologies for their

mitigation has not kept pace with the consequences of the releases. To date, the advances have been quite modest: early observations during the industrial revolution suggested the use of tall stacks for lessening the effects of large releases. The strong influence of the synoptic-scale weather on releases (first investigated in order to increase the effectiveness of chemical warfare agents) has largely motivated the Pasquill-type correlations of plume behavior. The hope of simply reducing the consequences by reducing the amount of effluents has stimulated an abundance of filtering, scrubbing, and effluent control technologies. However, increasingly important releases are certain to occur. A brief review here of the existing approaches to plume modeling can indicate the most promising avenue for study.

1.2.2 Characteristics of Bent-Over Buoyant Plumes

The character of the bent-over buoyant plume is central to all of the available plume models. When an effluent stream with a given upward momentum and initial buoyancy is released from a stack into a windy atmosphere, the plume is deflected downwind. This occurs partly because of pressure forces that develop around the plume, and partly because the plume entrains the ambient air, which mixes a lot of downwind momentum into the plume. The deflection quickly causes the plume to bend over (usually within about one stack height) and then to be

carried downstream. The buoyancy of the plume is converted into kinetic energy, and the plume rises under this action for a considerable distance downwind. About 20 years ago it was noted¹ that the motion of the plume in cross section during this rise was essentially that of a two-dimensional turbulent vortex pair. Initially the vortex pair rises and grows without being too dependent upon atmospheric turbulence (although atmospheric stratification is always important). After the kinetic energy of the cross-sectional motions has essentially died out, the plume continues to disperse solely by atmospheric motions. It will be found in the review of plume models that only the detailed numerical plume models provide a method that can easily bridge between the regimes where plume turbulence dominates and where atmospheric turbulence dominates.

1.2.3 Overview of Plume Models

With regard to the detailed three-dimensional nature of plume motions, existing models of plume behavior are found to possess a wide variety of sophistication. The Pasquill-type models, the entrainment models, and the numerical models are considered here.

The Pasquill-type models develop a highly idealized picture of the fluid motions in and around the plume. Pollutants in the plume cross section are assumed to fit Gaussian

distributions of height and width. In essence, the model parameters (standard deviations of the Gaussian distributions) are simply an ad-hoc replica of the experimental results; as such, the models are unable to predict in cases for which experiments have not been performed. The wealth of non-passive effluents and the rich variations in the meteorological state of the atmosphere serve to guarantee that cases outside of the Pasquill-type models will always exist.

The entrainment models develop a much less idealized, and much more physical picture of the fluid motions in the plume. In general, the models make use of the very elegant non-dimensional formulations and similarity relationships that are central to the theory of homogeneous isotropic turbulence. Typically the models are successful at analyzing the initial plume behavior, where the self-generated plume turbulence dominates over the atmospheric turbulence. The entrainment models are generally able to analyze plumes only in fairly simple atmospheres when analytical solutions are sought. But this is not the primary limitation of entrainment models, since in some cases their solutions are found on computers. The limitations of the entrainment models are the condition that the plume self-generated turbulence is dominant over the atmospheric turbulence, (which eventually breaks down for all plumes, commonly at

downwind distances for which the solution is still needed) and the basic entrainment velocity assumption, which cannot be obtained from fundamental constants and scales in a straightforward way.

Numerical plume models are capable of developing the most detailed picture of the fluid motions in the plume. In general, the models seek to integrate a closed set of Reynolds-averaged fluid mechanics equations, either in two or three dimensions. Turbulence leads to a fundamental closure problem in writing this set of equations, so that each model will have a collection of closure assumptions that together form a turbulence model, aside from other assumptions that are made concerning the plume behavior. Numerical plume models are becoming capable of analyzing the most detailed cases, yet they are often limited by the large computing costs. Aside from the computer costs, the tasks of initializing and validating the problem with fully two- or three-dimensional data can also quickly become intractable. Until computer costs are reduced greatly, the most useful numerical plume models will likely have to be two-dimensional. The greatest benefit that comes from such models is the wider range of application of the models, and the ease of extending them to new cases.

1.2.4 Scope of the Work

This work constructs a three-dimensional solution of a steady state plume from a sequence of time-dependent two-dimensional plume cross sections; each plume cross section of the sequence being spaced progressively further downwind as it is advected for a progressively longer time by the prevailing wind. The two-dimensional cross sections are simulated with a time-dependent turbulent fluid mechanics code which integrates the time-averaged equations of continuity, momentum, energy, moisture, and pollutant. The behavior of an individual plume is modeled in this way until the height or radius of the plume reaches several hundred meters, which roughly corresponds to the plume cross section being tens of kilometers downwind of the source.

The dynamics of the plume simulations are quite general. The buoyancy sources in the plume encompass the sensible heat in the plume, the latent heat absorbed or released in plume moisture processes, and the radioactive decay heating of the plume by a radioactive pollutant species in the plume. Buoyancy from chemical reactions could be easily included. The atmospheric state in the simulations accepts atmospheric wind, temperature, water vapor, liquid water, background pollutant, turbulent eddy viscosity, and turbulent kinetic energy as functions of height. The turbulence is treated

with the sophisticated second-order closure model of Stuhmiller², which allows the turbulent recirculation and entrainment of the plume cross section to be treated in a very natural way.

The model is validated against the Pasquill model³ and the entrainment model of Richards⁴ for idealized cases in which these models apply, and for several cases from the LAPPES⁵ field data for actual large power plant stacks. Simulations are obtained for cases outside of the Pasquill and entrainment models, and while no specific field data for these cases exists, the behavior of the simulation agrees with the physical changes imposed on the problems.

2. LITERATURE REVIEW

The literature review in this work undertakes a broad survey of plume modeling. In the first section, existing numerical plume models are discussed, along with the experimental data base that is available for the validation of these detailed plume models. The first section also includes the research that has been done on computational and experimental modeling of two-dimensional line vortex pairs. It is important to include them since the results of such work are very easily interpreted in the context of air pollution problems. In the second section, existing numerical models of the planetary boundary layer are discussed. Again, these models are very easily extended to air pollution problems (with the inclusion of a pollutant transport equation and pollutant source), so it is important to include them in the review.

2.1 Numerical Plume Models

A large number of plume models have been developed that are available as computer programs. Several recent reviews⁶⁻⁸ have reported dozens of such models, and it is important to make a distinction regarding them. A majority of the models employ the Gaussian plume assumption; as such, the computer

is simply being used to look up and present the standard handbook calculations, with minor modifications in some cases. These are not "numerical plume models" in the sense that the primitive equations are not being integrated to show the plume development, although computers are being used. Such models are not considered further here. The remaining models in the reviews are truly numerical plume models, and they will be considered next, along with several models that were reported elsewhere.

2.1.1 Three-Dimensional Models

The most sophisticated numerical plume models to date have not yet attempted a second-order turbulence closure to the fully three-dimensional flow field for non-passive pollutants. Some of these features are found in each of the models discussed here, but not all of them. The notes of Rao⁹ and Nappo¹⁰ discuss the desirable features of three-dimensional numerical plume models, and provide a good introduction to future work that may be undertaken.

Donaldson's modeling¹¹ has concentrated on a second-order turbulence closure for a three-dimensional planetary boundary layer simulation with a passive pollutant. Because the pollutant is passive, and hence does not affect the flow field or its turbulence, the turbulence closure only addresses PBL

turbulence, and is independent of the behavior of buoyant plumes. This is in contrast to the method in this work, where the second-order closure is "tuned" to the development of turbulent buoyant plumes, and is largely independent of PBL turbulence development. Lewellen's modeling¹² begins with a second-order closure to the passive pollutant transport equation, and then adopts the PBL flow field and turbulence from Donaldson's model.¹¹ Only integrations of the pollutant transport equation are needed in Lewellen's model because of the adoption of a complete PBL solution. Patankar's model¹³ of a deflected turbulent jet in three-dimensions also uses a second-order closure model, but does not allow for buoyancy and stratification, although it does allow for non-isotropic turbulent transports in the vertical and horizontal directions. A fundamentally different approach to three-dimensional modeling is found in the Atmospheric Release Advisory Capability (ARAC) system.¹⁵⁻²² A mass-consistent three-dimensional wind field is interpolated from a small set of local tower wind measurements and used to predict the advection of a passive pollutant. Turbulent diffusion is modeled with a zero equation model, although many other important features such as rainout, wet and dry deposition, and surface terrain have been added.

2.1.2 Two-Dimensional Models

Two two-dimensional numerical plume models have been found in the literature. Henninger's model²³ solves continuity, momentum, energy, and moisture with a less-sophisticated zero-equation turbulence closure, and with a more sophisticated treatment of moisture. For plumes in a wind, the model chooses the mesh alignment shown in Fig. 3.3.2.1b of Sec. 3.3.2, which is felt to be a less satisfactory choice than that of the present work. Taft's model²⁴ is much closer to the model in this work, since it adopts the same mesh alignment (see Fig. 3.3.2.1c in Sec. 3.3.2). The principal differences are that Taft's model employs a one-equation turbulence model, uses a more complex moisture model, and does not make any attempt to describe ambient atmospheric turbulence.

A number of two-dimensional numerical buoyant thermal models have evolved in the literature of meteorology, usually in support of efforts to parameterize the growth of rain clouds. The models have not been applied to air pollution directly, but could be easily converted. Lilly's model²⁵ seeks a self-preserving solution for the (dry) buoyant line thermal, and as such, would only be applicable for the early plume behavior when plume self-turbulence is dominating. Johnson's model²⁶ is used to study fog clearing on runways

with helicopter downwash; while the moisture equations are more complex than that in this work, the eddy viscosity is assumed to be constant. Ogura's model²⁷ of rain cloud development also assumes a constant eddy viscosity, while Arnason's model²⁸ ignores eddy transports altogether. Liu's model²⁹ employs a stratification of atmospheric turbulence into two constant eddy viscosity layers. While the treatment of turbulence in these models is very simple, it should be emphasized that these models are focussed on precipitation modeling, and they are likely to be helpful in the improvement of the moisture model in this work. A recent review of precipitation modeling is found in Cotton.³⁰

2.1.3 Experimental Studies

The field study that the model in this work is validated against is the Large Power Plant Effluent Study (LAPPES).⁵ Complete field data for stack plumes from three mine-mouth coal-fired plants are found in the four volumes of the study: wind, temperature, and humidity profiles, plant operating characteristics, and plume SO₂ concentration cross sections are of the most interest in this work. The Chalk Point Cooling Tower Project (CPCTP)³¹ is also of interest to this work since it provides cooling tower plume cross sections, but plant operating data³² was not available during this work.

The experimental laboratory studies that this work is validated against are the papers of Tsang³³ and Richards.⁴ The experiments study the behavior of two-dimensional line thermals released in a water tank. The ambient receiving fluid in the tank is both laminar and unstratified, and the thermals are fully turbulent.

2.2 Numerical Planetary Boundary Layer Modeling

A three-dimensional numerical model of the planetary boundary layer has been reported by Deardorff³⁴⁻³⁶ that could easily be adapted to local air pollution studies, although the expense is likely to be prohibitive. The model solves the complete set of primitive equations (with an eighteen-equation model of turbulence) in a box that ranges 5 km on a side and 2 km deep. The numerical experiments to date have compared very favorably with several well-documented planetary boundary layer field studies.

To apply the model to a single source of pollutant, a single mesh cell could be initialized with sources of momentum, heat, moisture, pollutant, and turbulence. To accommodate this, a pollutant transport equation would have to be added, and an additional three-equation model of turbulent pollutant fluxes would need to be developed. Time-dependent or steady-state releases could be modeled in great detail in this way.

However, the model currently requires 15 seconds of CPU on a CDC-7600 to simulate 1 second of flow in the atmosphere. Also, the specification of boundary conditions on a three-dimensional mesh with accurate time-dependent micrometeorological data would require a very elaborate reporting network. Nonetheless, the model represents a more sophisticated and potentially more accurate approach than the model in this work.

3. HYDRODYNAMIC MODEL DEVELOPMENT

3.1 Introduction

In order to model buoyant plumes in the atmosphere, the equation set contained in the VARR-II computer code is reinterpreted and expanded. A reinterpretation of the hydrodynamic variables is necessary in order to satisfactorily account for the compressible nature of an atmosphere that is at rest. The equations are expanded in Sec. 3.2.1 to include the transport of a pollutant and radioactive decay heating by the pollutant, and in Sec. 3.2.2, where the transport of water vapor, cloud liquid water, and the energy released or absorbed during the phase changes of water substance are considered. Since so many fundamental changes are made here in reinterpreting the VARR-II equation set, this discussion of the model development undertakes a derivation of the equations; for completeness it reiterates the important assumptions contained in the VARR-II code which were developed outside of this work.

3.2 Hydrodynamic Model Equation Sets

3.2.1 Equations for Dry Atmospheres

The equations for a dry atmosphere are derived in this

section. When the potential temperature is simply reinterpreted as the virtual potential temperature, these equations are applicable to moist plumes in moist atmospheres if none of the moisture undergoes a change of phase, and if the turbulent diffusion coefficients of heat and moisture are equal. A further discussion of virtual potential temperature is found in Sec. 3.2.2.1.

3.2.1.1 Reference State Decomposition

As a starting point for the model development, consider the three-dimensional compressible fluid mechanics equations, where the six primitive variables \tilde{p} , $\tilde{\rho}$, \tilde{T} , and \tilde{u}_i are physically measurable values of the fluctuating pressure, density, temperature, and velocity, respectively:

Continuity Eq:

$$\frac{\partial \tilde{\rho}}{\partial t} + \frac{\partial}{\partial x_j} (\tilde{\rho} \tilde{u}_j) = 0 \quad (3.1)$$

Momentum Eq:

$$\frac{\partial}{\partial t} (\tilde{\rho} \tilde{u}_i) + \frac{\partial}{\partial x_j} (\tilde{\rho} \tilde{u}_i \tilde{u}_j) = - \frac{\partial \tilde{p}}{\partial x_i} - \tilde{\rho} g_i + \mu \frac{\partial^2 \tilde{u}_i}{\partial x_j^2} \quad (3.2)$$

Energy Eq:

$$\frac{\partial}{\partial t} (\tilde{\rho} \tilde{T}) + \frac{\partial}{\partial x_j} (\tilde{\rho} \tilde{u}_j \tilde{T}) = \frac{\tilde{u}_j}{c_p} \frac{\partial \tilde{p}}{\partial x_j} + \frac{\partial}{\partial x_j} k \frac{\partial \tilde{T}}{\partial x_j} + \frac{1}{c_p} \frac{\partial \tilde{p}}{\partial t} \quad (3.3)$$

Equation of State:

$$\tilde{p} = \tilde{\rho} R_d \tilde{T} \quad (3.4)$$

These equations have property values μ , c_p , and k , which may depend upon temperature in general. The energy equation has neglected the kinetic energy in the fluid motions, and the equation of state is that for an ideal dry gas.

The variations of temperature, pressure, and density in a static atmosphere are usually "subtracted out" of these equations in meteorological analyses by a reference state decomposition. That is, equations of motion for perturbations about an adiabatic atmosphere are sought by decomposing the primitive variables as

$$\left\{ \begin{array}{l} \text{the value} \\ \text{of a primi-} \\ \text{tive variable} \end{array} \right\} = \left\{ \begin{array}{l} \text{its value in} \\ \text{an adiabatic} \\ \text{atmosphere} \\ \text{(function of} \\ \text{height only)} \end{array} \right\} + \left\{ \begin{array}{l} \text{a departure} \\ \text{from the} \\ \text{state at} \\ \text{rest} \end{array} \right\} \quad (3.5)$$

or, in terms of the notation in this work

$$\tilde{p} \rightarrow p_o + p \quad (3.6)$$

$$\tilde{\rho} \rightarrow \rho_o + \rho \quad (3.7)$$

$$\tilde{T} \rightarrow T_o + T \quad (3.8)$$

$$\tilde{u}_i \rightarrow 0 + u_i \quad (3.9)$$

The state of the dry, adiabatic atmosphere is found by

making the substitutions Eq. 3.6-Eq. 3.9 into Eq. 3.1-Eq. 3.4, and setting the time derivatives and the perturbations p , ρ , T , and u_i to zero. The continuity and energy equations become trivial under this substitution. The momentum equation becomes the hydrostatic equation:

$$\frac{dp_o}{dz} = -\rho_o g \quad (3.10)$$

The equation of state is simply

$$p_o = \rho_o R_d T_o \quad (3.11)$$

The First Law of Thermodynamics for an adiabatic process is

$$dQ = 0 = c_p dT_o - dp_o/\rho_o \quad (3.12)$$

Dividing by a displacement dz gives

$$\frac{dp_o}{dz} = \rho_o c_p \frac{dT_o}{dz} \quad (3.13)$$

and substitution of Eq. 3.13 into Eq. 3.10 gives Γ_d , the lapse rate of the dry adiabatic atmosphere:

$$\Gamma_d \equiv -\frac{dT_o}{dz} = \frac{g}{c_p} = 9.76 \text{ }^\circ\text{C/km} \quad (3.14)$$

To this point the solution of the adiabatic atmosphere has been presented. Substituting the reference state decomposition, Eq. 3.6-Eq. 3.9 into the equations of motion,

Eq. 3.1-Eq. 3.4, and using the results of the adiabatic atmosphere, Eq. 3.10 and Eq. 3.14, gives the equations of motion for the perturbations:

Continuity Equation

$$\frac{\partial u_j}{\partial x_j} = -\frac{u_j}{\rho_0} \frac{\partial \rho_0}{\partial x_j} + \frac{R_d}{c_p} \frac{k}{\rho_0} \frac{\partial^2 T}{\partial x_j^2} \approx 0 \quad (3.15)$$

Momentum Equation:

$$\rho_0 \frac{\partial u_i}{\partial t} + \rho_0 u_j \frac{\partial u_i}{\partial x_j} = -\frac{\partial p}{\partial x_i} - \rho g_i + \mu_0 \frac{\partial^2 u_i}{\partial x_j^2} \quad (3.16)$$

Energy Equation:

$$\rho_0 \frac{\partial T}{\partial t} + \rho_0 u_j \frac{\partial T}{\partial x_j} = \frac{R_d}{c_p} \frac{\partial^2 T}{\partial x_j^2} \quad (3.17)$$

Equation of State:

$$\frac{p}{\rho_0} = \frac{T}{T_0} + \frac{p}{\rho_0} + \frac{\rho T}{\rho_0 T_0} \quad (3.18)$$

The fluid perturbations will generally be assumed to be incompressible in the Boussinesq sense. That is, changes in fluid density are assumed to be produced only by temperature changes, and not by pressure fluctuations. Neglecting the pressure fluctuations in the equation of state, and noting that generally $\rho T \ll \rho_0 T_0$, the equation of state becomes

$$\rho/\rho_0 \approx -T/T_0 \quad (3.19)$$

which is the familiar Boussinesq equation of state. This equation allows the buoyancy term $(-\rho g_i/\rho_0)$ in the momentum equation (Eq. 3.16) to be similarly approximated. The continuity equation (Eq. 3.15) becomes that of an incompressible fluid, assuming that the fluid motions do not rapidly mix deep layers of the fluid,³⁷ e.g., comparing length scales of velocity and density:

$$\left(\frac{1}{|u_j|} \left| \frac{\partial u_j}{\partial x_j} \right| \right)^{-1} \ll \left(\frac{1}{\rho_0} \left| \frac{\partial \rho_0}{\partial x_j} \right| \right)^{-1} \quad (3.20)$$

and¹¹ that the heat conduction term in Eq. 3.1 is a small contribution to the divergence. Making these approximations, the equations for the perturbations may be written as

Continuity Eq.:

$$\frac{\partial u_j}{\partial x_j} = 0 \quad (3.21)$$

Momentum Eq:

$$\frac{\partial u_i}{\partial t} + u_j \frac{\partial u_i}{\partial x_j} = - \frac{1}{\rho_0} \frac{\partial p}{\partial x_i} - \frac{\rho}{\rho_0} g_i + \frac{\mu_0}{\rho_0} \frac{\partial^2 u_i}{\partial x_j^2} \quad (3.22)$$

Energy Eq:

$$\frac{\partial T}{\partial t} + u_j \frac{\partial T}{\partial x_j} = P_r^{-1} \frac{\mu_0}{\rho_0} \frac{\partial^2 T}{\partial x_j^2} \quad (3.23)$$

Define the potential temperature, θ , as

$$\theta \equiv \tilde{T} \left(\frac{1000\text{mb}}{\tilde{p}} \right)^{R_d/c_p} \quad (3.24)$$

Differentiating with respect to height finds that the adiabatic atmosphere has a lapse rate of potential temperature of zero,

$$\frac{d\theta_o}{dz} = 0 \quad (3.25)$$

or that the potential temperature is a constant in an adiabatic atmosphere. Errors introduced by evaluating density with θ instead of \tilde{T} are assumed to be small (this is investigated in Sec. 3.3.4). Neglecting the perturbation p with respect to p_o in Eq. 3.24, and approximating ρ_o as $\rho(\theta_o)$ in Eq. 3.22, the use of θ instead of T in the primitive equations (Eq. 3.21-Eq. 3.23) gives

Continuity Eq:

$$\frac{\partial u_j}{\partial \tilde{x}_j} = 0 \quad (3.26)$$

Momentum Eq:

$$\frac{\partial u_i}{\partial t} + u_j \frac{\partial u_i}{\partial \tilde{x}_j} = - \frac{1}{\rho(\theta_o)} \frac{\partial p}{\partial \tilde{x}_i} - \frac{\rho(\theta) - \rho(\theta_o)}{\rho(\theta_o)} g_i + \nu \frac{\partial^2 u_i}{\partial \tilde{x}_j^2} \quad (3.27)$$

Energy Eq:

$$\frac{\partial \theta}{\partial t} + u_j \frac{\partial \theta}{\partial \tilde{x}_j} = \nu \text{Pr}^{-1} \frac{\partial^2 \theta}{\partial \tilde{x}_j^2} \quad (3.28)$$

The utility of the potential temperature formulation is that strong variations of pressure and density with height in the hydrostatic approximation of Eq. 3.10 are no longer present in the primitive equations. Initialization errors to the hydrostatic state, if included in the primitive equations, lead to strong transient fluid motions.³⁸ The transients are neatly avoided by this formulation.

To this point the fully three-dimensional fluid mechanics equations have been decomposed into an adiabatic reference state, and a flow field of perturbations about this state. A number of approximations have simplified the equations for the perturbations to those of a Boussinesq incompressible flow. The equations need to be ensemble-averaged and a turbulence closure formulated, and then the set must be finite-differenced for computer solution.

3.2.1.2 Reynolds Decomposition and Closure

To model the effects of turbulence on the mean flow, each primitive variable in the equation set is decomposed into its time-averaged and fluctuating parts as

$$\left\{ \begin{array}{l} \text{the value of the} \\ \text{perturbation of} \\ \text{a primitive} \\ \text{variable} \end{array} \right\} = \left\{ \begin{array}{l} \text{its ensemble-} \\ \text{averaged} \\ \text{value} \end{array} \right\} + \left\{ \begin{array}{l} \text{any fluctua-} \\ \text{tions about} \\ \text{its ensemble-} \\ \text{average value} \end{array} \right\}$$

(3.29)

which is represented here by the decompositions

$$p \rightarrow \bar{p} + p' \quad (3.30)$$

$$\theta \rightarrow \bar{\theta} + \theta' \quad (3.31)$$

$$\rho \rightarrow \bar{\rho} + \rho' \quad (3.32)$$

$$u_i \rightarrow \bar{u}_i + u_i' \quad (3.33)$$

Under this transformation, by selectively ensemble-averaging and subtracting the equations, and by making use of the continuity equation, the primitive equations become

Continuity Equations

$$\partial \bar{u}_j / \partial x_j = 0 \quad (3.34)$$

$$\partial u_j' / \partial x_j = 0 \quad (3.35)$$

Momentum Equations:

$$\begin{aligned} \frac{\partial \bar{u}_i}{\partial t} + \bar{u}_j \frac{\partial \bar{u}_i}{\partial x_j} = & -\frac{1}{\rho(\theta_0)} \frac{\partial \bar{p}}{\partial x_i} + \frac{\rho(\bar{\theta}) - \rho(\theta_0)}{\rho(\theta_0)} g_i \\ & + \nu \frac{\partial^2 \bar{u}_i}{\partial x_j^2} - \frac{\partial}{\partial x_j} (\overline{u_i' u_j'}) \end{aligned} \quad (3.36)$$

$$\frac{\partial u_i'}{\partial t} + \bar{u}_j \frac{\partial u_i'}{\partial x_j} + u_j' \frac{\partial \bar{u}_i}{\partial x_j} + u_j' \frac{\partial u_i'}{\partial x_j} - \frac{\partial}{\partial x_j} (\overline{u_i' u_j'}) =$$

$$\frac{-1}{\rho(\theta_0)} \frac{\partial p'}{\partial x_i} - \frac{\rho(\theta') - \rho(\theta_0)}{\rho(\theta_0)} g_i + \nu \frac{\partial^2 u_i'}{\partial x_j^2} \quad (3.37)$$

Energy Equations:

$$\frac{\partial \bar{\theta}}{\partial t} + \bar{u}_j \frac{\partial \bar{\theta}}{\partial x_j} = \nu P_r^{-1} \frac{\partial^2 \bar{\theta}}{\partial x_j^2} - \frac{\partial}{\partial x_j} (\overline{u'_j \theta'}) \quad (3.38)$$

$$\frac{\partial \theta'}{\partial t} + \bar{u}_j \frac{\partial \theta'}{\partial x_j} + u_j \frac{\partial \bar{\theta}}{\partial x_j} + u_j \frac{\partial \theta'}{\partial x_j} - \frac{\partial}{\partial x_j} (\overline{u'_j \theta'}) = \nu P_r^{-1} \frac{\partial^2 \theta'}{\partial x_j^2} \quad (3.39)$$

The set of ensemble-averaged equations (i.e., Eq. 3.34, Eq. 3.36 and Eq. 3.38) suffer from the well-known closure problem due to the generation of the $\overline{u'_i u'_j}$ and $\overline{u'_i \theta'}$ terms by the non-linear advection terms in Eq. 3.27 and Eq. 3.28. Equations 3.37 and 3.39 may be manipulated to produce transport equations for these two new variables:

$$\begin{aligned} \frac{D}{Dt} (\overline{u'_i u'_j}) &= - \overline{u'_i u'_k} \frac{\partial \bar{u}_j}{\partial x_k} - \overline{u'_j u'_k} \frac{\partial \bar{u}_i}{\partial x_k} && \text{production terms} \\ &- \frac{\partial}{\partial x_k} (\overline{u'_i u'_j u'_k}) && \text{turbulent transport term} \\ &- \frac{1}{\rho_0} \frac{\partial}{\partial x_i} (\overline{p' u'_j}) - \frac{1}{\rho_0} \frac{\partial}{\partial x_j} (\overline{p' u'_i}) && \text{pressure diffusion terms} \\ &+ \frac{1}{\rho_0} \overline{p' \left(\frac{\partial u'_i}{\partial x_j} + \frac{\partial u'_j}{\partial x_i} \right)} && \text{tendency toward isotropy term} \end{aligned}$$

$$\begin{aligned}
 & + \frac{1}{\theta_0} (g_i \overline{u_j' \theta'} + g_j \overline{u_i' \theta'}) && \text{buoyant production terms} \\
 & + \nu \frac{\partial^2 (\overline{u_i' u_j'})}{\partial x_k^2} && \text{molecular diffusion terms} \\
 & - 2\nu \overline{\frac{\partial u_i'}{\partial x_k} \frac{\partial u_j'}{\partial x_k}} && \text{dissipation term}
 \end{aligned}$$

(3.40)

$$\begin{aligned}
 \frac{D}{Dt} (\overline{u_i' \theta'}) &= -\overline{u_j' u_i'} \frac{\partial \bar{\theta}}{\partial x_j} - \overline{u_j \theta'} \frac{\partial \bar{u}_i}{\partial x_j} && \text{production terms} \\
 & - \frac{\partial}{\partial x_j} (\overline{u_i' u_j' \theta'}) && \text{turbulent transport term} \\
 & - \frac{1}{\rho_0} \frac{\partial}{\partial x_i} (\overline{p' \theta'}) && \text{pressure diffusion term} \\
 & + \frac{1}{\rho_0} \overline{p' \frac{\partial \theta'}{\partial x_i}} && \text{tendency toward isotropy term} \\
 & + \frac{1}{\theta_0} g_i \overline{\theta' \theta'} && \text{buoyant production term} \\
 & + \nu \frac{\partial^2 (\overline{u_i' \theta'})}{\partial x_j^2} && \text{molecular diffusion term}
 \end{aligned}$$

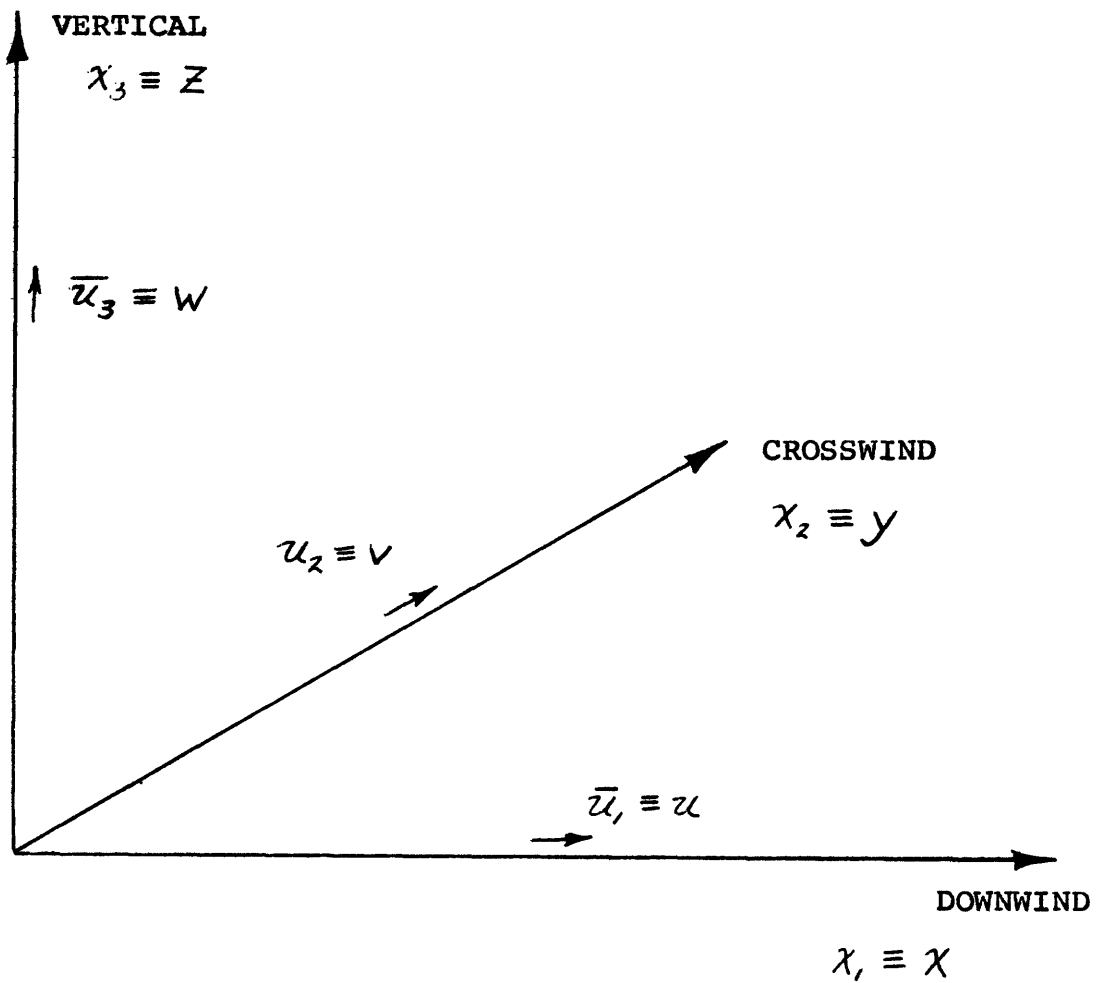
$$- 2\nu \frac{\overline{\frac{\partial u_i'}{\partial x_j} \frac{\partial \theta'}{\partial x_j}}}{\partial x_j} \quad \begin{array}{l} \text{dissipation} \\ \text{term} \end{array} \quad (3.41)$$

A discussion of the individual terms noted in Eq. 3.40 and Eq. 3.41 can be found elsewhere.¹¹ These equations were closed by Stuhmiller² and the results are listed here for completeness. In Eq. 3.40, the tendency toward isotropy term is neglected, because the turbulence is assumed to be homogeneous, and the molecular diffusion term is neglected because the flow is expected to be highly turbulent. The buoyant production term is also neglected, mainly in order to see how well the turbulence model can do without it, since it was neglected in Stuhmiller's turbulence model. It is found that the incorporation of this term would probably aid the model in reproducing the buoyant line-thermal results (see Sec. 5.2.2). By further making the assumption that the average flow is two-dimensional in the y-z axes of Fig. 3.1, the following closure is made for the trace of Eq. 3.40, which is the turbulence kinetic energy, q , $q \equiv \overline{u_i' u_i'}$,

$$\begin{aligned} \frac{Dq}{Dt} = & 2\sigma \left(\left(\frac{\partial v}{\partial y} \right)^2 + \frac{1}{2} \left(\frac{\partial v}{\partial z} + \frac{\partial w}{\partial y} \right)^2 + \left(\frac{\partial w}{\partial z} \right)^2 \right) - 4\alpha q^2 \sigma^{-1} \\ & + \Gamma \left(\frac{\partial}{\partial y} \sigma \frac{\partial q}{\partial y} + \frac{\partial}{\partial z} \sigma \frac{\partial q}{\partial z} \right) \end{aligned} \quad (3.42)$$

Figure 3.1
Flow Field Orientation

The flow field of Eqs. 3.42-3.47 is time-dependent and two-dimensional in the y-z axes. The relationship of the time-dependence to the (downwind) x-axis is discussed in Sec. 3.3.3.



The off-diagonal terms of the Reynolds stress tensor are related to a scalar eddy viscosity, σ , where $\overline{u'_i u'_j} = \frac{\sigma}{2} \left(\frac{\partial \bar{u}_i}{\partial x_j} + \frac{\partial \bar{u}_j}{\partial x_i} \right)$,

and σ has the following transport equation:

$$\begin{aligned} \frac{D\sigma}{Dt} = \frac{\sigma^2}{q} \left(\left(\frac{\partial v}{\partial y} \right)^2 + \frac{1}{2} \left(\frac{\partial v}{\partial z} + \frac{\partial w}{\partial y} \right)^2 + \left(\frac{\partial w}{\partial z} \right)^2 \right) - \alpha q \\ + \Gamma \frac{\sigma}{q} \left(\frac{\partial}{\partial y} \sigma \frac{\partial q}{\partial y} + \frac{\partial}{\partial z} \sigma \frac{\partial q}{\partial z} \right) - \Gamma_1 \left(\frac{\sigma^3}{q^2} \left(\frac{\partial}{\partial y} q \frac{\partial}{\partial y} \left(\frac{q}{\sigma} \right) + \frac{\partial}{\partial z} q \frac{\partial}{\partial z} \left(\frac{q}{\sigma} \right) \right) \right) \end{aligned} \quad (3.43)$$

Finally, the turbulent fluxes of heat in Eq. 3.41 are related to the turbulent momentum fluxes through a reciprocal turbulent Prandtl number, γ_T , which is specified along with the three other turbulence constants α , Γ , and Γ_1 . With this turbulence closure, the continuity, momentum, and energy equations become, in a two-dimensional flow

$$\frac{\partial v}{\partial y} + \frac{\partial w}{\partial z} = 0 \quad (3.44)$$

$$\frac{\partial v}{\partial t} + \frac{\partial}{\partial y} (v^2) + \frac{\partial}{\partial z} (vw) = - \frac{1}{\rho(\theta_0)} \frac{\partial \bar{p}}{\partial y} + \frac{\partial}{\partial y} \left(\sigma \frac{\partial v}{\partial y} \right) + \frac{\partial}{\partial z} \left(\sigma \frac{\partial v}{\partial z} \right) \quad (3.45)$$

$$\frac{\partial w}{\partial t} + \frac{\partial}{\partial y} (vw) + \frac{\partial}{\partial z} (w^2) = \frac{-1}{\rho(\theta_0)} \frac{\partial \bar{p}}{\partial z} + \frac{\partial}{\partial y} \left(\sigma \frac{\partial w}{\partial y} \right) + \frac{\partial}{\partial z} \left(\sigma \frac{\partial w}{\partial z} \right) - \left(\frac{\rho(\bar{\theta}) - \rho(\theta_0)}{\rho(\theta_0)} \right) g_z \quad (3.46)$$

$$\frac{\partial \bar{\theta}}{\partial t} + \frac{\partial}{\partial y}(\bar{\theta}v) + \frac{\partial}{\partial z}(\bar{\theta}w) = \frac{\partial}{\partial y}(\chi_T \sigma \frac{\partial \bar{\theta}}{\partial y}) + \frac{\partial}{\partial z}(\chi_T \sigma \frac{\partial \bar{\theta}}{\partial z}) \quad (3.47)$$

With an internal energy variable, I , defined as $I \equiv c_p \bar{\theta}$, equations 3.42-3.47 are solved by the VARR-II code. Additional pollutant and moisture transport equations are discussed in the next two sections, and possible modifications to these equations are discussed in section 6.2.

3.2.1.2 Pollutant Species Transport Equation

A transport equation for a pollutant species density, χ is added to the set of Eqs. 3.42-3.47. The pollutant is assumed to be a neutrally buoyant, passive species, although it may be contained in a buoyant stream of effluent. The assumption that the species is neutrally buoyant could be relaxed, but the model is felt to be useful in modeling most dilute pollutants in its present form. The turbulent diffusion of the pollutant is related to the eddy viscosity of momentum by a reciprocal turbulent Schmidt number, χ_χ . The transport equation may be written down as

$$\left[\begin{array}{c} \text{substantial derivative} \\ \text{of } \chi \end{array} \right] = \left[\begin{array}{c} \text{turbulent transport} \\ \text{of } \chi \end{array} \right] - \left[\begin{array}{c} \text{rate of} \\ \text{destruction} \\ \text{of } \chi \end{array} \right] \quad (3.48)$$

which is represented here as

$$\frac{\partial \chi}{\partial t} + v \frac{\partial \chi}{\partial y} + w \frac{\partial \chi}{\partial z} = \frac{\partial}{\partial y} (\sigma_{\chi} \frac{\partial \chi}{\partial y}) + \frac{\partial}{\partial z} (\sigma_{\chi} \frac{\partial \chi}{\partial z}) - \sum_{i=1}^N \lambda_{\chi}^{(i)} \chi \quad (3.49)$$

in the notation of Fig. 3.1.

The destruction of χ is assumed to be by radioactive decay into any of N decay channels, so that the rate of destruction of χ is the product of χ and the sum of its radioactive decay constants $\lambda_{\chi}^{(i)}$, in Eq. 3.49. This formulation makes no account of sources of the pollutant species through decay of radioactive precursors. It also ignores chemical reactions which could alter the pollutant concentration. However, the extension of the model to include these effects is straightforward.

3.2.1.4 Radioactive Decay Heating

The thermal energy released by radioactive decay of the pollutant is added to the specific internal energy of the fluid. Pollutants may decay by any one of N different decay channels with decay constant $\lambda_{\chi}^{(i)}$ and energy $E_{\chi}^{(i)}$. A fraction $F_{\chi}^{(i)}$ of the energy is deposited within the plume, yielding an energy release rate of

$$\left(c_p \frac{\partial \bar{\theta}}{\partial t}\right)_{\text{radioactive}} = \frac{4.151 \times 10^{10} \frac{\text{BTU-atoms}}{\text{MeV-lb}_m\text{-mole}}}{\rho W_{\text{mol}\chi} / \chi} \sum_{i=1}^N F_{\chi}^{(i)} E_{\chi}^{(i)} \lambda_{\chi}^{(i)}$$

(3.50)

where $W_{\text{mol}\chi}$ is the molecular weight of χ in $\text{lb}_m/\text{lb}_m\text{-mole}$. Daughter radiations have been ignored in this formulation, but could be included with their own transport equation. Similarly, alterations of the energy balance caused by chemical reactions has not been treated in this work, but would be easy to address in extensions of this work.

3.2.2 Moist Equations

The inclusion of moisture is considered in this section with the purpose of pointing out the assumptions that allow the equations to be formulated with the concept of virtual potential temperature, in addition to two other moisture variables. The assumptions that are made in this section are important--the moisture model is not meant to be perfectly general; it is expected to do poorly when these assumptions are not valid.

3.2.2.1 Reference State Decomposition

Atmospheric moisture is assumed to be in either the liquid or vapor phases. The amount of vapor is described by the vapor density moisture variable, $\tilde{\rho}_{\text{vap}}$, and the amount of cloud liquid water is described by the liquid density moisture variable, $\tilde{\rho}_{\text{liq}}$. Transport equations for these two variables are written that take note of the turbulent transports of vapor and liquid, and the processes of evaporation and condensation that cause the interchange of vapor and liquid. First, however, the effect of moisture on the buoyancy of a parcel of air is developed and applied to the description of a hydrostatic reference state.

The density of a parcel of moist air is the sum of the dry air, vapor, and liquid densities:

$$\tilde{\rho} = \tilde{\rho}_{\text{dry}} + \tilde{\rho}_{\text{vap}} + \tilde{\rho}_{\text{liq}} \quad (3.51)$$

In this work the contribution to the density of the typically small amount of cloud liquid water is ignored, (there is usually no liquid water present in the simulations, and when it is present, it is typically less than 1% of the mass of the fluid), so that the concept of virtual potential temperature can be explored. Dropping the $\tilde{\rho}_{\text{liq}}$ term and applying the perfect gas law to $\tilde{\rho}_{\text{dry}}$ and $\tilde{\rho}_{\text{vap}}$ yields:

$$\tilde{\rho} = \frac{\tilde{\rho}_{\text{dry}}}{R_d T} + \frac{\tilde{\rho}_{\text{vap}}}{R_v T} \equiv \frac{(\tilde{p}_{\text{dry}} + \tilde{p}_{\text{vap}})}{R_d T_v} = \frac{\tilde{p}}{R_d T_v} \quad (3.52)$$

where \tilde{p} is the total pressure, m_{vap} and m_{dry} are molecular weights and the virtual temperature, \tilde{T}_v , is

$$\tilde{T}_v = \tilde{T} \left[\frac{1 + \frac{m_{\text{dry}} \tilde{\rho}_{\text{vap}}}{m_{\text{vap}} \rho_{\text{dry}}}}{1 + \frac{\tilde{\rho}_{\text{vap}}}{\tilde{\rho}_{\text{dry}}}} \right] \quad (3.53)$$

It is very important to note in Eq. 3.52 that the virtual temperature is a fictitious temperature that is used in the dry gas equation of state to give the density of moist air. Generally the virtual temperature is no more than a few degrees higher than the thermodynamic temperature for typical atmospheric conditions.

Following the development in Sec. 3.2.1.1, the variations of virtual temperature, pressure, and density of a static atmosphere are "subtracted out" by making a reference state decomposition:

$$\left\{ \begin{array}{l} \text{the value of} \\ \text{a primitive} \\ \text{variable} \end{array} \right\} = \left\{ \begin{array}{l} \text{its value in a uni-} \\ \text{formly moist adiabatic} \\ \text{atmosphere (function} \\ \text{of height only)} \end{array} \right\} + \left\{ \begin{array}{l} \text{a departure} \\ \text{from the} \\ \text{state at} \\ \text{rest} \end{array} \right\} \quad (3.54)$$

Or, in the notation of this work:

$$\tilde{p} \rightarrow p_o + p \quad (3.55)$$

$$\tilde{\rho} \rightarrow \rho_o + \rho \quad (3.56)$$

$$\tilde{T}_v \rightarrow T_{vo} + T_v \quad (3.57)$$

$$\tilde{u}_i \rightarrow 0 + u_i \quad (3.58)$$

the only difference here to the reference state decomposition of Eqs. 3.6-3.9 is in the use of the (fictitious) virtual temperature in order to allow the use of an equation of state that is analogous to Eq. 3.4:

$$\tilde{p} = \tilde{p}/R_d \tilde{T}_v \quad (3.59)$$

Substituting Eqs. 3.55-3.58 into the primitive equation set (Eqs. 3.1-3.3 and Eq. 3.59), and setting the time derivatives and perturbations to zero yields the state of the moist adiabatic atmosphere. The continuity and energy equations are trivial (as before), and the momentum equation becomes the moist hydrostatic equation:

$$\frac{dp_o}{dz} = -\rho_o g \quad (3.60)$$

The equation of state is simply

$$p_o = \rho_o R_d T_{vo} \quad (3.61)$$

The first Law of Thermodynamics for an unsaturated adiabatic process in this atmosphere is

$$dQ = 0 = c_p^{\text{moist}} dT_{vo} - dp_o/\rho_o \quad (3.62)$$

Approximating the heat capacity for a moist gas, c_p^{moist} , as that of a dry gas, c_p , dividing by dz and substituting Eq. 3.62 into 3.60 yields an approximate lapse rate for a moist, unsaturated atmosphere which is the same as that for a dry adiabatic atmosphere:

$$\frac{-dT_{vo}}{dz} = \frac{g}{c_p} = 9.76^\circ\text{C/km} \quad (3.63)$$

To this point the resting state of a moist adiabatic atmosphere has been presented. The neglect of the effect of the liquid water on the total density has allowed the treatment of moisture to duplicate the dry atmosphere equations after the transformation of temperature to virtual temperature. The equations for the perturbations are identical to those of the dry atmosphere developed in Sec. 3.2.1.1, except that temperature is replaced by virtual temperature, and a latent heat release term is included:

Continuity Eq.

$$\frac{\partial u_j}{\partial x_j} = 0 \quad (3.64)$$

Momentum Eq.

$$\frac{\partial u_i}{\partial t} + u_j \frac{\partial u_i}{\partial x_j} = -\frac{1}{\rho_0} \frac{\partial p}{\partial x_i} + \frac{T_v}{T_{vo}} g_i + \frac{\mu_0}{\rho_0} \frac{\partial^2 u_i}{\partial x_j^2} \quad (3.65)$$

Energy Eq.

$$\frac{\partial T_v}{\partial t} + u_j \frac{\partial T_v}{\partial x_j} = \nu \text{Pr}^{-1} \frac{\partial^2 T_v}{\partial x_j^2} - \frac{L}{\rho c_p} \left(\frac{D\rho_{\text{vap}}}{Dt} \right)_{\text{phase}} \quad (3.66)$$

The latent heat release term is considered in Sec. 3.2.2.4.

Define the virtual potential temperature, θ_v , as

$$\theta_v \equiv \tilde{T}_v \left(\frac{1000}{p} \right)^{R_d/c_p^{\text{moist}}} \quad (3.67)$$

Again assume that c_p^{moist} is essentially equal to c_p . Differentiating with respect to height finds that the moist unsaturated adiabatic atmosphere has a lapse of virtual potential temperature that vanishes:

$$\frac{d\theta_{vo}}{dz} = 0 \quad (3.68)$$

The result here is that the virtual potential temperature is a constant in the reference state.

Neglecting the perturbation pressure, p , with respect to p_0 in Eq. 3.56, the use of θ_v instead of T_v in the primitive equations (Eq. 3.64-Eq. 366) gives

Continuity Eq:

$$\frac{\partial u_j}{\partial x_j} = 0 \quad (3.69)$$

Momentum Eq:

$$\frac{\partial u_i}{\partial t} + u_j \frac{\partial u_i}{\partial x_j} = \frac{-1}{\rho(\theta_{vo})} \frac{\partial p}{\partial x_i} - \frac{\rho(\theta_v) - \rho(\theta_{vo})}{\rho(\theta_{vo})} g_i + \nu \frac{\partial^2 u_i}{\partial x_j^2} \quad (3.70)$$

Energy Eq:

$$\frac{\partial \theta_v}{\partial t} + u_j \frac{\partial \theta_v}{\partial x_j} = \nu \text{Pr}^{-1} \frac{\partial^2 \theta_v}{\partial x_j^2} - \frac{L}{\rho c_p} \left(\frac{D\rho_{\text{vap}}}{Dt} \right)_{\text{phase}} \quad (3.71)$$

The result here is the same as in Sec. 3.2.1.1: the strong variation of pressure with height is no longer present in the primitive equations. This formulation is common (although in slightly different forms) among papers in meteorology.

Transport equations may be written down for the water vapor and liquid water densities according to the conservation scheme:

$$\left\{ \begin{array}{l} \text{Eulerian time} \\ \text{rate of change} \\ \text{of vapor or} \\ \text{liquid} \end{array} \right\} = \left\{ \begin{array}{l} \text{Diffusion of} \\ \text{vapor or} \\ \text{liquid} \end{array} \right\} + \left\{ \begin{array}{l} \text{Gain or loss of} \\ \text{vapor or liquid} \\ \text{due to phase} \\ \text{changes} \end{array} \right\} \quad (3.72)$$

or, in the notation of this work:

$$\frac{\partial \rho_{\text{vap}}}{\partial t} + u_j \frac{\partial \rho_{\text{vap}}}{\partial x_j} = v_{\text{Sc}_{\text{vap}}}^{-1} \frac{\partial^2 \rho_{\text{vap}}}{\partial x_j^2} + \left(\frac{D\rho_{\text{vap}}}{Dt} \right)_{\text{phase}} \quad (3.73)$$

$$\frac{\partial \rho_{\text{liq}}}{\partial t} + u_j \frac{\partial \rho_{\text{liq}}}{\partial x_j} = v_{\text{Sc}_{\text{liq}}}^{-1} \frac{\partial^2 \rho_{\text{liq}}}{\partial x_j^2} - \left(\frac{D\rho_{\text{vap}}}{Dt} \right)_{\text{phase}} \quad (3.74)$$

where the gain or loss of vapor due to phase changes,

$(D\rho_{\text{vap}}/Dt)_{\text{phase}}$, identically shows up as a loss or gain of liquid, and Schmidt numbers that describe the molecular diffusion of vapor and liquid are introduced, respectively. The terminal fall velocities of the liquid water droplets are ignored. The $\left(\frac{D\rho_{\text{vap}}}{Dt} \right)_{\text{phase}}$ term is discussed in Sec. 3.2.2.3.

Note that any constant background (ambient atmospheric) value of ρ_{vap} and ρ_{liq} trivially satisfied these equations, so that no new information would be brought into the specification of the reference state by decomposing the variables in these transport equations. That is, ρ_{vap} and ρ_{liq} do not have a reference state "subtracted away" from them, unlike the other primitive variables \tilde{p} , $\tilde{\theta}_v$, and $\tilde{\rho}$.

3.2.2.2 Reynolds Decomposition and Closure

A Reynolds decomposition of the primitive equations is made as in Sec. 3.2.1.2. Each primitive variable in the equation set is decomposed into its ensemble-averaged and fluctuating parts:

$$p \rightarrow \bar{p} + p' \quad (3.75)$$

$$\theta \rightarrow \bar{\theta} + \theta'_v \quad (3.76)$$

$$\rho \rightarrow \bar{\rho} + \rho' \quad (3.77)$$

$$u_j \rightarrow 0 + u'_j \quad (3.78)$$

$$\rho_{\text{vap}} \rightarrow \bar{\rho}_{\text{vap}} + \rho'_{\text{vap}} \quad (3.79)$$

$$\rho_{\text{liq}} \rightarrow \bar{\rho}_{\text{liq}} + \rho'_{\text{liq}} \quad (3.80)$$

By selectively ensemble-averaging and subtracting the equations, and by making use of the continuity equation, the primitive equations yield the following relationships:

Continuity Eq:

$$\frac{\partial \bar{u}_j}{\partial x_j} = 0 \quad (3.81)$$

Momentum Eq:

$$\frac{\partial u_i}{\partial t} + u_j \frac{\partial u_i}{\partial x_j} = \frac{-1}{\rho(\theta_{vo})} \frac{\partial \bar{p}}{\partial x_i} - \frac{\rho(\bar{\theta}_v) - \rho(\theta_{vo})}{\rho(\theta_{vo})} g_i + \nu \frac{\partial^2 u_i}{\partial x_j^2} - \frac{\partial}{\partial x_j} (\overline{u_i' u_j'}) \quad (3.82)$$

Energy Eq:

$$\frac{\partial \bar{\theta}_v}{\partial t} + u_j \frac{\partial \bar{\theta}_v}{\partial x_j} = \nu Pr^{-1} \frac{\partial^2 \bar{\theta}_v}{\partial x_j^2} - \frac{\partial}{\partial x_j} (\overline{u_j' \theta_v'}) - \frac{L}{\rho(\theta_v) c_p} \left(\frac{D\bar{\rho}_{vap}}{Dt} \right)_{\text{phase}} \quad (3.83)$$

and the transport equations for moisture, Eq. 3.73 and Eq. 3.74 yield

Vapor Eq:

$$\frac{\partial \bar{\rho}_{vap}}{\partial t} + u_j \frac{\partial \bar{\rho}_{vap}}{\partial x_j} = \nu Sc_{vap}^{-1} \frac{\partial^2 \bar{\rho}_{vap}}{\partial x_j^2} - \frac{\partial}{\partial x_j} (\overline{\rho_{vap}' u_j'}) + \left(\frac{D\bar{\rho}_{vap}}{Dt} \right)_{\text{phase}} \quad (3.84)$$

Liquid Eq:

$$\frac{\partial \bar{\rho}_{liq}}{\partial t} + u_j \frac{\partial \bar{\rho}_{liq}}{\partial x_j} = \nu Sc_{liq}^{-1} \frac{\partial^2 \bar{\rho}_{liq}}{\partial x_j^2} - \frac{\partial}{\partial x_j} (\overline{\rho_{liq}' u_j'}) - \left(\frac{D\bar{\rho}_{vap}}{Dt} \right)_{\text{phase}} \quad (3.85)$$

Rather than providing the full equations for the correlated fluctuations $\overline{u_i' u_j'}$, $\overline{u_j' \theta_v'}$, $\overline{u_j' \rho_{vap}'}$, and $\overline{u_j' \rho_{liq}'}$, the turbulence closure is simply extended from that developed in Sec. 3.2.1.2. The closed set of equations in two-dimensions is, in the

notation of Fig. 3.1

Continuity Eq:

$$\frac{\partial v}{\partial y} + \frac{\partial w}{\partial z} = 0 \quad (3.86)$$

Momentum Eqs:

$$\frac{Dv}{Dt} = \frac{-1}{\rho(\theta_{vo})} \frac{\partial \bar{p}}{\partial y} + \frac{\partial}{\partial y} \left(\sigma \frac{\partial v}{\partial y} \right) + \frac{\partial}{\partial z} \left(\sigma \frac{\partial v}{\partial z} \right) \quad (3.87)$$

$$\frac{Dw}{Dt} = \frac{-1}{\rho(\theta_{vo})} \frac{\partial \bar{p}}{\partial z} - \frac{\rho(\bar{\theta}_v) - \rho(\theta_{vo})}{\rho(\theta_{vo})} g_z + \frac{\partial}{\partial y} \left(\sigma \frac{\partial w}{\partial y} \right) + \frac{\partial}{\partial z} \left(\sigma \frac{\partial w}{\partial z} \right)$$

Energy Eq:

$$\frac{D}{Dt} (c_p \bar{\theta}_v) = \frac{\partial}{\partial y} \left(\gamma_T \sigma \frac{\partial (c_p \bar{\theta}_v)}{\partial y} \right) + \frac{\partial}{\partial z} \left(\gamma_T \sigma \frac{\partial (c_p \bar{\theta}_v)}{\partial z} \right) - \frac{L}{\rho(\theta_v)} \left(\frac{D\bar{\rho}_{vap}}{Dt} \right)_{\text{phase}} \quad (3.88)$$

Vapor Eq:

$$\frac{D}{Dt} \bar{\rho}_{vap} = \frac{\partial}{\partial y} \left(\gamma_v \sigma \frac{\partial \bar{\rho}_{vap}}{\partial y} \right) + \frac{\partial}{\partial z} \left(\gamma_v \sigma \frac{\partial \bar{\rho}_{vap}}{\partial z} \right) + \left(\frac{D\bar{\rho}_{vap}}{Dt} \right)_{\text{phase}} \quad (3.89)$$

Liquid Eq:

$$\frac{D}{Dt} \bar{\rho}_{liq} = \frac{\partial}{\partial y} \left(\gamma_L \sigma \frac{\partial \bar{\rho}_{liq}}{\partial y} \right) + \frac{\partial}{\partial z} \left(\gamma_L \sigma \frac{\partial \bar{\rho}_{liq}}{\partial z} \right) - \left(\frac{D\bar{\rho}_{vap}}{Dt} \right)_{\text{phase}} \quad (3.90)$$

Eddy Viscosity Eq:

$$\frac{D\sigma}{Dt} = \frac{\sigma^2}{q} \left(\left(\frac{\partial v}{\partial y} \right)^2 + \frac{1}{2} \left(\frac{\partial v}{\partial z} + \frac{\partial w}{\partial y} \right)^2 + \left(\frac{\partial w}{\partial z} \right)^2 \right) - \alpha q +$$

$$+ \Gamma \frac{\sigma}{q} \left(\left(\frac{\partial}{\partial y} \sigma \frac{\partial q}{\partial y} \right) + \left(\frac{\partial}{\partial z} \sigma \frac{\partial q}{\partial z} \right) \right) - \Gamma_1 \left(\frac{\sigma^3}{q^2} \frac{\partial}{\partial y} q \frac{\partial}{\partial y} \left(\frac{q}{\sigma} \right) + \frac{\partial}{\partial z} q \frac{\partial}{\partial z} \left(\frac{q}{\sigma} \right) \right) \quad (3.91)$$

Turbulence Kinetic Energy Eq:

$$\frac{Dq}{Dt} = 2\sigma \left(\left(\frac{\partial v}{\partial y} \right)^2 + \frac{1}{2} \left(\frac{\partial v}{\partial z} + \frac{\partial w}{\partial y} \right)^2 + \left(\frac{\partial w}{\partial z} \right)^2 \right) - 4\alpha q \sigma^{-1} + \Gamma \left(\frac{\partial}{\partial y} \sigma \frac{\partial q}{\partial y} + \frac{\partial}{\partial z} \sigma \frac{\partial q}{\partial z} \right) \quad (3.92)$$

Pollutant Eq:

$$\frac{D\chi}{Dt} = \frac{\partial}{\partial y} \left(\gamma_{\chi} \sigma \frac{\partial \chi}{\partial y} \right) + \frac{\partial}{\partial z} \left(\gamma_{\chi} \sigma \frac{\partial \chi}{\partial z} \right) - \sum_{i=1}^N \lambda_{\chi}^{(i)} \chi \quad (3.93)$$

where reciprocal turbulent Prandtl and Schmidt numbers have been introduced, and are assumed to be constants.

3.2.2.3 Equilibrium Cloud Microphysics Model

The cloud microphysics model simply assumes that water vapor and liquid are always in equilibrium. Further, the surface tension of the liquid droplets is ignored. That is, phase equilibrium over a flat surface of water is assumed to exist. A phase diagram that illustrates this equilibrium is

sketched in Fig. 3.2.2.3.1. The liquid-vapor equilibrium curve above 273^oK is the locus of points that the saturation vapor pressure, $e_{\text{sat}}(T)$, may take. The vapor density, ρ_{vap} , in the presence of liquid water would be $e_{\text{sat}}(T)/R_{\text{vap}}T$. If there is no liquid available to evaporate, then the vapor density may be less than this saturation value. Below 273^oK the subcooled liquid-vapor equilibrium (dashed line) is obeyed. No ice formation is allowed. The entire liquid-vapor equilibrium curve is given by Magnus' formula:³⁹

$$\log_{10}e_{\text{sat}} = -\frac{2937.4}{T} - 4.9283 \log_{10}T + 23.5518 \quad (3.94)$$

The $\left(\frac{D\bar{\rho}_{\text{vap}}}{Dt}\right)$ phase term of Eq. 3.89 and Eq. 3.90 is simply adjusted to make the liquid and vapor coexist. The logic of the moisture model is illustrated in Fig. 3.2.2.3.2. Liquid and vapor are advected and diffused in an initial calculation for each computer cell. This generally results in a non-equilibrium moisture state in the cell, so the cell is allowed to evaporate or condense water in order to restore the equilibrium. The amount of evaporation or condensation in each cell is noted in order to provide the latent heat release term in the energy equation.

3.2.2.4 Latent Heat Source Term

The latent heat source term is calculated in each cell

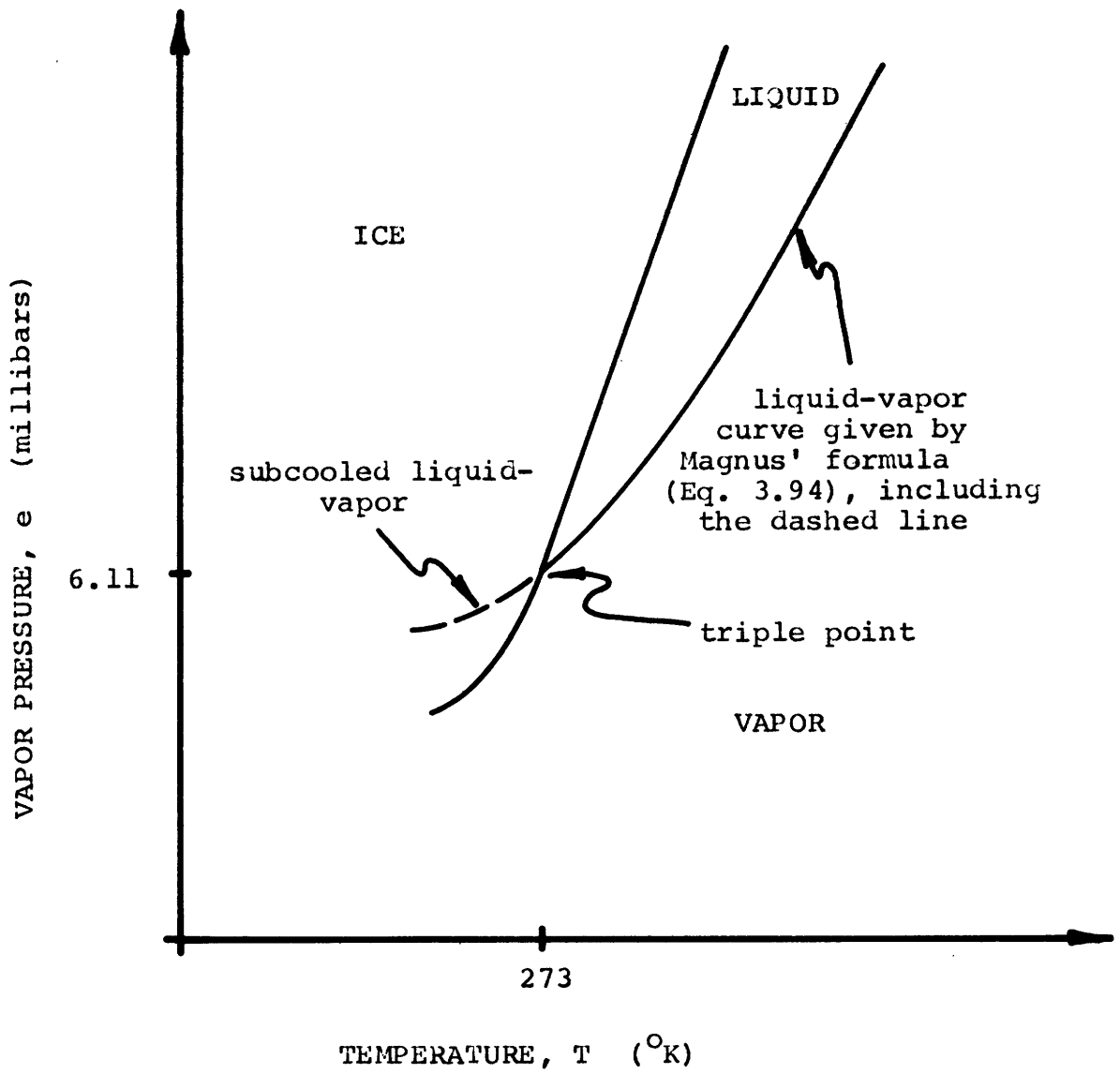


Fig. 3.2.2.3.1 Phase Diagram for Water Substance

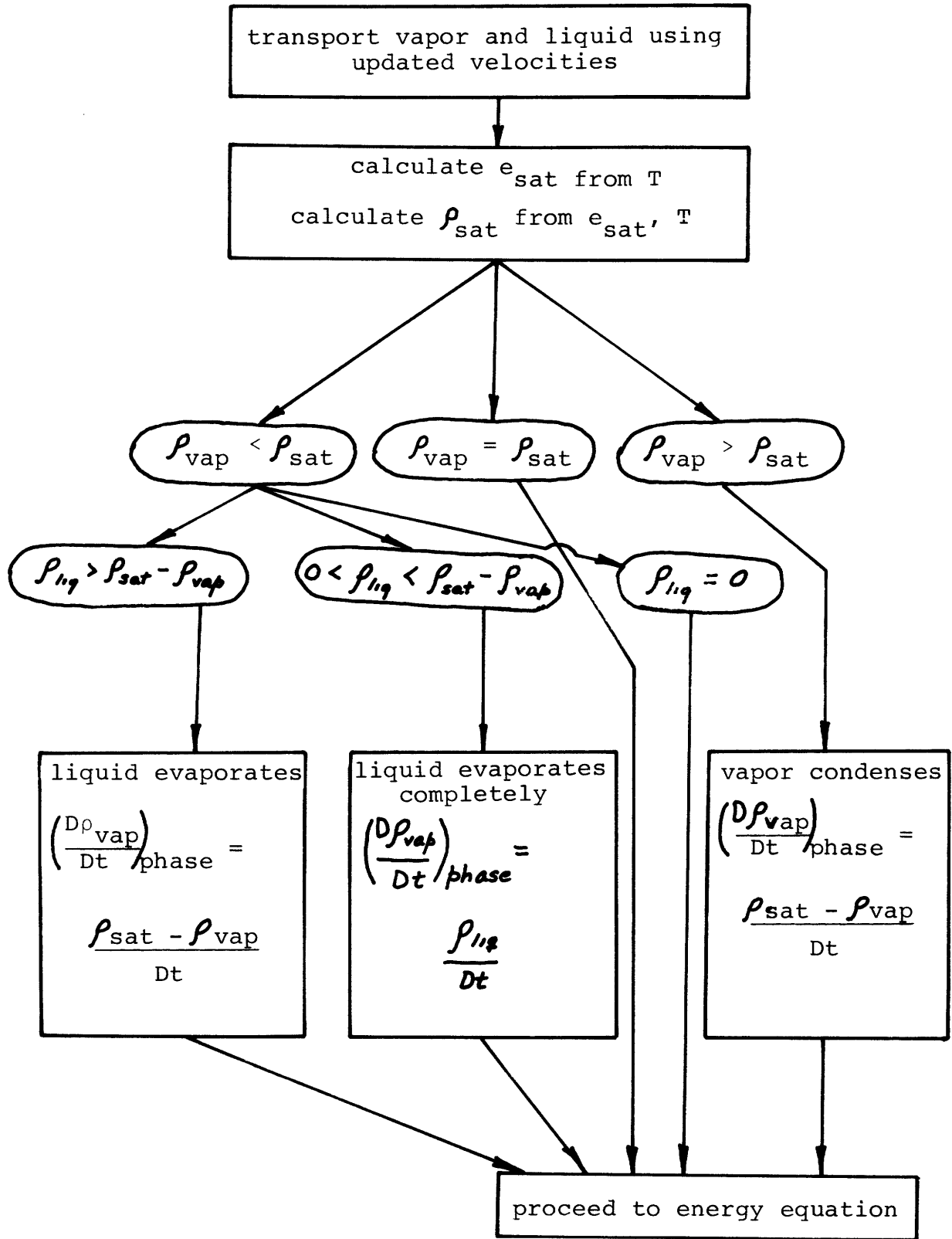


Fig. 3.2.2.3.2 Logic Diagram for the Equilibrium Moisture Calculation in a Single Cell during a Single Timestep

at every step depending on whether evaporation or condensation takes place. The latent heat release term is calculated as

$$\text{Latent Heat Release} \left[\frac{\text{BTU}}{\text{lb}_m \text{ sec}} \right] = - \frac{L}{\rho(\theta_v)} \left(\frac{D\bar{\rho}_{\text{vap}}}{Dt} \right)_{\text{phase}} \quad (3.95)$$

where the latent heat of vaporization, L , is assumed to be a constant, 1075 BTU/lb_m . The $\left(\frac{D\bar{\rho}_{\text{vap}}}{Dt} \right)_{\text{phase}}$ is found in the logic diagram of Fig. 3.2.2.3.2.

3.3 Model Solution Methodology

3.3.1 The VARR-II Fluid Mechanics Algorithm

The VARR-II computer code⁴⁰ is the starting point for the model development methodology in this work. In its original form, the VARR-II code solves the two-dimensional time-dependent turbulent fluid mechanics equations of continuity, momentum, and energy for a Boussinesq fluid. (The Boussinesq approximation to the momentum equation is considered in Sec. 3.2.1.1.) Two closure variables, the eddy viscosity, σ , and the turbulence kinetic energy, q , are also calculated from their own transport equations. The original VARR-II computer code is quite flexible in the choice of boundary conditions, allowing no-slip, free-slip, continuative inflow/outflow, or prescribed inflow/outflow boundaries.

The VARR-II fluid mechanics algorithm is the Simplified Marker and Cell (SMAC) method.⁴¹ The computer mesh for this method is Eulerian in either Cartesian or cylindrical geometry, and the primitive variables are solved directly, with no transformation to vorticity-stream function variables. The algorithm divides naturally into two sections during each time step: In the first section the velocity field is updated using the previous velocity and pressure fields with mixed central and donor-cell differencing⁴² of the equations. These velocities generally do not satisfy the continuity equation, so in a second section a pressure iteration adjusts these velocities until they satisfy continuity. Once the divergence-free updated velocity field is known, the energy and turbulence transport equations are updated, completing the calculational cycle of the time step.

The basic SMAC fluid mechanics algorithm has not been modified in this work. Pollutant and moisture transport equations have been added to the equation set, and they are updated in the same manner as the energy and turbulence variables, using the divergence-free updated velocity field. The stability of the method for problems of an atmospheric scale is considered in Sec. 5.2.1.

3.3.2 Orientation of the Computer Mesh

The optimal orientation of the two-dimensional computer

solution mesh is discussed here. Consider the representative three-dimensional plume in Fig. 3.3.2.1a. The plume has bent over in the imposed (one-dimensional) wind field, and the plume boundaries monotonically expand as the plume proceeds downwind. The most natural possibilities of orienting a two-dimensional solution mesh on this flow are: (1) to align the mesh parallel to the wind and through the center of the plume, as in Fig. 3.3.2.1b, or (2) to align the mesh perpendicular to the flow, as in Fig. 3.3.2.1c.

The advantages of the "crosswind" alignment of Fig. 3.3.2.1c over the "downwind" alignment of Fig. 3.3.2.1b are immediately apparent. In the crosswind alignment a three-dimensional simulation results since in the downwind Lagrangian translation of the computational mesh the time variable becomes a surrogate for the downwind position x , where

$$x = \int_0^t u(z(t))dt.$$

The downwind alignment is appropriate only for cases of line-source plumes--in which internal recirculation and entrainment will be of secondary importance to buoyant plume rise and atmospheric turbulent entrainment. Further, the crosswind alignment can take advantage of the centerline symmetry of the turbulent vortex pair to reduce the total mesh area by a factor of two, while the downwind

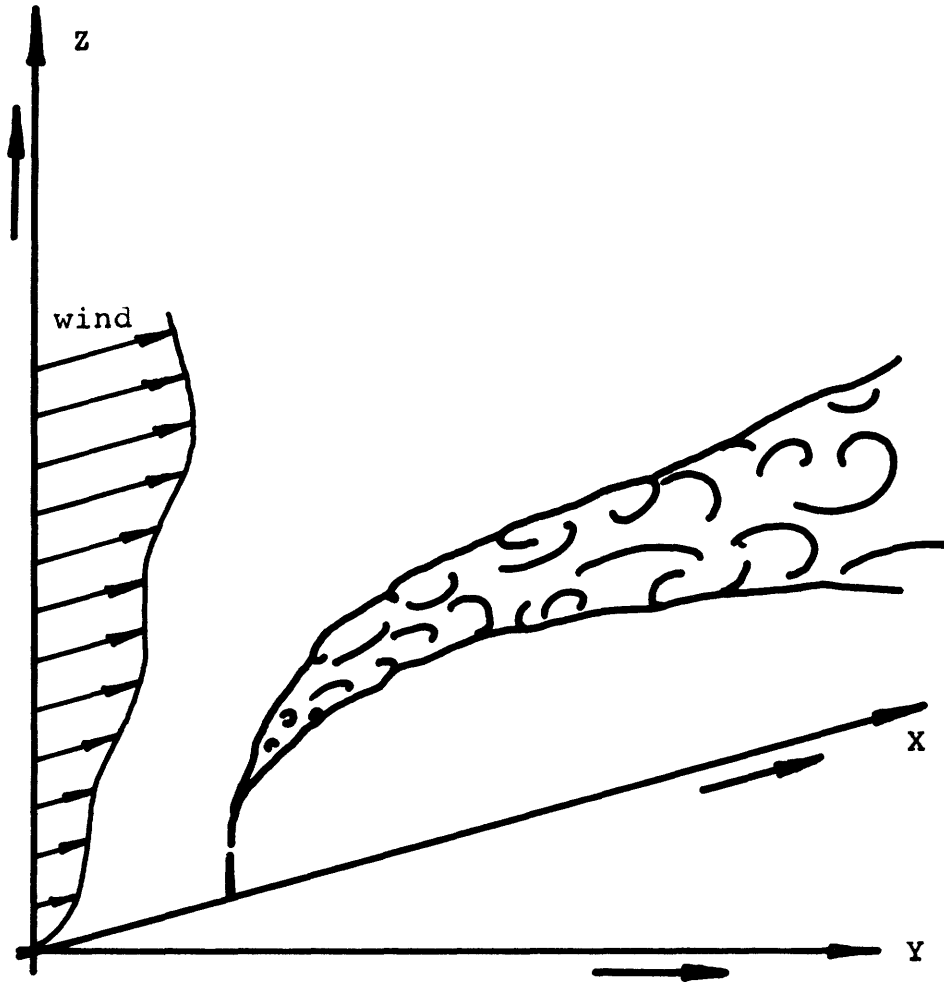


Fig. 3.3.2.1a Bent-Over Buoyant Plume with Ambient Thermal Stratification.

Fig. 3.3.2.1b

Mesh Alignment Appropriate for a Line Source Release

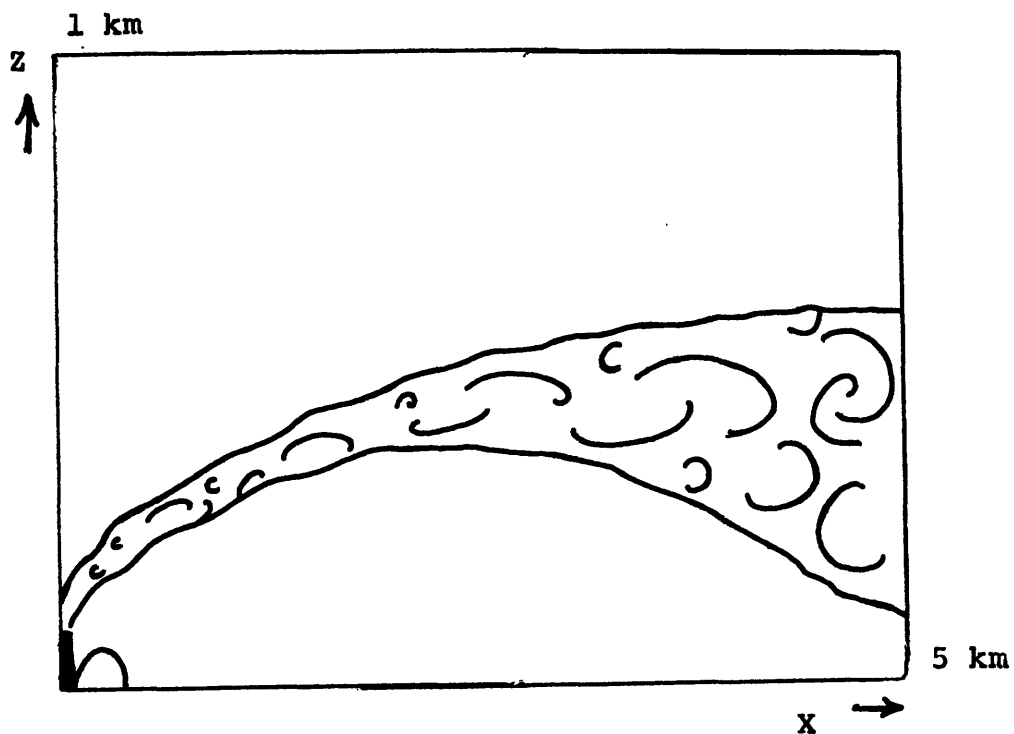
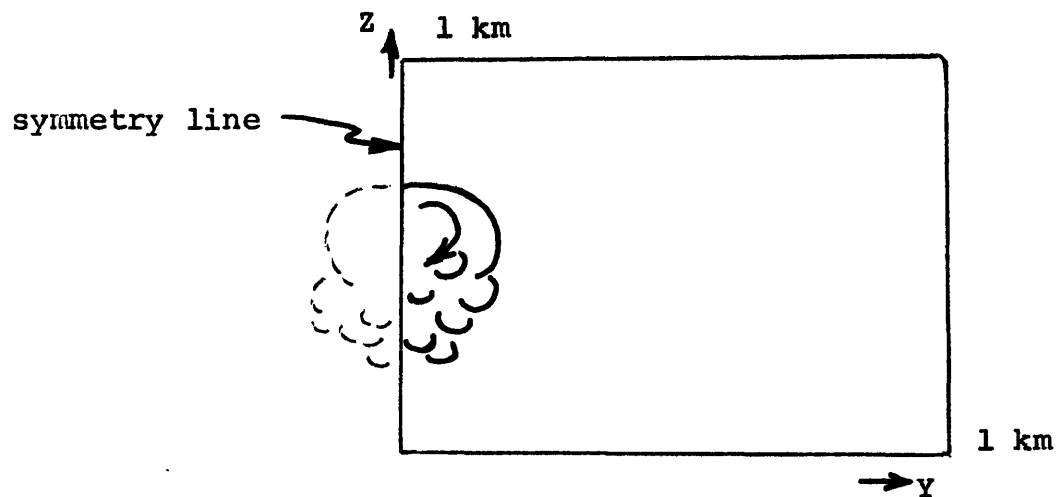


Fig. 3.3.2.1c

Mesh Alignment Appropriate for a Point Source Release



alignment scheme needs an extraordinarily long x-axis to model the same plume. Overall, the crosswind alignment scheme is about five times smaller than the downwind scheme. The velocity field in the crosswind alignment is that of a two-dimensional turbulent vortex, which typically exhibits strong shearing and entrainment of fluid. The velocity field in the downwind alignment is that of a two-dimensional turbulent deflected jet, which over most of the flow field exhibits a much smaller amount of shearing and entrainment. Clearly, the crosswind alignment scheme is expected to simulate the more important features of the flow.

The singular disadvantage of the crosswind alignment scheme is that it cannot explicitly calculate the shear-produced turbulence of the mean wind field, since the mean wind has no component in the y-z plane. The resolution of this problem is discussed in Sec. 4.3.3.

3.3.3 Downwind Advection of the Mesh

From the discussion in Sec. 3.3.2, the computer solution mesh is aligned perpendicular to the wind. The time evolution of the flow field of the plume cross section is drawn in Fig. 3.3.3.1. The choice of an appropriate downwind advection velocity of the computer mesh is needed in order to reconstruct

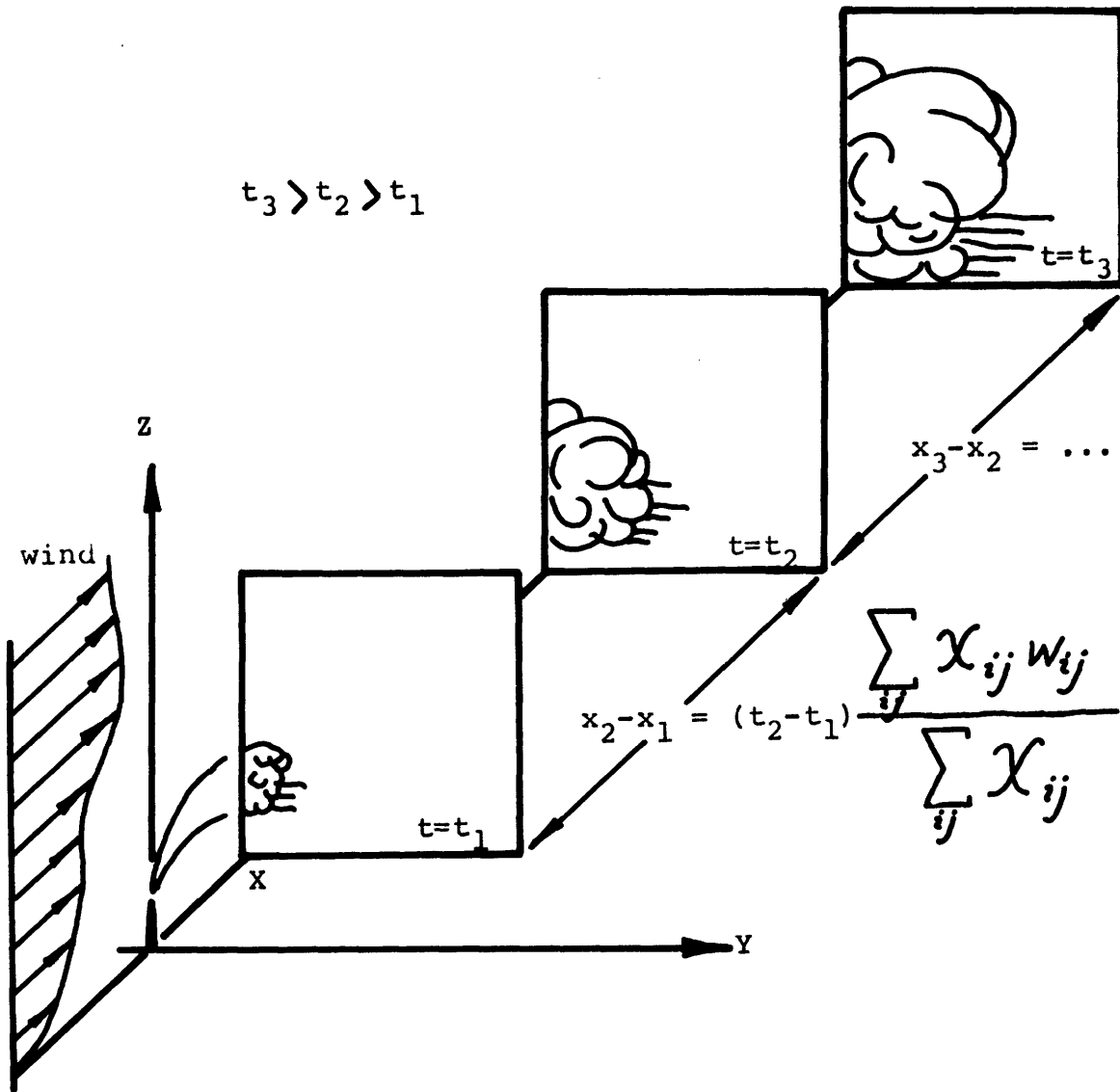


Fig. 3.3.3.1 Reconstruction of the Three-dimensional Plume. Wind vectors as a function of height are shown.

the full steady state plume, i.e., the time of the computer simulation must be related to a downwind distance. The choice is difficult because the wind profile dictates that fluid elements at different heights will advect downwind at different rates. A simple approximation is that the advection velocity should be equal to the "pollutant averaged" wind speed:

$$\frac{\Delta x}{\Delta t} = \frac{\int_0^{\infty} \int_0^{\infty} u(z) \chi(y, z) dy dz}{\int_0^{\infty} \int_0^{\infty} \chi(y, z) dy dz} \quad (3.96)$$

The finite difference form of Eq. 3.96 is written in Fig. 3.3.3.1. The calculation of this quantity is performed in the "statistics package" of Sec. 3.3.7. A further refinement of the solution scheme is discussed in Sec. 6.2.1.

In practice, for plumes that are released from tall stacks, the amount of wind shear that the plume encounters is ordinarily moderate and does not greatly alter the plume behavior.

3.3.4 Property Data

The original VARR-II computer code allows for quadratic fitting of air property data versus temperature. In view of the fact that potential temperature is substituted for

temperature in moist simulations, the scheme of fitting property data to temperature must be examined. The air property data to be fitted includes density, specific internal energy, dynamic viscosity, thermal conductivity, and heat capacity at constant pressure. The coefficients of the quadratic fits for dry air data⁴³ are listed in Table 3.3.4.1, along with the quadratic form that they are used in. The effect on the property value of the substitution of θ or θ_v for \tilde{T} is considered next.

The use of \tilde{T} or \tilde{T}_v in the perfect gas law yields, by definition, the correct density of a dry or moist parcel of air, respectively. A quadratic fit of the perfect gas law over a small temperature range of interest would yield essentially exact results for the density as well. The calculation of densities with θ or θ_v substituted into the formula for \tilde{T} is also appropriate because θ or θ_v vary from \tilde{T} by very little compared to the absolute temperature. Recall that θ or θ_v is used in the problem formulation to eliminate the compressible nature of the hydrostatic atmosphere. The relevant density variations in the momentum equation are the relative density variations, and the criteria for the use of, say θ_v for T is that

$$\frac{\rho(\tilde{T}) - \rho(T_o)}{\rho(T_o)} \approx \frac{\rho(\theta_v) - \rho(\theta_{vo})}{\rho(\theta_{vo})} \quad (3.97)$$

Table 3.3.4.1 Property Values of Air

<u>i</u>	<u>symbol</u>	<u>property</u>	<u>units</u>	<u>a_i</u>	<u>b_i</u>	<u>c_i</u>
1	ρ	density	lb _m /ft ³	2.0×10^{-7}	-1.78×10^{-4}	0.086394
2	I	internal energy	BTU/lb _m	4.3×10^{-6}	1.71×10^{-1}	78.357
3	ν	dynamic viscosity	lb _m /ft·sec	-1.0×10^{-6}	1.92×10^{-3}	1.0932
4	K	thermal conductivity	BTU/ft sec ^o R	0	2.59×10^{-5}	0.01313
5	C _p	heat capacity at constant pressure	BTU/lb _m ^o R	0	-2.00×10^{-6}	0.24008

$$\text{property } i = a_i (T-460^{\circ}\text{R})^2 + b_i (T-460^{\circ}\text{R}) + c_i$$

(T in ^oR)

with a similar condition for θ in dry simulations. This relation holds with about four percent accuracy for the most extreme cases encountered in this work.

The specific internal energy is originally fitted versus T . Again, the fact that θ or θ_v is close to T compared to the absolute temperature allows them to be interchanged without significant error. The specific internal energy is accurate to about 4 percent under this substitution.

The values of dynamic viscosity and thermal conductivity are important only if the flow becomes laminar. None of the simulations in this work are expected to encounter regions of laminar flow, so the fitted values of molecular viscosity and thermal conductivity are unimportant.

The specific heat varies slowly with temperature, and the substitution of θ or θ_v for T results in only a 0.02 percent error for typical cases.

The necessary property data for equilibrium conditions of water vapor and cloud liquid water are included in Secs. 3.2.2.3 and 3.2.2.4. The inclusion of water in the simulations is assumed to have a negligible effect on the property data of the air-water mixture, except for the density, which is corrected through the use of the virtual temperature.

3.3.5 Mesh Initialization and Boundary Conditions

3.3.5.1 Input Profiles

Seven vertical profiles are required for a simulation. Five of the profiles serve to specify the boundary conditions on the computer mesh, one profile (the mean wind speed) is needed by the statistics package, and one profile (the hydrostatic pressure) is needed by the equilibrium moisture thermodynamics model. The required profiles are listed in Table 3.3.5.1. Each vertical profile consists of a set of values that are representative of the cell-centered temperature, wind speed, etc. The number of values is obviously equal to the number of fluid cells in the z-direction. The extension of the model to time-dependent vertical profiles is considered in Sec. 6.2.2.

3.3.5.2 Boundary Conditions

Boundary conditions must be specified for each of eight variables on the four walls of the computer mesh. The walls of the computer mesh are numbered in Fig. 3.3.5.1. Wall #1 is in the plume centerline with the real computer simulation to its left. For this purpose, wall #1 is a free-slip solid wall. Wall #4 always represents the earth, and is specified to be a no-slip wall. The earth is assumed to be a perfect

Table 3.3.5.1
Required Input Profiles

<u>Atmospheric Profile</u>	<u>Units</u>
virtual potential temperature	$^{\circ}\text{F}$
water vapor density	lb_m/ft^3
cloud liquid water density	lb_m/ft^3
eddy viscosity	ft^2/sec
turbulence kinetic energy	ft^2/sec^2
mean wind speed ^A	ft/sec
hydrostatic pressure ^B	millibars

- A. The mean wind speed is required by the statistics package of Sec. 3.3.7.
- B. The hydrostatic pressure is required by the equilibrium moisture thermodynamics model of Sec. 3.2.2.3.

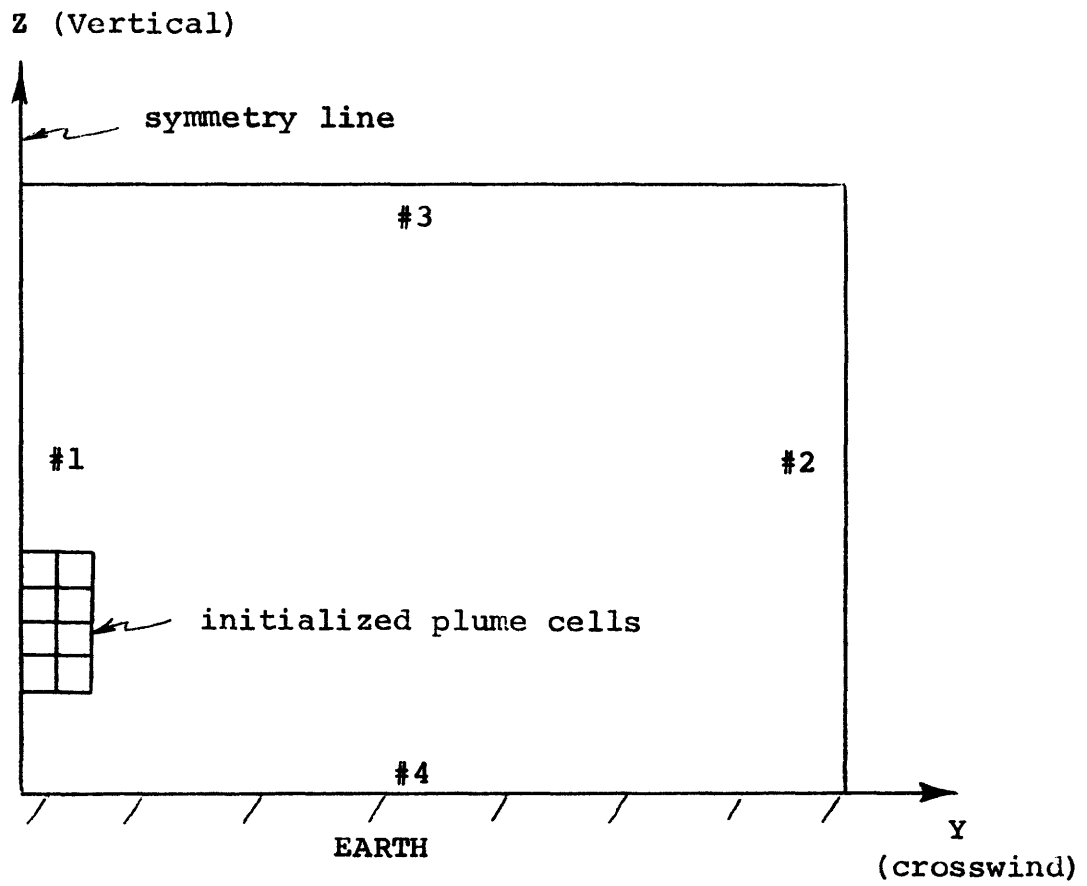


Fig. 3.3.5.1 Wall Numbering Scheme

reflector of pollutant and humidity in this work. This assumption could be easily modified to account for deposition of pollutant, sources of humidity, etc., for any case of specific interest. Walls #2 and #3 are chosen to be sufficiently far away from the plume so that negligible error is introduced in making them solid and free-slip. In practice, the plumes rise toward wall #3 and begin to deflect when their 10% boundary intersects the wall. This serves as a rough criterion on when to stop the computer simulation.

A summary of the boundary conditions is found in Table 3.5.5.2. The solid-wall, no-slip and free-slip conditions are found in the specification of the two velocity components, v and w . The reflective conditions are due to the "perfect reflecting walls" assumption; they are foregone at wall #2 for the five variables that are known as functions of height.

3.3.5.3 Mesh Initialization

The entire computer mesh in Fig. 3.3.5.2 is first initialized with the known atmospheric profiles of virtual potential temperature, eddy viscosity, turbulence kinetic energy, water vapor density, and cloud liquid water content. The entire mesh is initialized with a single background value of pollutant, and the velocity field is initialized to be at rest. The plume cells in the figure are then initialized by volume-averaging

Table 3.3.5.2

Boundary Conditions

<u>Variable</u>	<u>Wall #1</u>	<u>Wall #2</u>	<u>Wall #3</u>	<u>Wall #4</u>
y-velocity, v	S	S	F	N
z-velocity, w	F	F	S	S
virtual potential temperature	R	*	R	R
eddy viscosity	R	*	R	R
turbulence kinetic energy	R	*	R	R
pollutant	R	R	R	R
water vapor density	R	*	R	R
liquid water density	R	*	R	R

S--solid wall (normal velocity = 0)

N--no-slip (tangent velocity = 0)

F--free-slip (normal derivative of tangent velocity = 0)

R--reflective (normal derivative = 0)

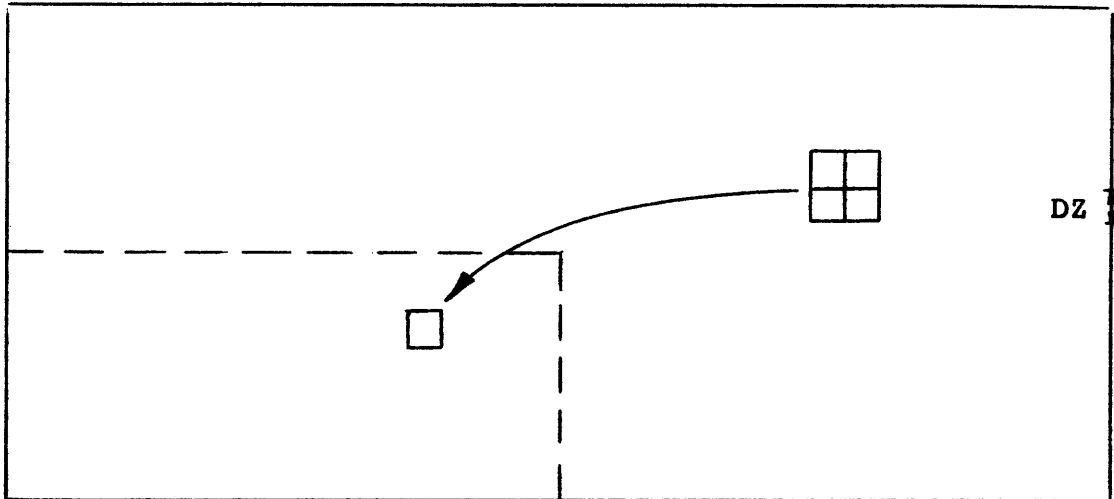
*--specified as profiles of height (z)

the plume sources of energy, pollutant, and moisture over those cells, using mean wind speed at that height to define the depth of the cells swept out in one second. The initial eddy viscosity and turbulence kinetic energy in the plume cells are set to about 100 times that of the surrounding atmosphere--in practice, the plume turbulence values very quickly relax into values that are consistent with the flow field. No initial volume-averaged momentum is given to the plume cells. Instead of this, an effective stack height increment due to momentum is added to the actual stack height in specifying the location of the center of the plume cells.

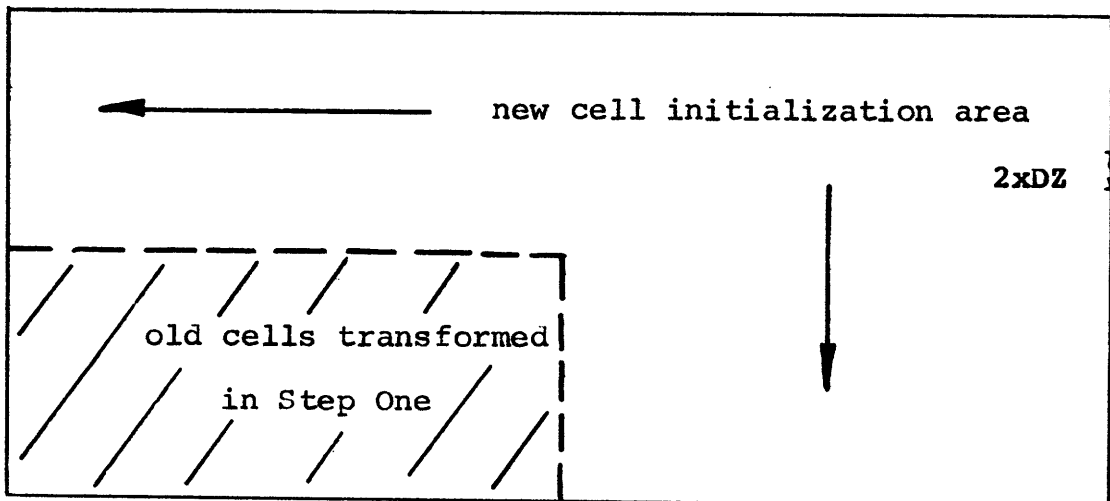
3.3.6 Mesh Coarsening Capability

Model programming has been undertaken to allow the mesh spacing to be doubled periodically during the simulations, while keeping the same number of fluid cells on the whole computer mesh. The motivation for this is the desire to keep the growing plume cross section away from the unphysical (solid wall) top and right mesh boundaries. When the simulation is "coarsened," the mesh spacing doubles, which reduces the plume cross section by a factor of four. The calculation is restarted, and the simulation proceeds on a mesh that has four times the area of the old mesh, but the same number of fluid cells.

The coarsening procedure is outlined in Fig. 3.3.6.1. In



(a) Step One - Four Cell Averaging



(b) Step Two - Initialization of New Cells

Figure 3.3.6.1 Mesh Coarsening Procedure Steps

a first step (a) the entire mesh is swept over, four cells at a time. Note that the number of cells vertically or horizontally must be even in order to do this. The fluid variables in these four cells are averaged in the following way: the cell specific internal energy, momenta, and turbulence kinetic energy are mass-averaged over the four cells, since these variables are defined on a per unit mass of air basis. The cell pollutant, eddy viscosity, and moisture variables are simply averaged over the four cells, since these variables are not defined on a per unit mass of air basis. The cell pressure is set to zero, which conforms with the usual starting guess procedures in running VARR-II. The average cell made up from these four cells is now stored in its proper place on the larger mesh, which is half of the distance to the origin vertically and horizontally. When the entire mesh has been swept, four cells at a time, the old mesh has now been relocated in the lower left corner, and is one-fourth of its old size.

In a second step (b) the remaining three-quarters of the mesh needs to be initialized. This "new" area is swept row-by-row in ascending order. The velocity field is assumed to be initially at rest, and the pressure field is initially set to zero. The remaining atmospheric state variables are all specified from a master library of profiles. When the "new" area has been initialized, the calculation is restarted with the

vertical and horizontal mesh spacings doubled.

The computer mesh may be coarsened up to five times during a simulation--this would result in a final mesh that is $2^5 \times 2^5 = 1024$ times as large as the original mesh. The five times are user specified, and need not take place at regular intervals.

3.3.7 Plume Statistics Package

At regular intervals specified by the user, the program calls on a statistics package to calculate a number of important plume statistics without printing out the data of the entire computer mesh. The quantities that are reported by the statistics package are listed in Table 3.3.7.1. The average plume advection velocity is the feature discussed in Sec. 3.3.3, and is defined in Eq. 3.96.

Table 3.3.7.1

Data Reported by the Plume Statistics Package

<u>Quantity</u>	<u>Units</u>
Time of Simulation	sec
Total Number of Problem Iterations	(none)
Current Number of Pressure Iterations	(none)
Current Time Step Size	sec
Center Height of Pollutant Field	ft
Total Specific Internal Energy on Mesh	BTU
Average Downwind Advection Velocity	ft/sec
Plume Downwind Distance	ft

4. DESCRIPTION OF ATMOSPHERIC TURBULENCE

4.1 Introduction

This chapter describes in detail how atmospheric turbulence is represented in the model. The description begins with the knowledge (e.g., from a set of measurements) of the common atmospheric variables as functions of height: the set includes the wind speed and direction, virtual potential temperature, water vapor density, and cloud liquid water density. The important processes that are responsible for the characteristic shapes of these profiles are outlined, and the concept of layers in the atmosphere arises naturally in the explanation of the interdependencies of the profiles. With a working knowledge of the dominant phenomena in the atmospheric layers, the problem of prescribing the atmospheric turbulence is undertaken. For the model in this work, the atmospheric turbulence is specified with profiles of eddy viscosity and turbulence kinetic energy. The relation of these two variables to the other profiles, and their inclusion into the model occupies most of this chapter.

4.2 Atmospheric Profiles of Wind, Temperature, and Humidity

The vertical atmospheric profiles considered in this work

are assumed to have been measured with some appropriate meteorological instruments over a flat terrain. For instance, a tower with a series of instruments at various heights would produce essentially pointwise values of the variables, which could then be linearly interpolated between the measurement heights to produce the full profiles. It is assumed that the measurements were time-averaged for at least 20 minutes so that there is very little time-dependence in the profiles. Alternatively, a radiosonde (balloon) ascent is commonly used for measuring vertical profiles, although the measurement averaging times are not long enough to completely average over the larger atmospheric eddies.

The measured atmospheric wind profiles have several common features. First, the atmospheric wind vanishes at the ground. This is in accord with the no-slip velocity boundary condition of real fluids. Second, the time-averaged (i.e., averaged over about 20 minutes) vertical velocity is very small at any height. This is because the very low frequency (of the order of 1 per day) vertical velocities are due to the synoptic scale subsiding or lifting motions associated with fronts; these velocities are usually only about 10 cm/sec. Because the average vertical velocities are small, the wind at any height is assumed to be parallel to the ground. Generally, the wind speed increases with height and commonly exhibits some turning with height--

especially in the first several hundred feet of elevation, where pressure gradient, Coriolis, and frictional forces are all important.

The fact that the wind vector may very roughly approximate a logarithmic profile,⁴⁴ an Ekman spiral,⁴⁵ or a thermal wind relation,⁴⁶ is only of minor interest here since the actual wind profile determines the behavior of an individual plume. In this work, the turning of the wind with height is not represented in the hydrodynamic simulations, although the prospect of including it is considered among the extensions of the model outlined in Sec. 6.2. Also, the difficulty of defining an average wind direction when there are only light, variable winds at a station dictates that the computer simulations are not expected to be accurate for winds of less than about 5 knots.

The temperature and humidity profiles directly provide the information about the local stability of vertical atmospheric and plume motions. No approximations to the temperature or humidity profiles are needed to incorporate them into the simulations. The temperature and humidity profiles are used to evaluate the virtual potential temperature profile: Note that in defining equations for virtual potential temperature (Eq. 3.53 and Eq. 3.67) the temperature, humidity, and pressure are required at any height. To this end the pressure profile could have been measured by itself, or calculated with any of

a number of approximations (dry hydrostatic, moist hydrostatic, various interpolations between points, etc.) Whatever assumptions are made, the pressure profile consistent with these assumptions must be input to the simulation where it is used to recalculate the correct temperature from the virtual potential temperature and humidity for the equilibrium moisture thermodynamics model.

4.3 Turbulence in the Planetary Boundary Layer

4.3.1 Introduction

The planetary boundary layer (PBL) is a boundary layer in a rotating, stratified, multi-component fluid whose moisture component can undergo changes of phase. Further, the boundary conditions on fluxes of momentum, sensible and latent heats, and radiant energy can vary greatly over large and small distances (i.e., distances that are large or small in comparison to the depth of the boundary layer), and are typically strongly coupled to the flow. Although a number of excellent reviews have been written⁴⁷⁻⁵⁷ at many levels of detail, the basic notions of turbulence in the planetary boundary layer are developed here with the aim of pointing out the limitations of the description of the PBL turbulence embodied in the computer simulations.

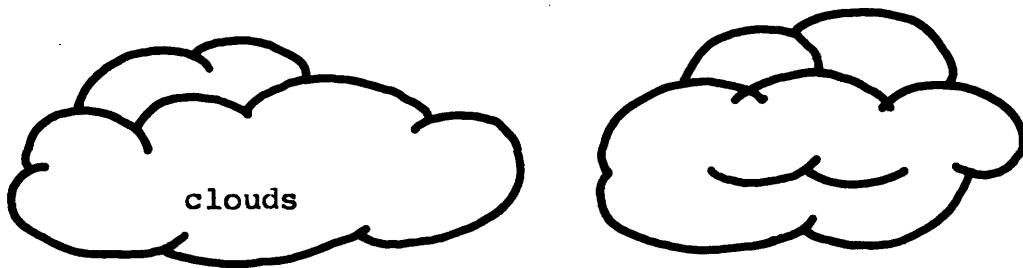
4.3.2 Layers in the PBL and Important Processes

Without much loss in generality, it is assumed in this work that all of the energy in turbulent atmospheric motions ultimately comes from the sun. Although it is possible to conceive of special situations where this is not quite true (for example, the turbulence near a busy expressway, much of which is caused by mechanical stirring and buoyant exhausts), the atmospheres which are encountered in this work are free of man-made turbulence, except for the buoyant plumes themselves! For the purposes of illustration, the solar energy which produces atmospheric turbulence may be divided into two streams: (1) that part of the solar energy that produces the large synoptic-scale pressure patterns on the earth, which in turn drives the wind and produces turbulence in regions of the atmosphere of sufficiently large wind shear, and (2) that part of the solar energy that produces the local thermal stratification of the atmosphere, which in turn produces turbulence in regions of sufficiently unstable stratification. The turbulence that is produced by the first stream is called "mechanically produced turbulence," and that produced by the second stream is called "buoyancy produced turbulence." The thermal stratification that is produced by the second stream is usually formulated in terms of virtual potential temperature, so that

moisture and latent heat effects are naturally included in the "buoyancy produced turbulence." There are two mechanisms that destroy atmospheric turbulence: (1) viscous dissipation, which is always at work in a turbulent flow, and (2) buoyant destruction, which is present in regions of stable thermal stratification.

From the preceding discussion it is expected that in a region in steady state the mechanisms of turbulence production and destruction will be balanced, and that the turbulence kinetic energy will maintain a value that is commensurate with the destruction rate. Very commonly in micrometeorological studies, the regions that these processes are studied in are simplified to layers, so that the description of atmospheric turbulence becomes one-dimensional--the single dimension is then height. The situation is illustrated in Fig. 4.3.2.1. In the uppermost layer of laminar flow, the strong geostrophic winds usually have very small wind shears with height, and are usually associated with stably stratified air, so that there is little or no turbulence. The next layer down usually is a region of buoyancy produced turbulence with only small wind shear--the buoyancy is typically from solar heating at the ground and latent heat release in cloud formation (clouds obviously affect the amount of solar heating at the ground, so that these effects are strongly coupled). The layer nearest

V_g
→
laminar (geostrophic) flow
(very small turbulence kinetic energy)



buoyancy \doteq dissipation
(small turbulence kinetic energy)

shear + buoyancy \doteq dissipation
(large turbulence kinetic energy)

—————
EARTH

Fig. 4.3.2.1 The Concept of Layers in the Planetary Boundary Layer. Atmospheric turbulence is assumed to be variable in one-dimension only in this figure. The turbulence is steady-state.

to the ground typically exhibits a lot of wind shear due to the no-slip condition at the ground, so that mechanically produced turbulence is present in addition to buoyant production, and turbulence kinetic energy is usually a maximum somewhere in this layer.

The particular illustration of atmospheric layers in Fig. 4.3.2.1 is certainly not unique. Many investigators have coined names for layers to illustrate different refinements on the processes in the PBL. Such terms as the surface layer, Ekman layer, subcloud layer, cloud layer, inner layer, outer layer, tower layer, convection layer, inversion layer, superadiabatic layer, and viscous sublayer are common, but they do not represent anything more sophisticated than treating the atmosphere as one-dimensional.

The prospect of treating the atmospheric state as two-dimensional--now including its downwind development as well as its profile with height--is considered in Sec. 5.4.1 in conjunction with the modeling of a fumigation episode.

4.3.3 Prescription of the Eddy Viscosity

The prescription of the eddy viscosity in the two-dimensional mesh of the crosswind alignment scheme of Fig. 3.3.2.1c is considered in this section. It was mentioned in Sec. 3.3.2

that the absence of any mean wind component (by definition) in the crosswind direction means that, away from the plume, and as far as the computer simulation is concerned, there is no explicit mechanical production of turbulence in the atmosphere. In fact, what takes place in the atmosphere is that the turbulence kinetic energy component, $\overline{u'^2}$, and the Reynolds stress, $\overline{u'w'}$, of the downwind x-z plane are feeding into the crosswind y-z plane turbulence kinetic energy component, $\overline{v'^2}$, and Reynolds stress, $\overline{v'w'}$, through the return to isotropy term in Eq. 3.40. For this work, the assumption is made that the return to isotropy term is very strong, so that the turbulence is isotropic. Experiments on atmospheric return to isotropy indicate that this assumption is reasonably good.⁵⁸ It is seen in the discussion of the results in Chapter Five that this is probably the most limiting assumption in the work with regard to being able to model real atmospheres. The eddy viscosity as a function of height in the downwind x-z plane is estimated from a number of prescriptions for eddy viscosity that are correlated from mean wind and temperature profiles, then the eddy viscosity in the crosswind y-z plane is assumed to be the same as in the x-z plane under the assumption of isotropy.

The incorporation of an ambient eddy viscosity profile on the simulation mesh finds two problems. First, any

arbitrary eddy viscosity imposed on the mesh cells at the start of the simulation will, in the absence of sufficient mechanical and buoyant production, rapidly decay down to the molecular kinematic viscosity. Second, the turbulence field inside the plume must be allowed to develop on its own. The method of incorporating the ambient eddy viscosity profile in light of these problems is as follows: to start the simulation, the cells outside of the initial plume cells are initialized with the eddy viscosity profile, depending on their height in the mesh. After each time step, each cell on the mesh is tested to see if it has fallen below the prescribed eddy viscosity profile at its height. If it has, its eddy viscosity is simply reset to the ambient value. If it has not fallen below the ambient value, presumably because either the plume-induced turbulence or the turbulently diffused turbulence from neighboring cells is dominating, then the cell eddy viscosity value is left alone. In this way, the far field always maintains the ambient atmospheric turbulence values, and the plume turbulence, if greater than the ambient turbulence, is left to develop on its own. Overall, this method has the effect of adding a non-uniform source term to the eddy viscosity equation--the term always adjusts itself to yield the original eddy viscosity in the far field, and to "turn itself off" if the plume turbulence is dominating. Mathematically, the

inequality

$$\sigma(y, z, t) \geq \sigma_{\text{library}}(z) \quad (4.1)$$

has been added to the equation set, where $\sigma_{\text{library}}(z)$ is the prescribed eddy viscosity profile as a function of height.

Before discussing the available prescriptions of eddy viscosity, it should be noted that the potentially most accurate method of prescribing the eddy viscosity for an individual release would be to actually measure it in the field--perhaps simply by estimating it from bivariate wind fluctuation data. The effort in this work to arrive at workable prescriptions from the micrometeorological literature is motivated by the total absence of these measurements in existing plume field data. The particular prescriptions that are recommended here are used only because they offer a simple way to estimate the eddy viscosity profile.

A number of prescriptions for the eddy viscosity in the outer boundary layer of the atmosphere as a function of height have been reviewed.⁵⁹⁻⁶⁴ A summary of the various prescriptions is presented in Table 4.3.3.1, where they are separated into two major groups--those that require wind speed and direction profiles, and those that do not. Those which do not require wind profiles as input are easier to use because the wind profiles need not be measured (e.g., with instrumented towers or

Table 4.3.3.1 Comparison of Eddy Viscosity Prescriptions

Atmospheric Stability in which the Prescription is Applicable

<u>Author(s)</u>	<u>Neutral</u>	<u>Stable</u>	<u>Unstable</u>
* * Prescriptions that require wind speed and direction versus height:			
Blackadar ⁵⁹	yes	no	no
Blackadar and Ching ⁶⁰	no	no	yes
Yamamoto and Shimanuki ⁶¹	yes	yes	yes
Nieuwstadt ⁶⁴	yes	yes	yes
Prescriptions that do not require wind profiles:			
O'Brien ⁶²	yes	yes	yes
Bornstein ⁶³	yes	yes	yes

balloons). However, they are not expected to be as accurate, since the wind profile has taken an ideal shape. All of the models in Table 4.3.3.1 are searched for applicability to neutral, stable, and unstable atmospheres.

It is recommended that if the wind speed and direction profiles have been measured, the prescriptions of Blackadar,^{59,60} and Yamamoto and Shimanuki⁶¹ should be used. If the wind speed and direction profiles have not been measured, the prescriptions of Bornstein⁶³ or O'Brien⁶² should be used. The prescription of Nieuwstadt⁶⁴ requires a substantial numerical analysis of the profiles and has not been tested.

Any of these prescriptions must be used with caution since all of them are only capable of providing an estimate to the eddy viscosity. The greatest difficulty in using these prescriptions is that they typically require values for quantities that were not measured, such as the heat flux at the ground, the roughness height, geostrophic velocity, etc.

4.3.4 Prescription of the Turbulence Kinetic Energy

The prescription of the turbulence kinetic energy (TKE) in the two-dimensional mesh of the crosswind alignment scheme of Fig. 3.3.2.1c is considered in this section. The turbulence kinetic energy suffers from exactly the same problem as the eddy viscosity in Sec. 4.3.3.: in the absence of explicit

buoyant and mechanical production of turbulence on the two-dimensional mesh, the turbulence kinetic energy would gradually decay away entirely. To satisfactorily avoid this problem, the concept of the turbulent "return to isotropy" is again invoked to allow the turbulent kinetic energy produced by the mean flow shearing and buoyancy to be fed into the crosswind motions. A turbulence kinetic energy profile is needed, so that it may maintain the turbulence for mesh cells that lack the sufficient turbulence production in exactly the same way that an eddy viscosity profile maintains the eddy viscosity for the mesh.

Ideally, the TKE profile should be measured or deduced from other profiles for an actual atmosphere. In fact, however, prescriptions for the turbulence kinetic energy from mean wind and temperature profiles are not generally available in the literature. The actual prescription of the turbulence kinetic energy profile in this work has had to come from the following, very approximate analysis of the transport equations.

Consider the TKE transport equation in a region away from the plume. The vertical and horizontal velocities, v and w , are zero, and the eddy viscosity, σ , and TKE, q , are functions of height, z , only; with the resulting expression being

$$\frac{\partial q}{\partial t} = \frac{4\alpha q^2}{\sigma} + \Gamma \frac{\partial}{\partial z} \left(\sigma \frac{\partial q}{\partial z} \right) \quad (4.2)$$

For a properly time-independent TKE, there must be a balance of dissipation and diffusion in Eq. 4.2; or

$$\frac{4\alpha q^2}{\sigma} = \Gamma \frac{\partial}{\partial z} \left(\sigma \frac{\partial q}{\partial z} \right) \quad (4.3)$$

Performing a scale analysis of the terms, noting that $\Gamma/4\alpha \sim 10$ and that the depth of the planetary boundary layer is taken equal to L_{eddy} , one obtains the result

$$q \sim 10 \frac{\sigma^2}{L_{eddy}^2} \quad (4.4)$$

For typical values in the atmosphere, $\sigma \sim 100 \text{ ft}^2/\text{sec}$ and $L_{eddy} \sim 10^3 \text{ ft}$, giving the value

$$\frac{q}{\sigma} \sim 10^{-3} \text{ sec}^{-1} . \quad (4.5)$$

Note that for a highly idealized picture of turbulence,⁶⁵ with eddies of a single size, L_{eddy} , and velocity, u_{eddy} ,

$$q \sim u_{eddy}^2 , \quad (4.6)$$

$$\sigma \sim u_{eddy} L_{eddy} , \quad (4.7)$$

and therefore

$$\frac{q}{\sigma} \sim \frac{u_{eddy}}{L_{eddy}} \quad [\text{sec}^{-1}] . \quad (4.8)$$

This states that q/σ is simply the inverse of the eddy turnover time. The scale analysis (Eq. 4.5) of the q transport equation shows that the choice $q \sim 10^{-3} \text{sec}^{-1} \sigma$ should roughly allow q to have a constant value. The fact that this choice of q agrees with the eddy turnover time of roughly the most diffusive atmospheric eddies⁶⁶ (10^3 seconds, or about 15 minutes) lends support to the idea that σ and q have been chosen consistently in this scheme.

The crude specification of $q_{\text{library}}(z)$ has been found to be satisfactory in this work primarily because the turbulence kinetic energy only indirectly influences the eddy viscosity, so that errors in estimating TKE are tolerated much more than the errors in estimating the eddy viscosity. The preceding analysis, since it is a scale analysis, only provides a very approximate estimate of the turbulence kinetic energy profile. Mathematically, the inequality

$$q(y,z,t) > q_{\text{library}}(z) = 10^{-3} \text{sec}^{-1} \sigma_{\text{library}}(z) \quad (4.9)$$

has been added to the equation set, where $q_{\text{library}}(z)$ is the prescribed turbulence kinetic energy profile as a function of height.

5. CARD INPUT AND SAMPLE PROBLEMS

The VARR-II⁴⁰ computer code has been modified for the modeling of buoyant plumes in turbulent, stratified atmospheres. This chapter is intended to illustrate the use of the modified code for users that are already familiar with the VARR-II code. Users that are not familiar with VARR-II should consult the VARR-II Users' Guide.⁴⁰ All users should note that a previous alteration⁶⁸ of the VARR-II code from CDC to IBM machines has removed the extensive film plotting routines (Sec. III.C in the VARR-II Users' Guide), and has also removed the packing of the cell flag index (Sec. III.F). The current modifications have not updated the program tape dump and restart capability (Sec. III.D), although this could be re-established with a minimal amount of programming.

The remainder of this chapter will discuss the alterations to the input data cards found in Sec. III.B of the VARR-II Users' Guide⁴⁰, and then several numerical examples are presented.

5.1 Overall Program Support

The modified program has a moderately larger storage requirement than the previous code, but the program support devices are the same. The code now stores 25 variables for each fluid cell (real or imaginary), where the previous code only stored 19. In the current version, the total program storage for a 20 x 20 (real) cell mesh is about 175K bytes of CPU. The program reads input on device 5 in card format (when IVDI=5 in Statement No. 94 in Appendix D), and writes output on device 6 (when IVDØ=6

in Statement No. 95 in Appendix D). Device 6 should be a line printer since nearly the full 120 characters per line are used. Of course, disc, mag tape, or microfiche could be used instead of a line printer.

Running time in CPU is, of course, dependent on the time step size in the problems. The time step size is selected by the program at each time step, and is usually from one-tenth of a second to several seconds. The selection of a time step size is performed by the code.⁶⁷ where it always chooses the smallest step size from a choice of a diffusion condition,

$$DT = \frac{TSTEP}{\max(\sigma) \left(\frac{1}{DY^2} + \frac{1}{DZ^2} \right)}, \quad (5.1)$$

a Courant condition,

$$DT = \frac{TSTEP \min(DY, DZ)}{\max(v, w)}, \quad (5.2)$$

or a simple rate of change condition,

$$\frac{.2 \max(v, w)}{(\max(v, w) - \max(v_{old}, w_{old})) + 10^{-6}}, \quad (5.3)$$

where TSTEP in the VARR-II Users' Guide has a value of 0.25. As a practical matter, it is found that the time steps have to be reduced beyond these conditions by about a factor of 25 for the mesh cell sizes encountered in this work. This 25-fold reduction is accomplished by giving TSTEP a value of 0.01

(note that Eq. 5.3 is virtually never the most limiting step size). This allows the code to conserve energy in the computer mesh cells within an acceptable tolerance. The non-conservation of energy arises from the first order accuracy of the differencing scheme for the advection terms. Full donor cell differencing of the advection terms is found to give the best answers in the simulations--less than full donor cell differencing produces noticeable nonlinear instabilities in the flow. Running times on the IBM370/168 are usually about 10 to 15 minutes per thousand time steps.

5.2 Card Input Decks

The generation of input decks is considered in detail in the Appendices, where the additional input variables are defined and the detailed card formats are listed. Many of the input variables are discussed in Section 3.3 and in Chapter 4. To illustrate several different problems, three input decks are listed in the following sections..

5.2.1 The Dry, Buoyant Line-Thermal

Card input for the dry, buoyant line-thermal is listed in Table 5.2.1. Briefly, the problem simulates the rise of an initially quiet, warm parcel of air in a neutrally stratified dry atmosphere. Results from this problem are given as a sample problem in Sec. 5.3.1.

5.2.2 LAPPES⁵ Plume of 20 October 1967

Card input for the essentially dry, buoyant plume from the Keystone #1 combustion stack is listed in Table 5.2.2.

Table 5.2.1 Card Input for the Dry, Buoyant
Line-Thermal (Continued)

86.9028	0.001	1.0	1000.00	1.00	0037
86.9028	0.001	1.0	1000.00	1.00	0038
86.9028	0.001	1.0	1000.00	1.00	0039
86.9028	0.001	1.0	1000.00	1.00	0040
86.9028	0.001	1.0	1000.00	1.00	0041
86.9028	0.001	1.0	1000.00	1.00	0042
86.9028	0.001	1.0	1000.00	1.00	0043
86.9028	0.001	1.0	1000.00	1.00	0044
86.9028	0.001	1.0	1000.00	1.00	0045
86.9028	0.001	1.0	1000.00	1.00	0046
86.9028	0.001	1.0	1000.00	1.00	0047
86.9028	0.001	1.0	1000.00	1.00	0048
86.9028	0.001	1.0	1000.00	1.00	0049
86.9028	0.001	1.0	1000.00	1.00	0050
86.9028	0.001	1.0	1000.00	1.00	0051
					0052

-1

Briefly, the problem simulates the behavior of the plume emanating from an 800 ft tall stack at about 7 A.M. Eastern Time. The plume and ambient weather were documented in the LAPPES study⁵ (Volume 2). Results from this problem are presented as a sample problem in Sec. 5.3.2. This input deck is included to illustrate the input of a pollutant (here SO₂ in gm/ft³), and to illustrate the input of available wind speed and temperature profiles, and the inclusion of ambient atmospheric turbulence profiles. The ambient turbulence in the neutral layer (above 350 m elevation) is calculated from Blackadar's prescription.⁵⁹ The ambient turbulence in the stable layer (below 350 m elevation) is simply Blackadar's prescription⁵⁹ suppressed by a factor of 100 to make a rough account of the suppression of the turbulence by the stable stratification. Comparisons between the numerical simulations and the LAPPES experiments are found in MIT-EL 79-002.

5.2.3 Moist, Buoyant Line-Thermal

Card input for the moist, buoyant line-thermal is listed in Table 5.2.3. Briefly, the problem simulates the rise of a very nearly saturated warm parcel of air in a cool environment. As the parcel begins to rise, its temperature falls rapidly and moisture begins to condense within a few seconds. This input deck is included to illustrate the input of moisture

Table 5.2.3 Card Input for the Moist, Buoyant
Line-Thermal (Continued)

86.9028	0.001	1.0	975.0	0037
86.9028	0.001	1.0	970.0	0038
86.9028	0.001	1.0	965.0	0039
86.9028	0.001	1.0	960.0	0040
86.9028	0.001	1.0	955.0	0041
86.9028	0.001	1.0	950.0	0042
86.9028	0.001	1.0	945.0	0043
86.9028	0.001	1.0	940.0	0044
86.9028	0.001	1.0	935.0	0045
86.9028	0.001	1.0	930.0	0046
86.9028	0.001	1.0	925.0	0047
86.9028	0.001	1.0	920.0	0048
86.9028	0.001	1.0	915.0	0049
86.9028	0.001	1.0	910.0	0050
86.9028	0.001	1.0	905.0	0051
				0052

-1

variables. Temperatures must now be interpreted as virtual potential temperatures since there is an appreciable amount of moisture in the cells. The absolute pressure profile is not a real profile, but simply is an estimated profile. In practice, the unstable nature of the explicit differencing of the moisture model imposes a very small time step on the problem (about 100 times smaller than usual). Results from this calculation are not given as a sample problem because of this restriction.

5.3 Sample Problem Results

The interpretation of the sample problem output listing is illustrated in Fig. 5.3.1. Each box in the figures that follow Fig. 5.3.1 represents an individual fluid cell. A map of the entire mesh cell storage is produced by the VRPRT subroutine. Only a small region of the entire problem is found in each of the figures--the figures are roughly centered on the regions of strongest flow.

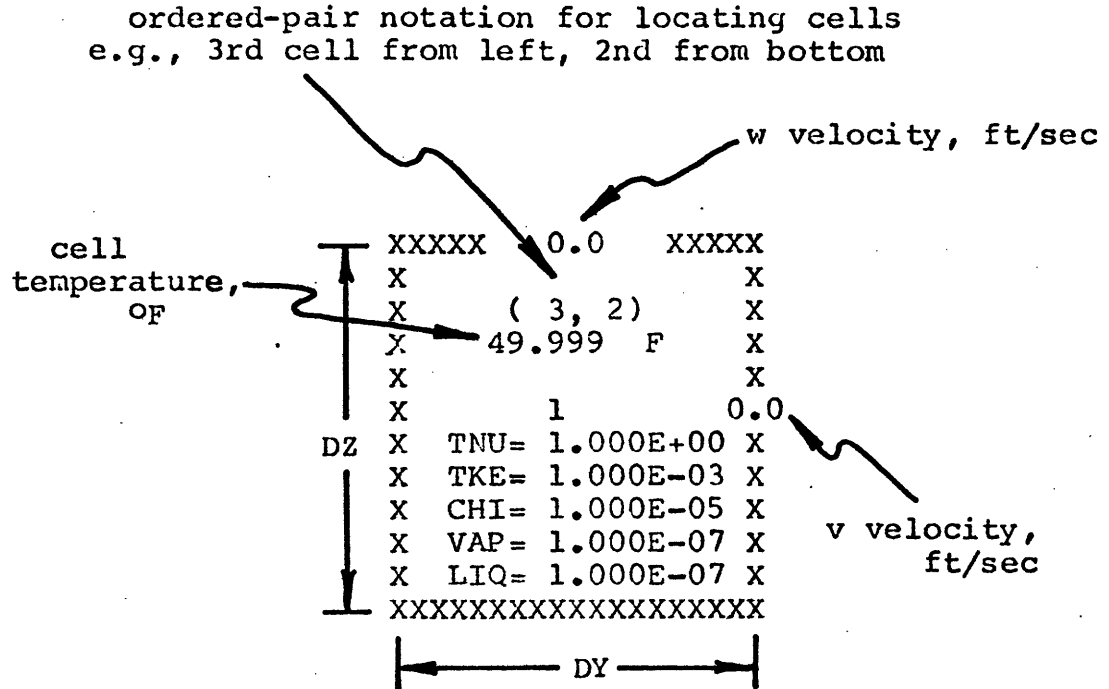
5.3.1 The Dry, Buoyant Line-Thermal

Results from the dry, buoyant line-thermal are presented in Figures 5.3.2 to 5.3.5. The moisture values may be disregarded in the figures. A further discussion of the results is found in MIT-EL 79-002.

5.3.2 LAPPES⁵ Plume of 20 October 1967

Results from the tall stack of the Keystone plant are presented in Fig. 5.3.6. Only the mesh cells at the beginning

of the simulation are shown. The plume several kilometers downwind extends over many cells and is discussed further in MIT-EL 79-002.



TNU is eddy viscosity in ft^2/sec
TKE is turbulence kinetic energy in ft^2/sec^2
CHI is pollutant concentration in lbm/ft^3
VAP is water vapor density in $\text{lbm H}_2\text{O}/\text{ft}^3$
LIQ is liquid water density in $\text{lbm H}_2\text{O}/\text{ft}^3$

Fig. 5.3.1. Key to Cellwise Quantities for Figs. 5.3.2, 5.3.3, 5.3.4, 5.3.5, and 5.3.6.


```

XXXXX 2.792 XXXXXXXXX 1.040 XXXXXXXXX 0.609 XXXXXXXXX 0.168 XXXXXXXXX -0.170 XXXXX
X      X      X      X      X      X      X      X      X      X
X      ( 2, 8) X      ( 3, 8) X      ( 4, 8) X      ( 5, 8) X      ( 6, 8) X
X      50.809 F X      50.137 F X      50.082 F X      49.999 F X      49.736 F X
X      X      X      X      X      X      X      X      X      X
O      1      1.592      1      1.860      1      1.545      1      1.118      1      0.843
X TNU= 5.087E+00 X TNU= 2.169E+00 X TNU= 1.658E+00 X TNU= 2.012E+00 X TNU= 1.370E+00 X
X TKE= 4.702E-01 X TKE= 1.135E-01 X TKE= 2.026E-02 X TKE= 6.234E-03 X TKE= 2.047E-03 X
X CHI= 4.895E-02 X CHI= 1.078E-02 X CHI= 1.448E-03 X CHI= 1.383E-04 X CHI= 1.682E-05 X
X VAP= 2.000E-07 X VAP= 2.000E-07 X VAP= 2.000E-07 X VAP= 2.000E-07 X VAP= 2.000E-07 X
X LIQ= 0.0 X LIQ= 0.0 X LIQ= 0.0 X LIQ= 0.0 X LIQ= 0.0 X
XXXXX 5.963 XXXXXXXXX 1.573 XXXXXXXXX 0.074 XXXXXXXXX -0.752 XXXXXXXXX -0.714 XXXXX
X      X      X      X      X      X      X      X      X      X
X      ( 2, 7) X      ( 3, 7) X      ( 4, 7) X      ( 5, 7) X      ( 6, 7) X
X      52.397 F X      50.927 F X      50.165 F X      49.888 F X      49.999 F X
X      X      X      X      X      X      X      X      X      X
O      1      1.790      1      2.327      1      1.898      1      1.345      1      0.966
X TNU= 1.364E+01 X TNU= 6.094E+00 X TNU= 2.564E+00 X TNU= 1.746E+00 X TNU= 1.560E+00 X
X TKE= 1.420E+00 X TKE= 5.864E-01 X TKE= 1.550E-01 X TKE= 3.042E-02 X TKE= 5.690E-03 X
X CHI= 1.422E-01 X CHI= 5.442E-02 X CHI= 1.527E-02 X CHI= 2.390E-03 X CHI= 2.249E-04 X
X VAP= 2.000E-07 X VAP= 2.000E-07 X VAP= 2.000E-07 X VAP= 1.999E-07 X VAP= 2.000E-07 X
X LIQ= 0.0 X LIQ= 0.0 X LIQ= 0.0 X LIQ= 0.0 X LIQ= 0.0 X
XXXXX 9.535 XXXXXXXXX 2.644 XXXXXXXXX -0.778 XXXXXXXXX -1.852 XXXXXXXXX -1.471 XXXXX
X      X      X      X      X      X      X      X      X      X
X      ( 2, 6) X      ( 3, 6) X      ( 4, 6) X      ( 5, 6) X      ( 6, 6) X
X      52.903 F X      51.870 F X      50.733 F X      50.137 F X      50.006 F X
X      X      X      X      X      X      X      X      X      X
O      1      0.651      1      1.127      1      0.740      1      0.562      1      0.313
X TNU= 1.802E+01 X TNU= 1.130E+01 X TNU= 4.335E+00 X TNU= 1.775E+00 X TNU= 1.980E+00 X
X TKE= 1.815E+00 X TKE= 1.200E+00 X TKE= 3.780E-01 X TKE= 7.838E-02 X TKE= 1.715E-02 X
X CHI= 1.763E-01 X CHI= 1.146E-01 X CHI= 4.295E-02 X CHI= 8.167E-03 X CHI= 9.445E-04 X
X VAP= 1.999E-07 X VAP= 2.000E-07 X VAP= 2.000E-07 X VAP= 2.000E-07 X VAP= 2.000E-07 X
X LIQ= 0.0 X LIQ= 0.0 X LIQ= 0.0 X LIQ= 0.0 X LIQ= 0.0 X
XXXXX 10.633 XXXXXXXXX 3.637 XXXXXXXXX -1.545 XXXXXXXXX -2.236 XXXXXXXXX -1.998 XXXXX
X      X      X      X      X      X      X      X      X      X
X      ( 2, 5) X      ( 3, 5) X      ( 4, 5) X      ( 5, 5) X      ( 6, 5) X
X      52.119 F X      51.607 F X      50.324 F X      50.096 F X      49.943 F X
X      X      X      X      X      X      X      X      X      X
O      1      -1.157      1      -1.622      1      -1.372      1      -0.988      1      -0.833
X TNU= 1.677E+01 X TNU= 1.198E+01 X TNU= 2.832E+00 X TNU= 1.397E+00 X TNU= 1.922E+00 X
X TKE= 1.643E+00 X TKE= 1.242E+00 X TKE= 2.058E-01 X TKE= 3.337E-02 X TKE= 8.061E-03 X
X CHI= 1.300E-01 X CHI= 1.046E-01 X CHI= 2.520E-02 X CHI= 2.410E-03 X CHI= 1.479E-04 X
X VAP= 2.000E-07 X VAP= 1.999E-07 X VAP= 2.000E-07 X VAP= 2.000E-07 X VAP= 2.000E-07 X
X LIQ= 0.0 X LIQ= 0.0 X LIQ= 0.0 X LIQ= 0.0 X LIQ= 0.0 X
XXXXX 8.533 XXXXXXXXX 2.676 XXXXXXXXX -1.061 XXXXXXXXX -1.458 XXXXXXXXX -1.665 XXXXX
X      X      X      X      X      X      X      X      X      X
X      ( 2, 4) X      ( 3, 4) X      ( 4, 4) X      ( 5, 4) X      ( 6, 4) X
X      50.858 F X      50.394 F X      50.061 F X      49.902 F X      49.811 F X
X      X      X      X      X      X      X      X      X      X
O      1      -1.958      1      -2.552      1      -2.173      1      -1.733      1      -1.269
X TNU= 1.359E+01 X TNU= 1.141E+01 X TNU= 4.348E+00 X TNU= 2.004E+00 X TNU= 2.577E+00 X
X TKE= 1.267E+00 X TKE= 8.776E-01 X TKE= 1.592E-01 X TKE= 1.617E-02 X TKE= 8.188E-03 X
X CHI= 5.792E-02 X CHI= 3.061E-02 X CHI= 8.101E-03 X CHI= 5.101E-04 X CHI= 2.975E-05 X
X VAP= 2.000E-07 X VAP= 2.000E-07 X VAP= 2.000E-07 X VAP= 2.000E-07 X VAP= 1.999E-07 X
X LIQ= 0.0 X LIQ= 0.0 X LIQ= 0.0 X LIQ= 0.0 X LIQ= 0.0 X
XXXXX 4.668 XXXXXXXXX 1.477 XXXXXXXXX -0.350 XXXXXXXXX -0.614 XXXXXXXXX -0.739 XXXXX
X      X      X      X      X      X      X      X      X      X
X      ( 2, 3) X      ( 3, 3) X      ( 4, 3) X      ( 5, 3) X      ( 6, 3) X
X      49.978 F X      49.735 F X      49.714 F X      49.936 F X      50.103 F X
X      X      X      X      X      X      X      X      X      X
O      1      -1.689      1      -1.970      1      -1.765      1      -1.500      1      -1.166
X TNU= 5.732E+00 X TNU= 3.192E+00 X TNU= 2.453E+00 X TNU= 2.150E+00 X TNU= 2.200E+00 X
X TKE= 4.311E-01 X TKE= 1.307E-01 X TKE= 4.032E-02 X TKE= 7.152E-03 X TKE= 5.154E-03 X
X CHI= 6.642E-03 X CHI= 2.758E-03 X CHI= 9.150E-04 X CHI= 5.188E-05 X CHI= 1.138E-05 X
X VAP= 2.000E-07 X VAP= 1.999E-07 X VAP= 1.999E-07 X VAP= 2.000E-07 X VAP= 2.000E-07 X
X LIQ= 0.0 X LIQ= 0.0 X LIQ= 0.0 X LIQ= 0.0 X LIQ= 0.0 X
XXXXX 1.202 XXXXXXXXX 0.886 XXXXXXXXX 0.151 XXXXXXXXX 0.019 XXXXXXXXX -0.036 XXXXX
X      X      X      X      X      X      X      X      X      X
X      ( 2, 2) X      ( 3, 2) X      ( 4, 2) X      ( 5, 2) X      ( 6, 2) X
X      49.583 F X      50.061 F X      50.089 F X      49.995 F X      49.874 F X
X      X      X      X      X      X      X      X      X      X
O      1      -0.619      1      -1.082      1      -1.137      1      -1.113      1      -1.078
X TNU= 2.115E+00 X TNU= 2.726E+00 X TNU= 3.230E+00 X TNU= 2.270E+00 X TNU= 1.936E+00 X
X TKE= 2.472E-02 X TKE= 1.924E-02 X TKE= 1.210E-02 X TKE= 5.171E-03 X TKE= 3.723E-03 X
X CHI= 7.881E-05 X CHI= 2.391E-05 X CHI= 1.320E-05 X CHI= 1.038E-05 X CHI= 1.001E-05 X
X VAP= 1.998E-07 X VAP= 2.000E-07 X VAP= 2.000E-07 X VAP= 2.000E-07 X VAP= 1.999E-07 X
X LIQ= 0.0 X LIQ= 0.0 X LIQ= 0.0 X LIQ= 0.0 X LIQ= 0.0 X
XXXXX 0.0 XXXXXXXXX 0.0 XXXXXXXXX 0.0 XXXXXXXXX 0.0 XXXXXXXXX 0.0 XXXXX

```

Fig. 5.3.4. Plume Cross Section at 80 sec.
 DY = 100 ft, DZ = 200 ft.
 Disregard moisture values.

6. RECOMMENDATIONS FOR MODEL EXTENSIONS

6.1 Calculational Scheme to Include Wind Shear Effects

A brief overview of a plausible calculational scheme that would address one of the important effects of wind shear on the plume dynamics is discussed here. The effect is that of the dilution of the plume properties as the plume rises into progressively stronger winds. The process is sketched in Fig. 6.2.1.1, and is well-known to plume modelers. A constant release of pollutant (illustrated in Fig. 6.2.1.1), momentum, sensible heat, moisture, etc., diluted into air that moves with a velocity $u(z_0)$ will have a density proportional to the inverse of the velocity. A plume property that is released into a stronger wind, $u(z)$, will be correspondingly more dilute. This effect is important in buoyant plumes when the plume updrafts and downdrafts in the presence of a wind shear cause parcels of the plume to change their downwind advection rate. Clearly, the problem is fully three-dimensional (although it can be in steady state), but a very restrictive assumption may afford a useful recasting of the two-dimensional problem. This assumption is discussed next.

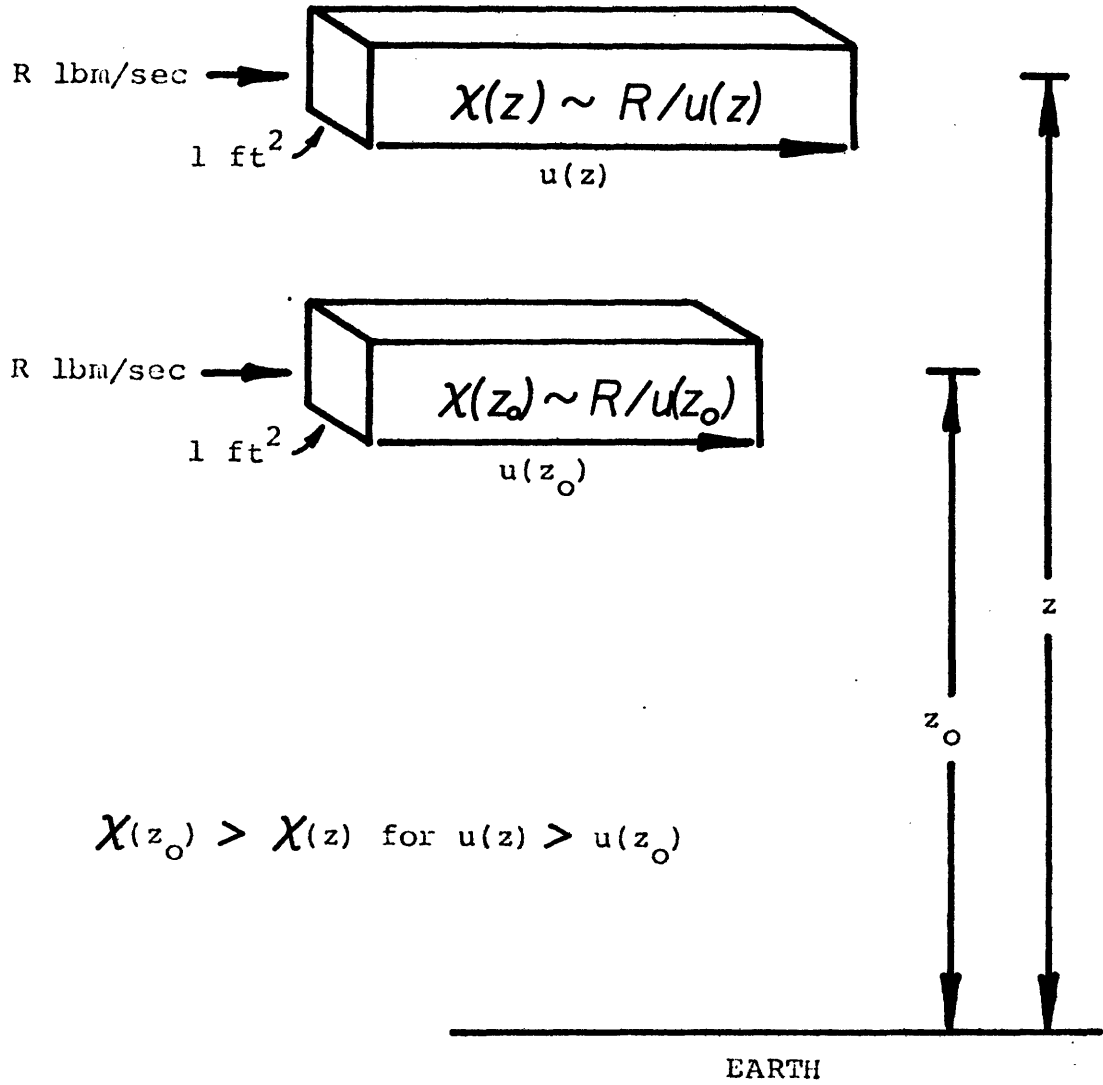


Fig. 6.2.1.1 Dilution of a Steady Release of Pollutant.

Consider the advection and turbulent diffusion of a pollutant in three dimensions (the results extend directly to momentum, sensible heat, etc.):

$$\frac{\partial \chi}{\partial t} + u \frac{\partial \chi}{\partial x} + v \frac{\partial \chi}{\partial y} + w \frac{\partial \chi}{\partial z} = \gamma_{\chi} \sigma \nabla^2 \chi \quad (6.1)$$

Assuming that the system is in steady state, we have

$$u \frac{\partial \chi}{\partial x} + v \frac{\partial \chi}{\partial y} + w \frac{\partial \chi}{\partial z} = \gamma_{\chi} \sigma \nabla^2 \chi \quad (6.2)$$

In the presence of a steady uniform wind field, u_0 , the first term is commonly interpreted as the time-rate-of-change for an observer moving with the wind, and is written as $\frac{\partial \chi}{\partial t_0}$, where $u_0 t_0 = x$. This contains the important assumption that the plume always has the downwind velocity u_0 --implying infinite accelerations at the stack exit, to be sure. In a strong wind field the downwind diffusion is commonly neglected with respect to the downwind advection, so the gradient operator has only y and z derivatives. If the wind field is allowed to have shears, then the first term may be represented as

$$u(z) \frac{\partial \chi}{\partial x} = \frac{u(z)}{u(z_0)} (u(z_0) \frac{\partial \chi}{\partial x}) = \frac{u(z)}{u(z_0)} \frac{\partial \chi}{\partial t_0} \quad (6.3)$$

where u_0 has been arbitrarily chosen to be $u(z_0)$. This interpretation allows the equation to be formulated as

$$\frac{\partial \chi}{\partial t_0} + \frac{u(z_0)}{u(z)} \left(v \frac{\partial \chi}{\partial y} + \frac{\partial \chi}{\partial z} \right) = \frac{u(z_0)}{u(z)} \gamma_{\chi} \sigma \left(\frac{\partial^2 \chi}{\partial y^2} + \frac{\partial^2 \chi}{\partial z^2} \right) \quad (6.4)$$

This equation holds the assumption that any parcel of air in the plume, when advected into a region of stronger wind, immediately takes on the local wind velocity and is correspondingly diluted. Note that it also causes parcels that are decelerated to concentrate their properties, which is physically unrealistic, but hopefully is not too serious an error since plume rise and updrafts are almost always stronger than downdrafts. The important feature that this scheme hopes to address is the dilution (usually by about 10 to 50 percent) of plume buoyancy, momentum, and moisture, which affect the plume dynamics. The procedure could be extended to every transport equation in the equation set--only the effect on the divergence condition in the fluid mechanics algorithm has not been studied. Its satisfaction would still be required as a constraint on the solution.

6.2 Calculational Scheme for Time-Dependent Release or Weather

The simulation of "mildly" time-dependent plumes can be made with the model. Essentially, the governing assumption here is that the prevailing weather or effluent properties

will advect downwind, and never affect the flow that precedes or follows it. The situation is developed in Fig. 6.2.2.1, where a stack is assumed to have a set of exit properties, Ω , that are piecewise-constant in time over periods of 100 sec. To reconstruct the behavior, an initial simulation with the properties at time t_0 , $\Omega(t_0)$ is made to 300 sec. The plume properties changed at time $t_0 + 100$ sec, so a second simulation is made with properties $\Omega(t_0 + 100)$ to 200 sec. Again the plume properties changed at time $t_0 + 200$ sec, so a third simulation is made with properties $\Omega(t_0 + 200)$ to 100 sec. The actual plume is then "cut and pasted" from the pertinent data in the simulations as shown at the bottom of the figure. The calculation is somewhat wasteful, since 600 sec of simulation produces only 300 sec of results--but the scheme surely saves time and storage over a fully three-dimensional calculation. Eventually, for sufficiently "strong" time-dependence the scheme becomes too laborious with respect to a three-dimensional calculation.

6.3 Cloud Microphysics Model

The limited success of the equilibrium moisture thermodynamics model is due to its explicit differencing. In short, the model is ignorant of the latent heat released in a current timestep, and it adjusts the equilibrium conditions without

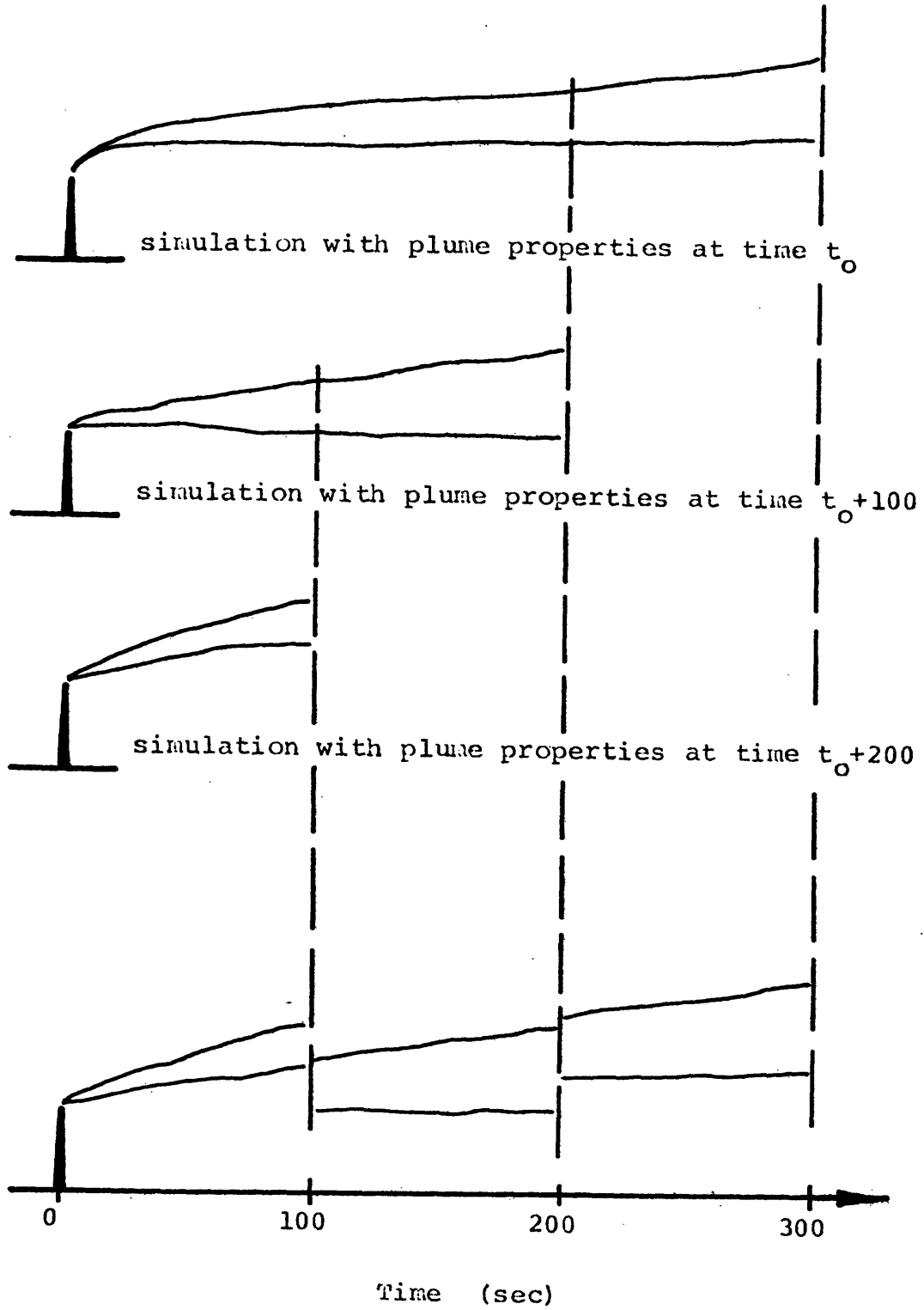


Fig. 6.2.2.1 Simulation of a Time-Dependent Plume in Steady-State Weather. Scheme is discussed in the text.

this knowledge. The resultant oscillations in the equilibrium conditions are not surprising, nor is the ability to control them with very small timesteps. If the calculation was made implicit--essentially iterating on the coupled latent heat release equation and Magnus' formula for liquid-vapor equilibrium--the timesteps could be relaxed back to their original size.

The prospect of incorporating a non-equilibrium moisture model is not investigated in this work. The limitations of the equilibrium model have not been sufficiently explored to justify the change at this point.

NOMENCLATURE

A_0	initial line-vortex area (ft ²)
C	experimental constant, 1.9
C_p	heat capacity at constant pressure (BTU/lb _m °R)
c_p^{moist}	heat capacity of moist air at constant pressure (BTU/lb _m °R)
DT	timestep size (sec)
DY	cell width (ft)
DZ	cell height (ft)
$e_{\text{sat}}(T)$	saturation vapor pressure of water (mb)
$E_{\chi}^{(i)}$	energy of the i^{th} decay channel from pollutant species χ (MeV)
$F_{\chi}^{(i)}$	fractional energy deposition for i^{th} radioactive decay channel from pollutant species χ
g	acceleration due to gravity (ft/sec ²)
g_i	vector acceleration due to gravity (ft/sec ²)
I	specific internal energy (BTU/lbm)
k	thermal conductivity (BTU/ft-sec-°R)
L	buoyancy parameter (ft)
L_{eddy}	eddy length scale (ft)
L_{vap}	latent heat of vaporization of water (BTU/lb _m)
N	experimental constant, 3.0
\tilde{p}	physically measurable pressure (millibars)
P	pressure perturbation about an adiabatic reference state (mb)
p_0	pressure in a quiet adiabatic atmosphere (mb)

\bar{p}	time average pressure perturbation (mb)
p'	fluctuating pressure perturbation (mb)
Pr	Prandtl number
$q, q(y, z, t)$	turbulence kinetic energy per unit lb_m (ft^2/sec^2)
$q_{library}^{(z)}$	prescribed turbulence kinetic energy profile (ft^2/sec^2)
Q	heat (BTU)
Q_H	heat emitted at stack exit (BTU/sec)
$R(T)$	plume radius as a function of time (ft)
R_{dry}, R_d	gas constant for dry air ($ft^3 mb/lb_m \text{ } ^\circ R$)
R_{vap}, R_v	gas constant for water vapor ($ft^3 mb/lb_m \text{ } ^\circ R$)
Sc_{liq}	Schmidt number for liquid water
Sc_{vap}	Schmidt number for water vapor
t, T	time (seconds)
t_o	x/u_o (sec)
T_*	time coordinate of virtual origin (sec)
\tilde{T}	physically measurable temperature ($^\circ R$)
T	temperature perturbation about an adiabatic reference state ($^\circ R$)
T_o	temperature in a quiet adiabatic atmosphere ($^\circ R$)
T_s	temperature of stack effluent ($^\circ R$)
\tilde{T}_v	virtual temperature ($^\circ R$)
T_{vo}	virtual temperature in a quiet adiabatic atmosphere ($^\circ R$)
u	downwind velocity (ft/sec)
u_o, U	windspeed, constant with height (ft/sec)
u_{eddy}	turbulent velocity scale in an eddy (ft/sec)
\tilde{u}_i, \tilde{u}_j	velocity (ft/sec)
u_i, u_j	velocity (ft/sec)

\bar{u}_i, \bar{u}_j	time average velocity (ft/sec)
u_i', u_j'	fluctuating velocity (ft/sec)
$\overline{u_i' u_j'}$	Reynolds stress tensor (ft ² /sec ²)
$\overline{u_i' \theta'}$	correlation of fluctuating velocity and temperature
$\overline{u_i' u_j' u_k'}$	triple correlation of fluctuating velocity (ft ³ /sec ³)
v	crosswind velocity (ft/sec)
V_g	geostrophic wind (ft/sec)
w	vertical velocity (ft/sec)
$W_{mol, \chi}$	molecular weight of the pollutant species (lb _m /lb _m -mole)
X	downwind distance (ft)
X_i, X_j	cartesian coordinate (ft)
y	crosswind distance (ft)
z	height (ft)
z_*	height coordinate of virtual origin (ft)

α, α_1	turbulence constants
γ_L	reciprocal turbulent Schmidt number for liquid water
γ_T	reciprocal turbulent Prandtl number for heat
γ_V	reciprocal turbulent Schmidt number for water vapor
γ_χ	reciprocal turbulent Schmidt number for pollutant
Γ	turbulence constant
Γ_l	turbulence constant
Γ_d	dry adiabatic lapse rate ($^{\circ}\text{R}/\text{ft}$)
ϵ_h	eddy diffusivity of heat (ft^2/sec)
ϵ_m	eddy diffusivity of momentum (ft^2/sec)
ϵ_χ	eddy diffusivity of pollutant (ft^2/sec)
$\tilde{\theta}$	potential temperature ($^{\circ}\text{R}$)
θ	potential temperature perturbation about an adiabatic reference state ($^{\circ}\text{R}$)
θ_o	potential temperature in a quiet adiabatic atmosphere ($^{\circ}\text{R}$)
$\bar{\theta}$	time average potential temperature ($^{\circ}\text{R}$)
θ'	fluctuating potential temperature ($^{\circ}\text{R}$)
θ_v	virtual potential temperature ($^{\circ}\text{R}$)
θ_{vo}	virtual potential temperature in a quiet adiabatic atmosphere ($^{\circ}\text{R}$)
$\bar{\theta}_v$	time average virtual potential temperature ($^{\circ}\text{R}$)
θ'_v	fluctuating virtual potential temperature ($^{\circ}\text{R}$)
(i) λ_x	decay constant for i^{th} radioactive decay channel from pollutant species χ (sec^{-1})

μ	dynamic viscosity ($\text{lb}_m/\text{sec ft}$)
ν	kinematic viscosity (ft^2/sec)
ρ_{dry}	density of dry air (lbm/ft^3)
ρ_{liq}	liquid water density (lbm/ft^3)
$\bar{\rho}_{\text{liq}}$	time average liquid water density (lbm/ft^3)
ρ'_{liq}	fluctuating liquid water density (lbm/ft^3)
ρ_s	density of stack effluent (lbm/ft^3)
ρ_{sat}	saturation water vapor density (lbm/ft^3)
ρ_{vap}	water vapor density (lbm/ft^3)
$\bar{\rho}_{\text{vap}}$	time average water vapor density (lbm/ft^3)
ρ'_{vap}	fluctuating water vapor density (lbm/ft^3)
$\sigma, \sigma(y, z, t)$	eddy viscosity (same as ϵ_m) (ft^2/sec)
$\sigma_{\text{library}}(z)$	prescribed eddy viscosity profile (ft^2/sec)
χ	pollutant density (lbm/ft^3)

LIST OF FIGURES AND TABLES

		page
Figure 3.1	Flow Field Orientation	35
Figure 3.2.2.3.1	Phase Diagram for Water Substance	51
Figure 3.2.2.3.2	Logic Diagram for the Equilibrium Moisture Calculation in a Single Cell during a Single Timestep	52
Figure 3.3.2.1a	Bent-Over Buoyant Plume with Ambient Thermal Stratification	56
Figure 3.3.2.1b	Mesh Alignment Appropriate for a Line Source Release	57
Figure 3.3.2.1c	Mesh Alignment Appropriate for a Point Source Release	57
Figure 3.3.3.1	Reconstruction of the Three-dimensional Plume. Wind vectors as a function of height are shown.	59
Figure 3.3.4.1	Property Values of Air	62
Table 3.3.5.1	Required Input Profiles	65
Figure 3.3.5.1	Wall Numbering Scheme	66
Table 3.3.5.2	Boundary Conditions	68
Figure 3.3.6.1	Mesh Coarsening Procedure Steps	70
Table 3.3.7.1	Data Reported by the Plume Statistics Package	73
Figure 4.3.2.1	The Concept of Layers in the Planetary Boundary Layer	80
Table 4.3.3.1	Comparison of Eddy Viscosity Prescriptions	85
Table 5.2.1	Card Input for the Dry, Buoyant Line-Thermal	93
Table 5.2.2	Card Input for the LAPPES ⁵ Plume of 20 October 1967	95
Table 5.2.3	Card Input for the Moist, Buoyant Line-Thermal	99

		page
Figure 5.3.1	Key to Cellwise Quantities for Figs. 5.3.2, 5.3.3, 5.3.4, 5.3.5, and 5.3.6.	103
Figure 5.3.2	Initialized Plume Cross Section at 0 sec.	104
Figure 5.3.3	Plume Cross Section at 20 sec.	105
Figure 5.3.4	Plume Cross Section at 80 sec.	106
Figure 5.3.5	Plume Cross Section at 200 sec.	107
Figure 5.3.6	Initialized Plume Cross Section for the Keystone No. 1 Stack on 20 October 1967.	108
Figure 6.2.1.1	Dilution of a Steady Release of Pollutant	110
Figure 6.2.2.1	Simulation of a Time-Dependent Plume in Steady-State Weather	114
Figure B.1	Profile Generation for Problems with Mesh Coarsening.	134
Figure B.2	Profile Generation for a Particular Problem.	135

REFERENCES

1. R. Scorer, Natural Aerodynamics, New York, Pergamon Press, 1958, p. 194.
2. J. Stuhmiller, "Development and Validation of a Two-Variable Turbulence Model," SAI-74-509-LJ, 1974.
3. F. Pasquill, Atmospheric Diffusion, Second Ed., England, Ellis Horwood Ltd., 1974.
4. J. Richards, "Experiments on the Motions of Isolated Cylindrical Thermals Through Unstratified Surroundings," Int. Jour. Air Water Poll., 7, pp 17-34, 1963.
5. F. Schiermeier, Large Power Plant Effluent Study, Vol. 1-4, Research Triangle Park, NC, EPA, Office of Air Programs, 1971.
6. R. Sklarew, and J. Wilson, "Air Quality Models Required Data Characterization," Palo Alto, CA, EPRI EC-137, May, 1976.
7. F. Hoffman, et. al., "Computer Codes for the Assessment of Radionuclides Released to the Environment," Nuclear Safety, Vol. 18, No. 3, pp 343-354, May-June, 1977.
8. M. Winton, "Computer Codes for Analyzing Nuclear Accidents," Nuclear Safety, Vol. 15, No. 5, pp 535-552, Sept.-Oct., 1973.
9. K. Rao, "Numerical Simulation of Turbulent Flows-- A Review," ARATDL internal note, April, 1976.
10. C. Nappo, "The Detailed Numerical Simulation of Vorticity Concentration Downwind of Large Heat Sources," (unpublished notes).
11. C. DuP. Donaldson, "Construction of a Dynamic Model of the Production of Atmospheric Turbulence and the Dispersal of Atmospheric Pollutants," in D. Haugen, ed., Workshop on Micrometeorology, Ephrata, PA, Science Press, AMS, 1973, pp 313-392.
12. W. Lewellen, and M. Teske, "Second-Order Closure Modeling of Diffusion in the Atmospheric Boundary Layer," Boun. Lay. Met., 10, pp 69-90, March 1976.

13. S. Patankar, et. al., "Prediction of the Three-Dimensional Velocity Field of a Deflected Turbulent Jet," Trans. ASME, J. Flu. Eng., pp 758-762, Dec. 1977.
14. K. Rao, et. al., "Mass Diffusion from a Point Source in a Neutral Turbulent Shear Layer," Jour. Heat Transfer, 99, pp 433-438, Aug. 1977.
15. M. Dickerson, and R. Orphan, "Atmospheric Release Advisory Capability," Nuc. Safety, Vol. 17, No. 3, May-June, pp 281-289.
16. R. Lange, "ADPIC: A 3-D Computer Code for the Study of Pollutant Dispersal and Deposition Under Complex Conditions," UCRL-51462, Oct. 1973.
17. M. Dickerson, et. al., "Concept for an Atmospheric Release Advisory Capability," UCRL-51656, Oct. 1974.
18. J. Knox, "Numerical Modeling of the Transport, Diffusion, and Deposition of Pollutants for Regions and Extended Scales," UCRL-74666, Mar. 1973.
19. J. Knox, "Atmospheric Release Advisory Capability: Research and Progress," UCRL-75644 (Rev. 2), May 1974.
20. R. Lange, and J. Knox, "Adaptation of a 3-D Atmospheric Transport Diffusion Model to Rainout Assessments," UCRL-75731, Sep. 1974.
21. R. Lange, "ADPIC: A 3-D Transport-Diffusion Model for the Dispersal of Atmospheric Pollutants and its Validation Against Regional Tracer Studies," UCRL-76170, May 1975.
22. C. Sherman, "Mass-Consistent Model for Wind Fields Over Complex Terrain," UCRL-76171, May 1975.
23. R. Henninger, "A Two-Dimensional Dynamic Model for Cooling Tower Plumes," Trans. ANS, Vol. 17, 1973, pp 65-66.
24. J. Taft, "Numerical Model for the Investigation of Moist Buoyant Cooling-Tower Plumes," in S. Hanna and J. Pell, coords., Cooling Tower Environment-1974, ERDA Symposium Series No. 35, Oak Ridge, Tenn., USERDA, Conf-740302, April, 1975.
25. D. Lilly, "Numerical Solutions for the Shape-Preserving Two-Dimensional Thermal Convection Element," Jour. of the Atmos. Sci., 21, pp 83-98, Jan. 1964.

26. D. Johnson, et. al., "A Numerical Study of Fog Clearing by Helicopter Downwash," Jour. Appl. Met., 14, pp 1284-1292, 1975.
27. Y. Ogura, "The Evolution of a Moist Convective Element in a Shallow, Conditionally Unstable Atmosphere: A Numerical Calculation," Jour. Atmos. Sci., 20, pp 407-424, Sept. 1963.
28. G. Arnason, et. al., "A Numerical Experiment in Dry and Moist Convection Including the Rain Stage," Jour. Atmos. Sci., 25, pp 404-415, May 1968.
29. J. Liu, and H. Orville, "Numerical Modeling of Precipitation and Cloud Shadow Effects on Mountain-Induced Cumuli," Jour. Atmos. Sci., 26, pp 1283-1298, Nov. 1969.
30. W. Cotton, "Theoretical Cumulus Dynamics," Rev. Geophys. and Space Phys., Vol. 13, No. 2, pp 419-448, May 1975.
31. Chalk Point Cooling Tower Project, Vol. 1-3, PPSP-CPCTP-16, Applied Physics Lab., Johns Hopkins Univ., Laurel, MD, August, 1977.
32. Chalk Point Cooling Tower Project, PPSP-CPCTP-11 and PPSP-CPCTP-12, Applied Physics Lab., Johns Hopkins Univ., Laurel, MD, 1978.
33. G. Tsang, "Laboratory Study of Line Thermals," Atmos. Environ., 5, pp 445-471, 1971.
34. J. Deardorff, "Numerical Investigation of Neutral and Unstable Planetary Boundary Layers," Jour. Atmos. Sci., 29, pp 91-115, 1972.
35. J. Deardorff, "Three-Dimensional Numerical Modeling of the Planetary Boundary Layer," in D. Haugen, ed., Workshop on Micrometeorology, Ephrata, PA, Science Press, AMS, 1973.
36. J. Deardorff, "Three-Dimensional Numerical Study of the Height and Mean Structure of a Heated Planetary Boundary Layer," Boun. Lay. Met., 7, pp 81-106, 1974.
37. E. Spiegel, and G. Veronis, "On the Boussinesq Approximation for a Compressible Fluid," Astrophys. Jour., 131, pp 442-447, 1960.
38. L. Cloutman, C. Hirt, and N. Romero, "SOLA-ICE: A Numerical Algorithm for Transient Compressible Fluid Flows," UC-34, July, 1976.

39. J. Iribarne, and W. Godson, Atmospheric Thermodynamics, Holland, Reidel Publ. Co., 1973.
40. VARR-II--A Computer Program for Calculating Time-Dependent Turbulent Fluid Flows with Slight Density Variation, Vols 1,2,3, Madison, PA, Westinghouse Adv. React. Div., May 1975.
41. A. Amsden, and F. Harlow, "The SMAC Method: A Numerical Technique for Calculating Incompressible Fluid Flows," LA-4370, May 1970.
42. R. Gentry, et. al., "An Eulerian Differencing Method for Unsteady Compressible Flow Problems," Jour. of Comp. Phys., Vol. 1, 1966, pp 87-118.
43. E. Eckert, and R. Drake, Heat and Mass Transfer, New York, McGraw-Hill Book Co., 1959.
44. S. Hess, Introduction to Theoretical Meteorology, New York, Holt, Rinehart, and Winston, 1959, Chap 18.6.
45. Ibid., Chapter 18.7.
46. Ibid., Chapter 12.
47. H. Tennekes, "The Atmospheric Boundary Layer," Physics Today, Jan. 1974, pp 52-63.
48. C. Priestly, Turbulent Transfer in the Lower Atmosphere, Chicago, U. of Chicago Press, 1959.
49. R. Scorer, Natural Aerodynamics, New York, Pergamon Press, 1958.
50. A. Monin, "The Atmospheric Boundary Layer," in M. Van Dyke, ed., Ann. Rev. of Fluid Mechanics, Vol. 2, pp 225-250, 1970.
51. J. Businger, "The Atmospheric Boundary Layer," V. Derr, ed., Remote Sensing of the Troposphere, Washington, D.C., U.S.Dept. of Commerce, NOAA, Govt. Printing Office, Aug. 1972.
52. H. Panofsky, "The Boundary Layer Above 30 M," Bound. Lay. Met., 4, pp 251-264, 1973.
53. H. Panofsky, "The Atmospheric Boundary Layer Below 150 M," in Annual Review of Fluid Mechanics, pp 147-177, 1974.

54. G. Csanady, Turbulent Diffusion in the Environment, Boston, MA, Reidel Publ., 1973.
55. J. Lumley, and H. Panofsky, The Structure of Atmospheric Turbulence, New York, John Wiley & Sons, 1964.
56. A. Monin, and A. Yaglom, Statistical Fluid Mechanics, Vol. 1, Cambridge, MA, MIT Press, 1971.
57. A. Monin, and A. Yaglom, Statistical Fluid Mechanics, Vol. 2, Cambridge, MA, MIT Press, 1975.
58. Ibid., Vol. 1, p 280.
59. A. Blackadar, "The Vertical Distribution of Wind and Turbulent Exchange in a Neutral Atmosphere," Jour. Geophys. Res., 67, pp 3095-3102, 1962.
60. A. Blackadar, and J. Ching, "Wind Distribution in a Steady State Planetary Boundary Layer of the Atmosphere with Upward Heat Flux," AF(604)-6641, Dept. of Meteor., Penn. State Univ., pp 23-48, 1965.
61. G. Yamamoto, and A. Shimanuki, "Turbulent Transfer in Diabatic Conditions," J. Meteor. Soc. Japan, Ser. 2, 44, pp 301-307, 1966.
62. J. O'Brien, "A Note on the Vertical Structure of the Eddy Exchange Coefficient in the Planetary Boundary Layer," J. Atmos. Sci., 27, pp 1213-1215, Nov. 1970.
63. R. Bornstein, "The Two-Dimensional URBMET Urban Boundary Layer Model," J. Appl. Met., 14, pp 1459-1477, Dec. 1975.
64. F. Nieuwstadt, "The Computation of the Friction Velocity, u_* , and the Temperature Scale, T_* , from Temperature and Wind Velocity Profiles by Least-Square Methods," Bound. Lay. Met., 14, pp 235-246, 1978.
65. H. Tennekes, and J. Lumley, A First Course in Turbulence, Cambridge, MA, MIT Press, 1972.
66. A. Monin, Weather Forecasting as a Problem in Physics, Cambridge, MA, MIT Press, 1972.
67. VARR-II Users' Guide, Op. Cit., p. 88.
68. Y. Chen, "Coolant Mixing in the LMFBR Outlet Plenum," MIT PhD Thesis, Nuclear Engineering Dept., May 1977.

APPENDIX A

Definitions of Important Variables Added to the VARR-II Code
for Simulating Plume Behavior

Definitions of Important Variables Added to VARR-II for
 Simulating Plume Behavior

<u>Variable</u>	<u>Meaning</u>	<u>Units</u>
BKGND	background pollutant concentration	lbm/ft ³
CHI(IK)	pollutant concentration, χ	lbm/ft ³
CHIØ(IK)	pollutant concentration at the previous timestep	lbm/ft ³
CHII	pollutant concentration input variable	lbm/ft ³
DWNDS	downwind distance	ft
EFAC(J)	fraction of the energy of the J th radiation deposited in the plume, $F_x^{(j)}$	-
ELAM(J)	energy of the J th radioactive decay channel, $E_x^{(j)}$	MeV
GAML	reciprocal turbulent Schmidt number for cloud liquid water, γ_L	-
GAMV	reciprocal turbulent Schmidt number for water vapor, γ_V	-
GAMX	reciprocal turbulent Schmidt number for pollutant, γ_X	-
LIQ(IK)	cloud liquid water density, ρ_{liq}	lbm/ft ³
LIQØ(IK)	cloud liquid water density at the previous timestep	lbm/ft ³
LIQI	cloud liquid water density input variable	lbm/ft ³
NCHAN	number of decay channels to be input	-
NPRØF	number of input profiles to be input	-
RLAM(J)	decay constant of the J th decay channel, $\lambda_x^{(j)}$	sec ⁻¹
RLAMB	net decay constant, $\sum_{j=1}^{NCHAN} \lambda_x^{(j)}$	sec ⁻¹
SER	specific energy release rate of the radioactive pollutant	MeV/sec
SMSIE	total internal energy on the mesh (assumed 1 ft deep)	BTU

<u>Variable</u>	<u>Meaning</u>	<u>Units</u>
TRSTRT(J)	time for program coarsening (J=1, 2, ... 5)	sec
VELCHI	pollutant-averaged velocity	ft/sec
VAP(IK)	water vapor density, ρ_{vap}	lbm/ft ³
VAPØ(IK)	water vapor density, at the previous timestep	lbm/ft ³
VAPI	water vapor density input variable	lbm/ft ³
WMØLX	molecular weight of the pollutant	lbm/lbm-mole
WWSP(J)	wind speed profile variable	ft/sec
WZAP(J)	absolute pressure profile variable	mb
WZLQ(J)	liquid water profile variable	lbm/ft ³
WZSIE(J)	specific internal energy profile variable	BTU/lbm
WZTQ(J)	turbulence kinetic energy profile variable	ft ² /sec
WZTS(J)	eddy viscosity profile variable	ft ² /sec
WZVP(J)	water vapor profile variable	lbm/ft ³
YPLUME	plume center height	ft

APPENDIX B

Card Formats for Input Variables

Card Formats for Input Variables

<u>Card No.</u>	<u>Input Variables/Card</u>	<u>Format</u>
1*	IBR, KBR, IPRFM	(2(5X,I5),7X,I2)
2	LABEL	(10A8)
3*	DT, TPRT, TPLT, TWTD, TFIN, ITAPW, NPRT, IDIAG, LPR, IØBS, IDG, KDG	(5F8.3, 5I2, 2I3)
4*	DX, DZ, GX, GZ, ALX, ALZ, CYL, B _O , EPS, VMIN	(10F8.3)
5	KWR, KWL, KWT, KWB, FSLIP, ALP, GAM, ALP _O , GAM ₁ , NU, TQJET, TSJET	(4I2, 8F8.3)
6	AW, BW, CW, WEPS, KDERBC, UBRI, UBRI, UBLI, WBTI, WBI	(4F8.3,I2,4F8.3)
7	WØBI, UØBI, CSUBPØ	(3F8.3)
8*	TGAM, T _O , TI, TSTEP, MAT, NRESEX	(4F8.3, 2I2)
9	AI, BI, CI, AR, BR, CR, AMU, BMU, CMU	(10F8.3)
10	AK, BK, CK, ACP, BCP, CCP	(10F8.3)
11*	NFLOW, NT1, NT2, NT3, NT4, NT5, NTAU	(7X, I3,5(5X,I3), 7X, I3)
12*	TYMF(I), FN(I)	(8F8.3)
13*	TYMYT1(I), T1N(I)	(8F8.3)
14*	TYMT2(I), T2N(I)	(8F8.3)
15*	TAU(I)	(8F8.3)
16*	I, CØFA, CØFB, CØFC	(3X,I3,2X,3F8.3)
17*	I, CØFA, CØFB,CØFC	(3X,I3,2X,3F8.3)
18*	I, CØFA, CØFB,CØFC	(3X,I3,2X,3F8.3)

<u>Card No.</u>	<u>Input Variables/Card</u>	<u>Format</u>
19*	I, CØFA, CØFB, CØFC	(3X,I3,2X,3F8.3)
20*	I, CØFA, CØFB, CØFC	(3X,I3,2X,3F8.3)
21*	I, CØFA, CØFB, CØFC	(3X,I3,2X,3F8.3)
22*	I, K, RXC, RZC	(2(3X,I3),2(5X,F8.3))
23*	NL, NR, NB, NT, ICELTYP	(4I5,I2)
24*	SIEI, TQI, TSI, UI, WI, CHII, VAPI, LIQI	(8F8.3)
25**	NGØP, NOVP, DRØU, XDIV, YDIV	(2(7X,I2),3(6X,F8.3))
26	IGØP(I)	(6X,6I2)
27	VNTP(I), NCVTYP(I)	(4(5X,I2,1X,I3))
28	IBR, KBR, IPRFM	(2(5X,I5),7X,I2)
29*	GAMX, NCHAN, WMØLX, GAMV, GAML, BKGND, DWNDS	(F8.3,I8,5F8.3)
30*	RLAM, ELAM, EFRAC	(3F8.3)
31*	NPRØF, TRSTRT(1), TRSTRT(2), TRSTRT(3), TRSTRT(4), TRSTRT(5)	(I8,5F8.3)
32*	WZSIE, WZTQ, WZTS, WZVP, WZLQ, WZAP, WWSP	(7F8.3)
33*	IBR, KBR, IPRFM	(2(5X,I5),7X,I2)

* See Special Notes to Input

** Cards No. 25-28 in the original VARR-II input have been omitted entirely in this version.

Special Notes to Input

Card No.

- 1 Do not attempt to "restart" the program (i.e., storing or retrieving the program storage on or from magnetic tape or disc) unless additional programming has been performed that would "restart" the variables added to VARR-II. Set IPRFM=1 to allow the statistics package (instead of the film generated plots) to be printed out.
- 3 TPLT is now "time when to print statistics" (sic). Always set TWTD > TFIN, and/or make device 8 equal to DUMMY. Set ITAPW = 8. In IDIAG, grind time and CPU time have been omitted. Set LPR = 3, and IØBS = 0.
- 4 Set ALX = ALZ = 1.0, and CYL = 0.0
- 8 TI is ignored by the program. TSTEP should have a value of about 10⁻².
- 11-15 All of the values on these cards are unimportant for problems that have no inflow/outflow and no obstacle cells. However, the code cannot skip these cards, so dummy information must be supplied.
- 16-22 Set I = 0.
- 23-24 Because of the solid-wall boundary conditions, only the real fluid cells on the mesh need to be initialized. Cards of type 23 and 24 can be repeated as many times as desired when initializing; the sequence is terminated when NL = 0 on Card 23. Note that CHII, VAPI, and LIQI have been added to Card 24.
- 25-28 These cards have been dropped from the input list.
- 29 See Appendix A for definitions.
- 30 This card is repeated NCHAN times with the values corresponding to J=1,...NCHAN. See Appendix A for definitions.
- 31 See Appendix A for definitions.

Card No.

- 32 This card is repeated NPROF times with the values corresponding to J=1, ... NPROF. For a problem that is 20 real cells high, the code needs 20 values for each variable if there are no mesh coarsenings. If there is one mesh coarsening carried out, the code needs 30 values (consisting of the first 20 plus 10 more to initialize the new cell area). If there are two mesh coarsenings carried out, the code needs 40 values, etc. The cell center height at which a profile needs to be defined can be generated by considering Figs B.1 and B.2. See Appendix A for definitions.
- 33 Set IBR = -1 to terminate the problem.

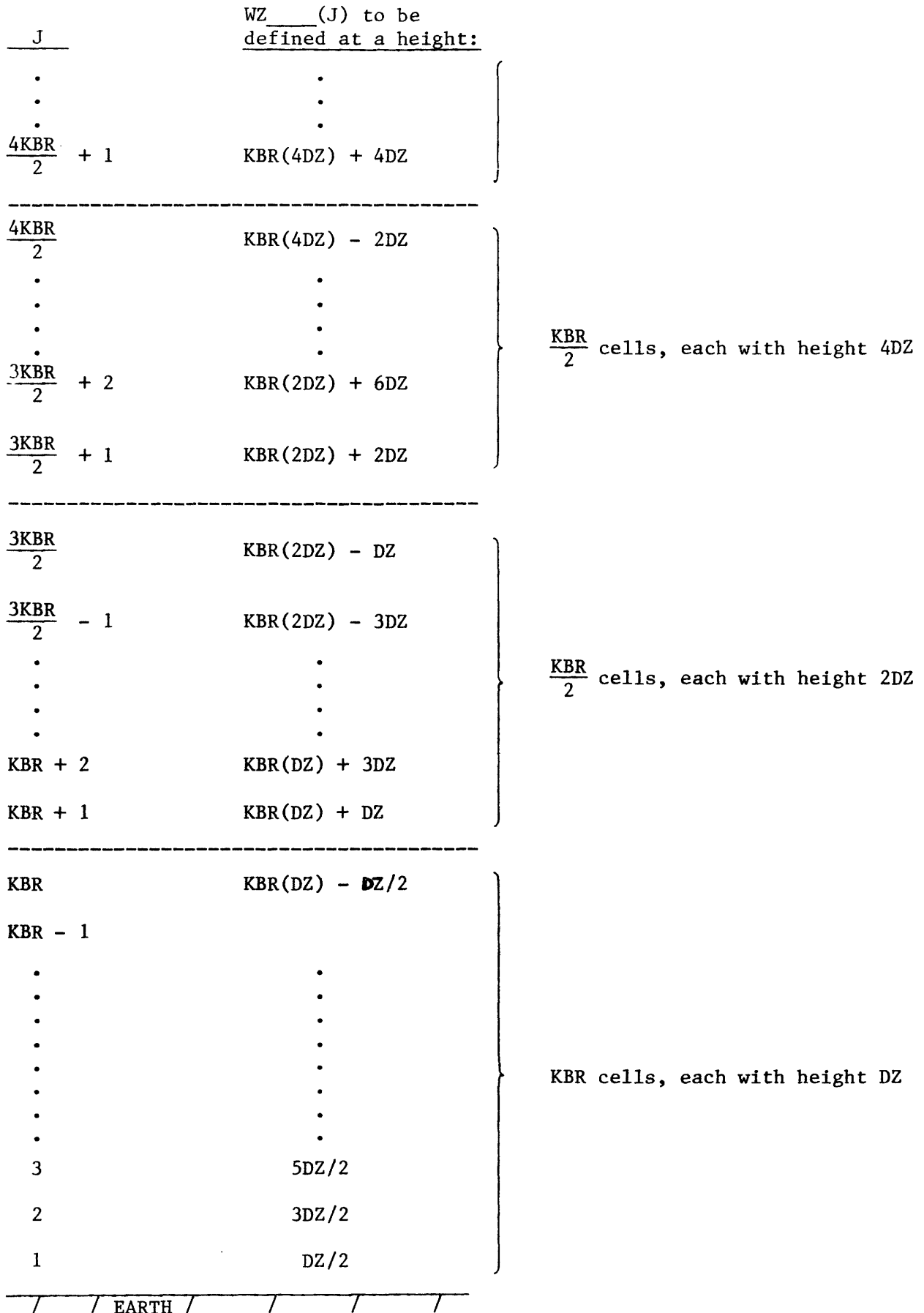


Figure B.1 Profile generation for problems with mesh coarsening. KBR real cells are placed on the computer mesh at a time. The cell height is DZ initially. The cell center height at which each of the seven profiles must be specified is developed in the figure.

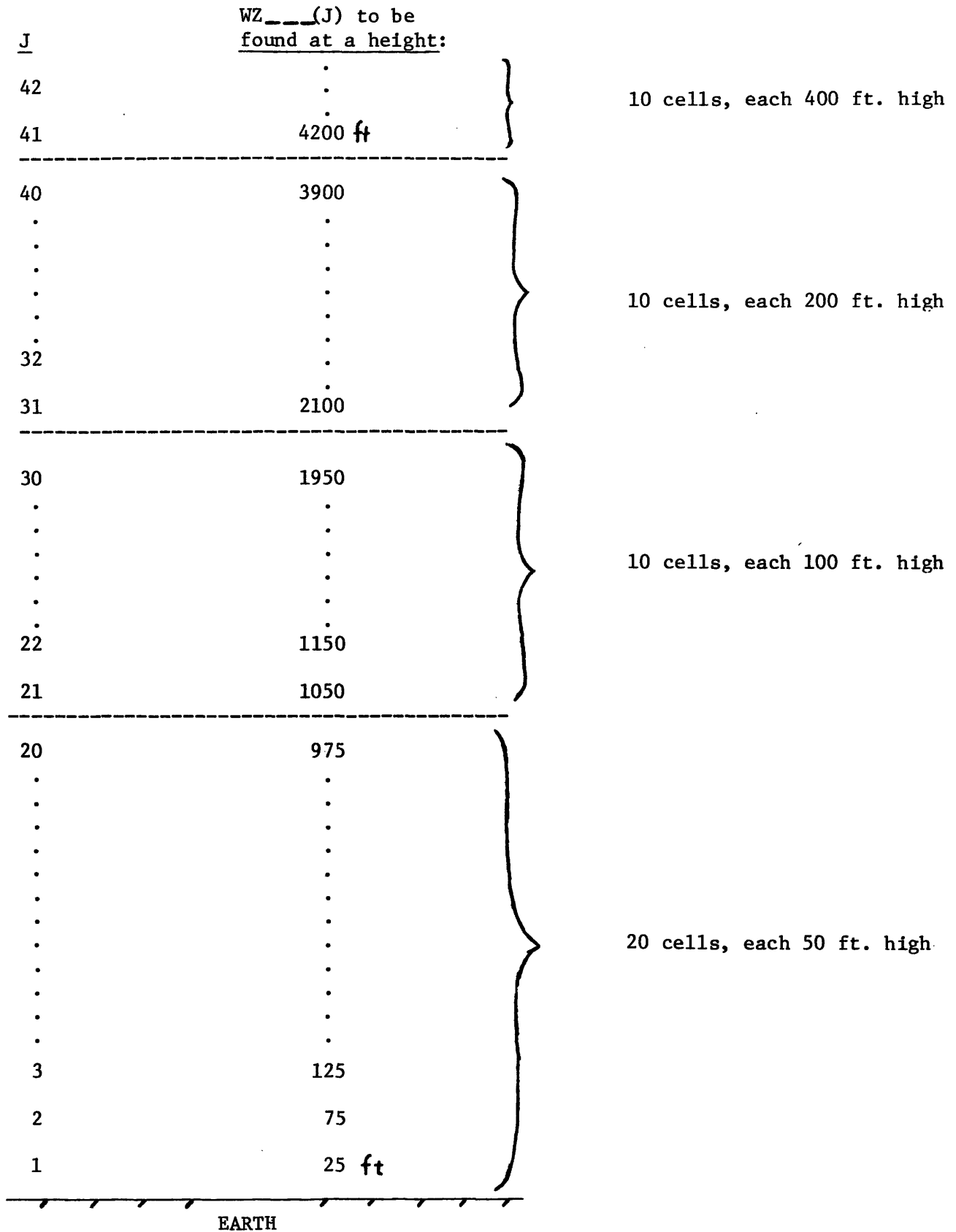


Fig. B.2. Profile generation for a particular problem. The problem is 20 cells high, each of which is 50 feet tall initially.

APPENDIX C

Statement Number Cross-References

Statement Number Cross-References

The statement number cross-references are intended to aid the user in understanding the purpose of the altered or added FORTRAN statements. Any statement that was altered or added is labeled in columns 73-80 with a "card entry" that begins with the initials RGB or MWG.

The first cross-reference consists of 12 effects or problems that are solved by the cards that are listed below the problem statement. For example, a constant heat flux from the top wall of an obstacle cell (Effect No. 12) is permitted when a single statement (No. 1688) is altered. Statements that were removed from the code are not listed.

A second cross-reference allows any altered or added statement to be identified with the problem that it helps to solve. For example, statement #1688 is identified with effect #12--and looking up effect #12 in the first cross-reference shows that no other cards were involved in the solution to that problem.

EFFECTS OR PROBLEM(S) CONSIDERED

EFFECT NO. 1

1. Non-executable statements for COMMON, DIMENSION,
REAL, INTEGER, or EQUIVALENCE CARDS.

(Two executable statements (91,92) are included here
since they are related to program control.)

<u>SUBROUTINE(S)</u>	<u>CARD ENTRIES</u>	<u>PROGRAM STATEMENT NUMBERS</u>
MAIN	RGB MN60A, B	32, 36, 53, 55, 56, 86, 91, 92
"	RGB MN01A	35, 85
"	RGB VM62A	50, 52
"	RGB VM55A, B	51, 54
IDLE	RGB MN60A, B	125, 129, 146, 148, 149, 179
"	RGB MN01A	128, 178
"	RGB VM62A	143, 145
"	RGB VM55A, B	144, 147
VRPRT	RGB MN60A, B	392, 398, 415, 417, 418, 448
"	RGB MN01A	397, 447
"	RGB VM62A	412, 414
"	RGB VM55, A, B	413, 416
VSET	RGB MN60, A, B	512, 516, 533, 535, 536, 566
"	RGB MN01A	515, 565
"	RGB VM62A	530, 532
"	RGB VM55, A, B	531, 534

EFFECTS OR PROBLEM(S) CONSIDERED

EFFECT NO. 1

non-executable (continued)

<u>SUBROUTINE(S)</u>	<u>CARD ENTRIES</u>	<u>PROGRAM STATEMENT NUMBERS</u>
MESHMK	RGB MN60A,B	685,689,706,708,709,739
"	RGB MN01A	688,738
"	RGB VM62A	703,705
"	RGB VM55A,B	704,707
VM	RGB MN60A,B	1071,1077,1094,1096,1097,1127
"	RGB MN01A	1076,1126
"	RGB VM62A	1091,1093
"	RGB VM55A,B	1092,1095

EFFECTS OR PROBLEM(S) CONSIDERED

EFFECT NO. 2

1. Boundary conditions for crosswind runs for the variables U, W, SIE, TQ, TS.
2. Set $\sigma \geq \sigma_{\text{library}}(z)$ and $q \geq q_{\text{library}}(z)$

<u>SUBROUTINE(S)</u>	<u>CARD ENTRIES</u>	<u>PROGRAM STATEMENT NUMBERS</u>
VM	RGB VM50A	1466,1847
VM	RGB VM51A	1301,1305,1307,1309,1467, 1489,2199,2200
VM	RGB VM02A	1302,1369-71,1379

EFFECTS OR PROBLEM(S) CONSIDERED

EFFECT NO. 3

1. Boundary conditions for crosswind runs for the variable, CHI.
2. Pollutant transport equation.

SUBROUTINE(S)

CARD ENTRIES

PROGRAM STATEMENT NUMBERS

VM

RGB VM52A,B,C

1310-12,1475-77,1959,1980,
1988,2047-52,2277-78,2358,2366,
2469

EFFECTS OR PROBLEM(S) CONSIDERED

EFFECT NO. 4

1. Cell initialization from input data.

<u>SUBROUTINE(S)</u>	<u>CARD ENTRIES</u>	<u>PROGRAM STATEMENT NUMBERS</u>
MESHMK	RGB MK01A,02A	946,952,960
"	RGB MK60A	930-31,953-54,961-62,1027, 1049-50

EFFECTS OR PROBLEM(S) CONSIDERED

EFFECT NO. 5

1. Atmospheric profile read-in and printout for variables,

WZSIE	(internal energy)
WZTQ	(turbulence kinetic energy)
WZTS	(eddy viscosity)
WZVP	(water vapor)
WZLQ	(cloud liquid water)
WZAP	(pressure)
WWSP	(wind speed)

<u>SUBROUTINE(S)</u>	<u>CARD ENTRIES</u>	<u>PROGRAM STATEMENT NUMBERS</u>
VM	RGB VM62A	1153-58,1162,1169
VM	RGB VM55A	1151-52, 1159-60, 1165-67, 1172-74, 1179-81
VM	RGB VM70A	1161,1168,1175

EFFECTS OR PROBLEM(S) CONSIDERED

EFFECT NO. 6

1. Moisture model in subroutine VM (initialization of cell moisture is done elsewhere), including input, boundary conditions, and transport equations.

<u>SUBROUTINE(S)</u>	<u>CARD ENTRIES</u>	<u>PROGRAM STATEMENT NUMBERS</u>
VM	RGB VM60A,B	1072,1133-37,1163-64,1170-71, 1177-78,1313-16,1478-81, 1960-61, 1981-82,1989-90, 2053-64,2359-60,2367-68,2470-71
VM	RGB VM62A	2225-26,2230-55
VM	RGB VM61A	2201-24

EFFECTS OR PROBLEM(S) CONSIDERED

EFFECT NO. 7

1. Mesh coarsening capability.

<u>SUBROUTINE(S)</u>	<u>CARD ENTRIES</u>	<u>PROGRAM STATEMENT NUMBERS</u>
IDLE	RGB ID55A	202-209, 214-327
IDLE	RGB ID70A	210-213
VM	RGB VM55A,B	1132,2553-56,2564-68
VM	RGB ID55A,B	2557-63

EFFECTS OR PROBLEM(S) CONSIDERED

EFFECT NO. 8

1. Cell by cell output of variables by the printing subroutine.

<u>SUBROUTINE(S)</u>	<u>CARD ENTRIES</u>	<u>PROGRAM STATEMENT NUMBERS</u>
VRPRT	RGB MØ60A	394
"	RGB MØ01A	451-507*

*The entire section was altered, although not all of the cards have card entries.

EFFECTS OR PROBLEM(S) CONSIDERED

EFFECT NO. 9

1. Plume statistics package.

<u>SUBROUTINE(S)</u>	<u>CARD ENTRIES</u>	<u>PROGRAM STATEMENT NUMBERS</u>
VM	RGB VM54A,B	2518-21, 2529-30,2545-47
VM	RGB VM70A	2514-17,2522-28,2531-33
VM	RGB VM55B	2548-50

EFFECTS OR PROBLEM(S) CONSIDERED

EFFECT NO. 10

1. Radioactive decay heating.

SUBROUTINE(S)

CARD ENTRIES

PROGRAM STATEMENT NUMBERS

VM

RGB VM56A

1073,1138-50,2227-29,2273-74,
2276

EFFECTS OR PROBLEM(S) CONSIDERED

EFFECT NO. 11

1. Turbulence model errors.
2. SIEX error.

SUBROUTINE(S)

CARD ENTRIES

PROGRAM STATEMENT NUMBERS

VM	RGB VM000	2193-94
"	MWG 04/78	2195-96
"	RGB VM01A	1361,1416,1526,1591,1816, 1877

EFFECTS OR PROBLEM(S) CONSIDERED

EFFECT NO. 12

1. Constant heat flux from obstacle top wall.

SUBROUTINE (S)

VM

CARD ENTRIES

RGB VM03A

PROGRAM STATEMENT NUMBERS

1688

Statement Number	Effect Number	Statement Number	Effect Number
32	1	946	4
35	1	9-954	4
36	1	960-962	4
50-56	1	1027	4
85-86	1	1049-50	4
91-92	1	1071	1
125	1	1072	6
128-129	1	1073	10
143-149	1	1076-77	1
178-179	1	1091-97	1
202-209	7	1126-27	1
210-213	7	1132	7
214-327	7	1133-37	6
392	1	1138-50	10
394	8	1151-62	5
397-398	1	1163-64	6
412-418	1	1165-69	5
447-448	1	1170-71	6
451-507	8	1172-76	5
512	1	1177-78	6
515-516	1	1179-81	5
530-536	1	1301-02	2
56-566	1	1305	2
685	1	1307	2
688-689	1	1309	2
73-709	1	1310-12	3
738-739	1	1313-16	6
930-931	4	1361	11

Statement Number	Effect Number	Statement Number	Effect Number
1369-71	2	2276	10
1379	2	2277-88	3
1416	11	2358	3
1466-67	2	2359-60	6
1475-77	3	2366	3
1478-81	6	2367-68	6
1489	2	2469	3
1526	11	2470-71	6
1591	11	2514-33	9
1688	12	2545-50	9
1816	11	2553-68	7
1847	2		
1877	11		
1959	3		
1960-61	6		
1980	3		
1981-82	6		
1988	3		
1989-90	6		
2047-52	3		
2053-64	6		
2193-96	11		
2199-00	2		
2201-26	6		
2227-29	10		
2230-55	6		
2273-74	10		

APPENDIX D

Computer Code Listing

3 , TYMP (25), FN (25), TYMT1 (25), T1N (25), TYMT2 (25), T2N (25),
 4 COFBA (25), COFBB (25), COFBC (25), COFTA (25), COFTB (25), COFTC (25),
 5 COFRA (25), COFRB (25), COFRC (25), COFLA (25), COFLB (25), COFLC (25),
 6 OFOBA (25), OFOBB (25), OFOBC (25),
 7 OFOBRA (25), OFOBRB (25), OFOBR C (25), TAU (10), USL (32), USLOB (20),
 8 USROB (20), USTOB (20), USBOB (20)
 9, COFBD (25), COFBE (25), COFTD (25), COFTE (25), COFTP (25), COFBF (25),
 * COFRD (25), COFRE (25), COFLD (25), COFLE (25), COFRF (25), COFLF (25),
 A OFOBD (25), OFOBE (25), OFOBRD (25), OFOBR E (25),
 B OFOBF (25), OFOBRF (25),
 C TYMT3 (25), TYMT4 (25), TYMT5 (25), T3N (25), T4N (25), T5N (25),
 * IICFR (1), IICFL (1), IICFT (1), IICFB (1)
 * , ZERO1 (1165), ZERO2 (608), ZERO3 (16), ZERO4 (3)
 DIMENSION ZSIE (22), ZTQ (22), ZTS (22), ZVP (22), ZLQ (22), ZAP (22), WSP (22) RGBVM62A
 DIMENSION TRSIRT (5), WZSIE (100), WZTQ (100), WZTS (100) RGBVM55A
 A, WZVP (100), WZLQ (100), WZAP (100), WWSP (100) RGBVM62A
 COMMON /VRCON/A (14000) RGBMN60A
 COMMON /RGB/RLAMB, CHIL, GAMX, NRSIRT, TRSIRT, ZSIE, ZTQ, ZTS, WZSIE, WZTQ, RGBMN60A
 AWZTS, NPROF, WZVP, WZLQ, ZVP, ZLQ, GAML, GAMV, VAPI, LIQI RGBVM55A
 B, WSP, WWSP, BKGND, DWNDS RGBMN60A
 COMMON /VRCON/ ALP, ALPO, ALX, ALZ, B0, BETA, BUPL, CFI (9), CFS (9), CYL, RGBMN60B
 1 DT, DX, DZ, EM6, EPS, ERF, FSLIP, GAM, GAM1, GX, GZ, HDX, HDZ, I, I1, I2, I2K2,
 2 IBP1, IBP2, IBR, IDAIN, IDIAG, IKP2, IOBS, IRSIRT, ITAPW, ITER, IVDI,
 3 IVD0, K, K1, K2, K2NC, KBP1, KBP2, KBR, KNC, KWB, KWL, KWR, KWT, LABEL (20),
 4 LPR, NCYC, NCYCB, NPR T, NU, NWPC, RDT, RDX, RDZ, RDZS, RIBKB, ROI, TD, TFIN,
 5 TIMET, TIOSUM, TPL, TPLT, TPR, TPRT, TQI, TSI, TTD, TWTD, UI, WI
 * , USR (32), UST (22), USB (22), USO (10), PFX3, PFY3
 6 , AW, BW, CW, EPSB, UBLI, UBRI, WBI, WBTI, WEPS, W0BI, NTPAS, T GAM, CSUBP,
 7 T0, SIEI, I DG, KDG, TI, MAT, RHO0, AT, TMU, TK, TYMF, FN, TYMT1, T1N, TYMT2,
 8 T2N, RPRAN, NRESEK, NFLOW, NT1, NT2, TSTEP, KDERBC, U0BI, COFBA, COFBB,
 9 COFBC, COFTA, COFTB, COFTC, COPRA, COFRB, COFRC, COFLA, COFLB, COFLC,
 * OFOBA, OFOBB, OFOBTB, OFOBT C, OFOBRA, OFOBRB, OFOBR C, TAU, NTAU, USL,
 1 USLOB, USROB, USTOB, USBOB, UMAX, WMAX
 * , CSUBPO, EPS0, RDXDZS, RLENGTH, TQJET, TSJET
 COMMON /FLMCON/ DROU, DROU0, IPRPM
 COMMON /VRMAT3/ AI, BI, CI, AR, BR, CR, AMU, BMU, CMU, AK, BK, CK, ACP, BCP, CCP


```

1      COMMON/PROP/SIGN,VMIN
COMMON/EXTRA/NT3,NT4,NT5,TYMT3,TYMT4,TYMT5,T3N,T4N,T5N,COFBD,
1COFBE,COFBF,COFTD,COFTE,COFTF,COFRD,COFRE,COFRF,COFLD,COFLE,
2COFLF,OFBTD,OFBTE,OFBTF,OFBRD,OFBRE,OFBRF,IRESET,
*NCYCLS,TADD,NIV,I0BRAN
COMMON/INDEX/NWPCL,K2NCL
COMMON/LARGE/DIFFCO(2400)
EQUIVALENCE (A(1),CF),(A(2),U),(A(3),W),(A(4),P),(A(5),TQ),
1 (A(6),TS),(A(7),ER,CQ),(A(8),UO),(A(9),WO),(A(10),TQO),
2 (A(11),TSO),(A(12),SIE),(A(13),SIEO),(A(14),RX),(A(15),RZ),
3 (A(16),IICFR),(A(17),IICFL),(A(18),IICFT),(A(19),IICFB),
A (A(20),CHI),(A(21),CHIO),
B (A(22),VAP),(A(23),VAPO),(A(24),LIQ),(A(25),LIQO),
4 (ZERO1(1),ALP),(ZERO2(1),NT3),(ZERO3(1),AI),(ZERO4(1),DROU)
C NOTE. END - END OF NON-EXECUTABLE STATEMENTS .
C
C NOTE. NWPC = NUMBER OF WORDS PER MESH CELL .
CALL ERASE (ZERO1,1155,ZERO2,608,ZERO3,16,ZERO4,3,A,14000)
NWPC=25
NWPCL = 4
IVDI=5
IVDO=6
100 WRITE(IVDO,1)
READ(IVDI,2) IBR,KBR,I PRFM,NCYCLS,TADD,IRESET
ERF=0
IF( IPRFM.GT.0 ) CALL FLMINI
IF( IBR ) 700,400,400
400 PRINT 11
CALL VSET
WRITE(IVDO,3)
IF( ERF.EQ.1 ) GO TO 700
PRINT 12
CALL VM
IF( ERF.EQ.1 ) GO TO 700
GO TO 100

```

```

0073
0074
0075
0076
0077
0078
0079
0080
0081
0082
0083
0084
0085
0086
0087
0088
0089
0090
0091
0092
0093
0094
0095
0096
0097
0098
0099
0100
0101
0102
0103
0104
0105
0106
0107
0108

```

```

RGBMN01A
RGBMN60A

RGBMN60A
RGBMN60A

VRC42002

VRC50002

PAGE 3

```

```

700 IF( IPRFM.GT.0 ) CALL FLMFIN
C ***** FORMATS ***** FORMATS ***** .
1  FORMAT(1H1,22H MAIN PROGRAM CALLED .)
2  FORMAT(2(5X,I5),7X,I2,I11,F10.4,5X,I5)
3  FORMAT(1H ,27H SUBROUTINE VSET FINISHED .)
11  FORMAT(1H ,25H SUBROUTINE VSET CALLED .)
12  FORMAT(1H ,23H SUBROUTINE VM CALLED .)
STOP
END
VRC70004
BLOCK DATA
COMMON/LARGE/DIFFCO(2400)
REAL DIFFCO/2400*1.0/
END
SUBROUTINE IDLE
INTEGER BUFL,CF,CP1,CFB,CFC,CPI,CFL,CFR,CFS,CPT,CQF,ERF,TD,VNTP,
1  VTP
REAL NU,LIQ,LIQO,LIQI,LOUT
DIMENSION CF(1),CQ(1),QCON(1),P(1),RX(1),RZ(1),TQ(1),TS(1),U(1),
1  W(1),ER(1),FFX3(102),FFY3(102),PBTIM(2),UO(1),WO(1),TQO(1),
2  TSO(1),SIE(1),SIEO(1),CHI(1),CHIO(1)
A,VAP(1),VAP(1),LIQ(1),LIQO(1)
3  ,TYMP(25),FN(25),TYMT1(25),T1N(25),TYMT2(25),T2N(25),
4  COFBA(25),COFBB(25),COFBC(25),COFTA(25),COFTB(25),COFTC(25),
5  COFRA(25),COFRB(25),COFRC(25),COFLA(25),COFLB(25),COFLC(25),
6  OFOBA(25),OFOBB(25),OFOBTC(25),
7  OFORA(25),OFORB(25),OFORC(25),TAU(10),USL(32),USLOB(20),
8  USROB(20),USTOB(20),USBOB(20)
9,COFBD(25),COFBE(25),COFTD(25),COFTE(25),COFTF(25),COFBF(25),
*COFRD(25),COFRE(25),COFLD(25),COFLE(25),COFRF(25),COFLF(25),
AOFBTD(25),OFOBTE(25),OFOBRD(25),OFOBRE(25),
B OFORTP(25),OFOBRF(25),
CTYMT3(25),TYMT4(25),TYMT5(25),T3N(25),T4N(25),T5N(25),
* IICPR(1),IICFL(1),IICPT(1),IICFR(1)
* ,ZERO1(1165),ZERO2(608),ZERO3(16),ZERO4(3)
DIMENSION ZSIE(22),ZTQ(22),ZTS(22),ZVP(22),ZLQ(22),ZAP(22),WSP(22) RGBVM62A
DIMENSION TRSTRT(5),WZSIE(100),WZTQ(100),WZTS(100) RGBVM55A

```

A, WZVP (100), WZLQ (100), WZAP (100), WWSP (100)
 COMMON /VRCON /A (14000)
 COMMON /RGB /RIAMB, CHII, GAMX, NRSTRT, TRSTRT, ZSIE, ZTQ, ZTS, WZSIE, WZTQ,
 WZTS, NPROF, WZVP, WZLQ, ZVP, ZLQ, GAML, GAMV, VAPI, LIQI
 B, WSP, WWSP, BKGND, DWNDS
 COMMON /VRCON / ALP, ALPO, ALX, ALZ, BO, BETA, BUFL, CFI (9), CFS (9), CYL,
 1 DT, DX, DZ, EM6, EPS, ERF, FSLIP, GAM, GAM1, GX, GZ, HDX, HDZ, I, I1, I2, I2K2,
 2 IBP1, IBP2, IBR, IDATIN, IDIAG, IKP2, IOBS, IRSTRT, ITAPW, ITER, IVDI,
 3 IVD0, K, K1, K2, K2NC, KBP1, KBP2, KBR, KNC, KWB, KWL, KWR, KWT, LABEL (20),
 4 LPR, NCYC, NCYCB, NPRT, NU, NWPC, RDT, RDX, RDZ, RDZS, RIBKB, ROI, TD, TFIN,
 5 TIMET, TIOSUM, TPL, TPLT, TPR, TPRT, TQI, TSI, TTD, TWTD, UI, WI
 * USR (32), UST (22), USB (22), USO (10), FFX3, FFY3
 6 AW, BW, CW, EPSB, UBLI, UBRI, WBI, WBTI, WEPS, WOBI, NTPAS, TGAM, CSUBP,
 7 T0, SIEI, IDG, KDG, TI, MAT, RHOO, AT, THU, TK, TYMP, FN, TYMT1, T1N, TYMT2,
 8 T2N, RPRAN, NRESEX, NFLOW, NT1, NT2, TSTEP, KDERBC, UOBI, COFBA, COFBB,
 9 COPBC, COFTA, COFTB, COFTC, COFRA, COFRB, COFRC, COFLA, COFLB, COFLC,
 * OFOBT, OFOBTB, OFOBT, OFOBR, OFOBRB, OFOBR, OFOBR, OFOBR, OFOBR, OFOBR, OFOBR,
 1 USLOB, USROB, USTOB, USBOB, UMAX, WMAX
 * CSUBPO, EPSO, RDXDZS, RLENGTH, TQJET, TSJET
 COMMON /FLMCON / DROU, DROU0, IPRFM
 COMMON /VRMAT3 / AI, BI, CI, AR, BR, CR, AMU, BMU, CMU, AK, BK, CK, ACP, BCP, CCP
 1
 COMMON /PROP /SIGN
 COMMON /EXTRA /NT3, NT4, NT5, TYMT3, TYMT4, TYMT5, T3N, T4N, T5N, COFBD,
 1 COFBE, COFBF, COFTD, COFTE, COFTF, COFRD, COFRE, COFRF, COFLD, COFLE,
 2 COFLF, OFOBT, OFOBTB, OFOBT, OFOBR, OFOBR, OFOBR, OFOBR, OFOBR, OFOBR,
 * NCYCLS, TADD, NIV, IOBRAN
 COMMON /INDEX /NWPCL, K2NCL
 COMMON /LARGE /DIFCO (2400)
 EQUI VALENCE (A (1), CF), (A (2), U), (A (3), W), (A (4), P), (A (5), TQ),
 1 (A (6), TS), (A (7), ER, CO), (A (8), UO), (A (9), WO), (A (10), TQO),
 2 (A (11), TSO), (A (12), SIE), (A (13), SIEO), (A (14), RX), (A (15), RZ),
 3 (A (16), IICFR), (A (17), IICFL), (A (18), IICFT), (A (19), IICFB),
 A (A (20), CHI), (A (21), CHIO),
 B (A (22), VAP), (A (23), VAPO), (A (24), LIQ), (A (25), LIQO),
 4 (ZERO1 (1), ALP), (ZERO2 (1), NT3), (ZERO3 (1), AI), (ZERO4 (1), DROU)

0145 RGBVM62A
 0146 RGBMN60A
 0147 RGBVM55A
 0148 RGBMN60A
 0149 RGBMN60B
 0150
 0151
 0152
 0153
 0154
 0155
 0156
 0157
 0158
 0159
 0160
 0161
 0162
 0163
 0164
 0165
 0166
 0167
 0168
 0169
 0170
 0171
 0172
 0173
 0174
 0175
 0176
 0177
 0178
 0179
 0180

RGBMN01A
 RGBMN60A
 PAGE 5

RGBID55A 0217
 RGBID70A 0218
 RGBID70A 0219
 RGBID70A 0220
 RGBID70A 0221
 RGBID55A 0222
 RGBID55A 0223
 RGBID55A 0224
 RGBID55A 0225
 RGBID70A 0226
 RGBID70A 0227
 RGBID70A 0228
 RGBID70A 0229
 RGBID55A 0230
 RGBID55A 0231
 RGBID55A 0232
 RGBID55A 0233
 RGBID70A 0234
 RGBID70A 0235
 RGBID70A 0236
 RGBID70A 0237
 RGBID55A 0238
 RGBID55A 0239
 RGBID55A 0240
 RGBID55A 0241
 RGBID55A 0242
 RGBID55A 0243
 RGBID55A 0244
 RGBID55A 0245
 RGBID55A 0246
 RGBID55A 0247
 RGBID55A 0248
 RGBID55A 0249
 RGBID55A 0250
 RGBID55A 0251
 RGBID55A 0252

ZTQ (1) = ZTQ (2)
 ZLQ (1) = ZLQ (2)
 ZVP (1) = ZVP (2)
 ZAP (1) = ZAP (2)
 WSP (1) = WSP (2)
 KHP1 = KHALF + 1
 DO 95 K = KHP1, KBP1
 ZTQ (K) = WZTQ ((NRSTRT * KBR / 2) + K - 1)
 ZTS (K) = WZTS ((NRSTRT * KBR / 2) + K - 1)
 ZLQ (K) = WZLQ ((NRSTRT * KBR / 2) + K - 1)
 ZVP (K) = WZVP ((NRSTRT * KBR / 2) + K - 1)
 ZAP (K) = WZAP ((NRSTRT * KBR / 2) + K - 1)
 WSP (K) = WZSP ((NRSTRT * KBR / 2) + K - 1)
 ZSIE (K) = WZSIE ((NRSTRT * KBR / 2) + K - 1)
 ZSIF (KBP2) = ZSIE (KBP1)
 ZTS (KBP2) = ZTS (KBP1)
 ZTQ (KBP2) = ZTQ (KBP1)
 ZLQ (KBP2) = ZLQ (KBP1)
 ZVP (KBP2) = ZVP (KBP1)
 ZAP (KBP2) = ZAP (KBP1)
 WSP (KBP2) = WSP (KBP1)
 95
 C RECOMPUTES DATA ASSOCIATED WITH DZ, DX FOR USE IN VM
 DX = 2.0 * DX
 DZ = 2.0 * DZ
 RDX = 1. / DX
 RDZ = 1. / DZ
 HDX = .5 * DX
 HDZ = .5 * DZ
 RDZS = 1. / (DZ * DZ)
 BETA = 5 * R0 / (RDX * RDX + RDZ * RDZ)
 EPSB = 4. * NU / A MIN1 (DX, DZ)
 FDXDZS = 1. / (RDX * RDX + RDZ * RDZ)
 X1 = FLOAT (IBR) * DX
 Z1 = FLOAT (KBR) * DZ
 RLENGTH = 1. / A MAX1 (X1, Z1)
 C BEGINS CELL BY CELL AVERAGING

```

DO 100 I=2,IBP1
DO 100 K=2,KBP1
IK=1+NWPC*((I-1)*KBP2)+K-1
IF(I.GT.IHALF.OB.K.GF.KHALF) GO TO 200
C COMPUTES INDICES FOR FLUID CELLS
J=2*(I-1)
L=2*(K-1)
IKR=1+NWPC*((J-1)*KBP2)+L-1
J=2*I-1
IPKP=1+NWPC*((J-1)*KBP2)+L-1
L=2*K-1
IPKPR=1+NWPC*((J-1)*KBP2)+L-1
J=2*(I-1)
IKPR=1+NWPC*((J-1)*KBP2)+L-1
C COMPUTES FLUID CELL DENSITIES FOR CELL MASS AVERAGING
CIT=CI-SIE(IKPR)
TEMPLL=SI(AI,BI,CIT,-1)
CIT=CI-SIE(IPKR)
TEMPLR=SI(AI,BI,CIT,-1)
CIT=CI-SIE(IKPR)
TEMPUL=SI(AI,BI,CIT,-1)
CIT=CI-SIE(IPKPR)
TEMPUR=SI(AI,BI,CIT,-1)
RHOLL=AR*TEMPLL+BR*TEMPLL+CR
RHOLR=AR*TEMPLR+BR*TEMPLR+CR
RHOUL=AR*TEMPUL+BR*TEMPUL+CR
RHOULR=AR*TEMPUR+BR*TEMPUR+CR
RHOSUM=RHOLL+RHOLR+RHOUL+RHOULR
C MASS AVERAGING OF FLUID CELLS FOR RESTART ON COARSER MESH
U(IK)=(U(IKPR)*RHOLL+U(IPKR)*RHOLR+U(IKPR)*RHOUL+U(IPKPR)*RHOULR)/RHOSUM
AOSUM
U(IK)=(U(IKPR)*RHOLL+U(IPKR)*RHOLR+U(IPKR)*RHOUL+U(IPKPR)*RHOULR)/RHOSUM
AOSUM
W(IK)=(W(IKPR)*RHOLL+W(IPKR)*RHOLR+W(IPKPR)*RHOUL+W(IPKPR)*RHOULR)/RHOSUM
AOSUM
WO(IK)=(WO(IKPR)*RHOLL+WO(IPKR)*RHOLR+WO(IPKPR)*RHOUL+WO(IPKPR)*RHOULR)/RHOSUM
AOSUM

```

```

RGBID55A 0253
RGBID55A 0254
RGBID55A 0255
RGBID55A 0256
RGBID55A 0257
RGBID55A 0258
RGBID55A 0259
RGBID55A 0260
RGBID55A 0261
RGBID55A 0262
RGBID55A 0263
RGBID55A 0264
RGBID55A 0265
RGBID55A 0266
RGBID55A 0267
RGBID55A 0268
RGBID55A 0269
RGBID55A 0270
RGBID55A 0271
RGBID55A 0272
RGBID55A 0273
RGBID55A 0274
RGBID55A 0275
RGBID55A 0276
RGBID55A 0277
RGBID55A 0278
RGBID55A 0279
RGBID55A 0280
RGBID55A 0281
RGBID55A 0282
RGBID55A 0283
RGBID55A 0284
RGBID55A 0285
RGBID55A 0286
RGBID55A 0287
RGBID55A 0288

```

```

A*RHOUR)/RHOSUM
TS(IK)=(TS(IKR)+TS(IPKR)+TS(IPKR))/4.00
TSO(IK)=(TSO(IKR)+TSO(IPKR)+TSO(IPKR))/4.0
TQ(IK)=(TQ(IKR)+RHOLL+TQ(IPKR)+RHOLR+TQ(IPKR)+RHOU+TQ(IPKR)
A*RHOUR)/RHOSUM
TQO(IK)=(TQO(IKR)+RHOLL+TQO(IPKR)+RHOLR+TQO(IPKR)+RHOUL+TQO(IPKR)
A*RHOUR)/RHOSUM
SIE(IK)=(SIE(IKR)+RHOLL+SIE(IPKR)+RHOLR+SIE(IPKR)+RHOUL+SIE(IPKR)
A*RHOUR)/RHOSUM
SIEO(IK)=(SIEO(IKR)+RHOLL+SIEO(IPKR)+RHOLR+SIEO(IPKR)+RHOUL+SIEO
APKPR)*RHOUR)/RHOSUM
CHI(IK)=(CHI(IKR)+CHI(IPKR)+CHI(IPKR))/4.0
CHIO(IK)=(CHIO(IKR)+CHIO(IPKR)+CHIO(IPKR))/4.0
VAP(IK)=(VAP(IKR)+VAP(IPKR)+VAP(IPKR))/4.0
VAPO(IK)=(VAPO(IKR)+VAPO(IPKR)+VAPO(IPKR))/4.0
LIQ(IK)=(LIQ(IKR)+LIQ(IPKR)+LIQ(IPKR))/4.0
LIQO(IK)=(LIQO(IKR)+LIQO(IPKR)+LIQO(IPKR))/4.0
P(IK)=0.0
GO TO 100
C INITIALIZATION OF CELLS THAT WEREN'T IN THE PREVIOUS RUN
200 U(IK)=0.0
UO(IK)=0.0
W(IK)=0.0
WO(IK)=0.0
SIE(IK)=ZSIE(K)
SIEO(IK)=ZSIEO(K)
TS(IK)=ZTS(K)
TSO(IK)=ZTSO(K)
TQ(IK)=ZTQ(K)
TQO(IK)=ZTQO(K)
CHI(IK)=BKGND
CHIO(IK)=BKGND
LIQ(IK)=ZLQ(K)
LIQO(IK)=ZLQO(K)
VAP(IK)=ZVP(K)
VAPO(IK)=ZVPO(K)

```

```

RGBID55A 0289
RGBID55A 0290
RGBID55A 0291
RGBID55A 0292
RGBID55A 0293
RGBID55A 0294
RGBID55A 0295
RGBID55A 0296
RGBID55A 0297
IRGBID55A 0298
RGBID55A 0299
RGBID55A 0300
RGBID55A 0301
RGBID70A 0302
RGBID70A 0303
RGBID70A 0304
RGBID70A 0305
RGBID55A 0306
RGBID55A 0307
RGBID55A 0308
RGBID55A 0309
RGBID55A 0310
RGBID55A 0311
RGBID55A 0312
RGBID55A 0313
RGBID55A 0314
RGBID55A 0315
RGBID55A 0316
RGBID55A 0317
RGBID55A 0318
RGBVM70A 0319
RGBVM70A 0320
RGBVM70A 0321
RGBVM70A 0322
RGBVM70A 0323
RGBVM70A 0324

```

```

P(IK) = 0.0
100 CONTINUE
    RETURN
    ENTRY FILMCO
    RETURN
    ENTRY FLMCAL
    RETURN
    ENTRY FLMINI
    RETURN
    ENTRY FLMFIN
    RETURN
    ENTRY FLMGEN
    RETURN
    ENTRY VREQ
    RETURN
    ENTRY VRFLM
    RETURN
    END
    FUNCTION SI(XTBL,YTBL,X,N)
    COMMON/PROP/SIGN
    DIMENSION XTBL(1),YTBL(1)
    IF(N.LT.0) GO TO 200
    IF(X.LT.XTBL(1)) GO TO 16
    IF(X.GT.XTBL(N)) GO TO 31
    DO 10 I=1,N
    IF(X.EQ.XTBL(I)) GO TO 21
    IF(X.LT.XTBL(I)) GO TO 26
10 CONTINUE
16 J1 = 1
   J2 = 2
   GO TO 50
21 SI = YTBL(I)
   GO TO 100
26 J1 = I-1
   J2 = I
   GO TO 50

```

```

RGBID55A
RGBID55A
RGBID55A

```

```

0325
0326
0327
0328
0329
0330
0331
0332
0333
0334
0335
0336
0337
0338
0339
0340
0341
0342
0343
0344
0345
0346
0347
0348
0349
0350
0351
0352
0353
0354
0355
0356
0357
0358
0359
0360

```



```

31 J1 = N-1
362 J2 = N
363 50 SI=YTBL(J1)+(YTBL(J2)-YTBL(J1))*(X-YTBL(J1))/(YTBL(J2)-YTBL(J1))
364 100 RETURN
365 C NOTE. ROOTS OF QUADRATIC EQUATION - A*X**2 + B*X + C =0.0 .
366 200 A=YTBL(1)
367 B=YTBL(1)
368 C=X
369 IF (A.NE.0.0) GO TO 205
370 SI=-1.0*C/B
371 RETURN
372 205 CONTINUE
373 D=B*B - 4.*A*C
374 IF ( D ) 210,220,220
375 210 PRINT 211
376 RETURN
377 220 DS=SQRT( D )
378 IF (SIGN) 224,224,226
379 224 SI = -1.0 * (B + DS) / (2.0 * A)
380 GO TO 230
381 226 SI = (DS - B) / (2.0 * A)
382 GO TO 230
383 230 CONTINUE
384 RETURN
385 C ***** FORMATS ***** FORMATS ***** .
386 211 FORMAT(1H ,28H ERROR - ROOTS ARE COMPLEX .)
387 END
388 SUBROUTINE VRPRT
389 DIMENSION TPT(50,50)
390 INTEGER BUFL,CF,CF1,CFB,CFC,CFL,CFR,CFS,CFT,CQF,ERF,TD,VNTP,
391 1VTP,CFOUT
392 REAL NU,LIQ,LIQO,LIQI,LOUT
393 DIMENSION UOUT(7),VOJT(7),IOUT(7),KOUT(7),CFOUT(7),QOUT(7),
394 1SOUT(7),TOUT(7),XOUT(7),GOUT(7),LOUT(7)
395 DIMENSION CF(1),CQ(1),QCON(1),P(1),RX(1),RZ(1),TQ(1),TS(1),U(1),
396 1 W(1),ER(1),FFX3(102),FFY3(102),PBTIN(2),UO(1),WO(1),TQO(1),

```

OLAY0029

RGBMN60A

RGBM06 0A

2 TSO (1), SIE (1), SIEO (1), CHI (1), CHIO (1)
 A, VAP (1), VAPO (1), LIQ (1), LIQO (1)
 3 , TYMF (25), FN (25), TYMT1 (25), T1N (25), TYMT2 (25), T2N (25),
 4 COFBA (25), COFBB (25), COFBC (25), COFTA (25), COFTB (25), COFTC (25),
 5 COFRA (25), COFRB (25), COFRC (25), COFLA (25), COFLB (25), COFLC (25),
 6 OFOFTA (25), OFOFTB (25), OFOFTC (25),
 7 OFOBFA (25), OFOBRB (25), OFOBRC (25), TAU (10), USL (32), USLOB (20),
 8 USROB (20), USTOB (20), USBOB (20)
 9, COFBD (25), COFBE (25), COFTD (25), COFTE (25), COFTF (25), COFBF (25),
 *COFRD (25), COFRE (25), COFLD (25), COFLE (25), COFRF (25), COPLF (25),
 AOFBTD (25), OFOBTE (25), OFOBRD (25), OFOBRE (25),
 B OFOBT (25), OFOBRF (25),
 C TYMT3 (25), TYMT4 (25), TYMT5 (25), T3N (25), T4N (25), T5N (25),
 * IICFR (1), IICFL (1), IICFT (1), IICFB (1)
 * , ZERO1 (1165), ZERO2 (608), ZERO3 (16), ZERO4 (3)
 DIMENSION ZSIE (22), ZIQ (22), ZTS (22), ZVP (22), ZLQ (22), ZAP (22), WSP (22) RGBVM62A
 DIMENSION TRSTRT (5), WZSIE (100), WZTQ (100), WZTS (100) RGBVM55A
 A, WZVP (100), WZLQ (100), WZAP (100), WWSP (100) RGBVM62A
 COMMON /VRCON /A (14000) RGBMM60A
 COMMON /RGB/RLAMB, CHII, GAMX, NRSTRT, TRSTRT, ZSIE, ZTQ, ZTS, WZSIE, WZTQ, RGBMM60B
 A WZTS, NPROF, WZVP, WZLQ, ZVP, ZLQ, GAML, GAMV, VAPI, LIQI
 B, WSP, WWSP, BKGND, DWNDS
 COMMON /VRCON/ ALP, ALPO, ALX, ALZ, B0, BETA, BUFL, CFI (9), CFS (9), CYL,
 1 DT, DX, DZ, EM6, EPS, ERF, PSLIP, GAM, GAM1, GX, GZ, HDX, HDZ, I, I1, I2, I2K2,
 2 IBP1, IBP2, IBR, IDATIN, IDIAG, IKP2, IOBS, IRSTRT, ITAPH, ITER, IVDI,
 3 IVDO, K, K1, K2, K2NC, KBP1, KBP2, KBR, KNC, KWB, KWL, KWR, KWT, LABEL (20),
 4 LPR, NCYC, NCYCB, NPRT, NU, NWPC, RDT, RDX, RDZ, RDZS, RIBKB, ROI, TD, TFIN,
 5 TIMET, TIOSUM, TPL, TPLT, TPR, TPRT, TQI, TSI, TTD, TWT, UI, WI
 * ,USR (32), UST (22), USB (22), USO (10), FFX3, FFX3
 6 ,AW, BW, CW, EPSB, UBLI, UBRI, WBI, WBTI, WEPS, WOB, WOT, NTPAS, TGAM, CSUBP,
 7 T0, SIEI, IDG, KDG, TI, MAT, RHO0, AT, TMU, TK, TYMF, FN, TYMT1, T1N, TYMT2,
 8 T2N, RPRAN, NRESEX, NFLOW, NT1, NT2, TSTEP, KDERBC, UOBI, COFBA, COFBB,
 9 COFBC, COFTA, COFTB, COFTC, COFRA, COFRB, COFRC, COFLA, COFLB, COFLC,
 * OFOFTA, OFOFTB, OFOFTC, OFOBRA, OFOBRB, OFOBR C, TAU, NTAU, USL,
 1 USLOB, USROB, USTOB, USBOB, UMAX, WMAX
 * ,CSUBPO, EPS0, RDXDZS, RLENGH , TQJET, TSJET

RGBMN01A
 RGBMN60A

0397
 0398
 0399
 0400
 0401
 0402
 0403
 0404
 0405
 0406
 0407
 0408
 0409
 0410
 0411
 0412
 0413
 0414
 0415
 0416
 0417
 0418
 0419
 0420
 0421
 0422
 0423
 0424
 0425
 0426
 0427
 0428
 0429
 0430
 0431
 0432

```

COMMON /VRMAT3/ AI,BI,CI,AR,BR,CR,AMU,BMU,CMU,AK,BK,CK,ACP,BCP,CCP
1      ,VMIN
COMMON/PROP/SIGN
COMMON/EXTRA/NT3,NT4,NT5,TYMT3,TYMT4,TYMT5,T3N,T4N,T5N,COFBD,
1COFBE,COFBE,COFTD,COFTE,COFTF,COFRD,COFRE,COFEF,COFLD,COFLE,
2COPLF,OFOBTD,OFOBTE,OFOBTF,OFOBRD,OFOBRE,OFOBRF,IRESET,
*NCYCLS,TADD,NIV,IOBRAN
COMMON/INDEX/NWPCL,K2NCL
COMMON /FLMCON/ DROU,DROU0,IPRFM
COMMON/LARGE/DIFFCO(2400)
EQUIVALENCE (A(1),CF), (A(2),U), (A(3),W), (A(4),P), (A(5),TQ),
1 (A(6),TS), (A(7),ER,CQ), (A(8),UO), (A(9),WO), (A(10),TQO),
2 (A(11),TSO), (A(12),SIE), (A(13),SIEO), (A(14),RX), (A(15),RZ),
3 (A(16),IICFR), (A(17),IICFL), (A(18),IICFT), (A(19),IICFB),
A (A(20),CHI), (A(21),CHIO),
B (A(22),VAP), (A(23),VAPO), (A(24),LIQ), (A(25),LIQO),
4 (ZERO1(1),ALP), (ZERO2(1),NT3), (ZERO3(1),AI), (ZERO4(1),DROU)
C NOTE. END - END OF NON-EXECUTABLE STATEMENTS .
C PRODUCES A CELL BY CELL OUTPUT OF STORED VARIABLES (22 X 22 ONLY)
WRITE(IVDO,5)
96 DO 103 ILOOP=1,4
IREST=(ILOOP-1)*5
97 DO 102 KLOOP=1,5
KREST=(KLOOP-1)*5
98 DO 100 KINV=1,5
K=23-KINV-KREST
IF(K.EQ.0) GO TO 101
DO 99 IPART=1,7
I=IPART+IREST
IK=1+NWPC*((I-1)*KBP2)+K-1)
UOUT(IPART)=U(IK)
VOUT(IPART)=W(IK)
IOUT(IPART)=I
KOUT(IPART)=K
CFOUT(IPART)=CF(IK)
QOUT(IPART)=TQ(IK)

```

RGBMN01A
RGBMN60A

```

SOUT (IPART) =TS (IK)
XOUT (IPART) =CHI (IK)
GOUT (IPART) =VAP (IK)
LOUT (IPART) =LIQ (IK)
SIEC =SIE (IK)
CIT =CI -SIEC
TOUT (IPART) =SI (AI, BI, CIT, -1)
IF (CF (IK) .GE. 30) TOUT (IPART) =P (IK)
99 CONTINUE
WRITE (IVDO, 20) (VOUT (L), L=1, 7)
WRITE (IVDO, 10)
WRITE (IVDO, 30) (IOUT (L), KOUT (L), L=1, 7)
WRITE (IVDO, 40) (TOUT (L), L=1, 7)
WRITE (IVDO, 10)
WRITE (IVDO, 50) (CFOUT (L), UOUT (L), L=1, 7)
WRITE (IVDO, 70) (SOUT (L), L=1, 7)
WRITE (IVDO, 60) (QOUT (L), L=1, 7)
WRITE (IVDO, 80) (XOUT (L), L=1, 7)
WRITE (IVDO, 85) (GOUT (L), L=1, 7)
WRITE (IVDO, 90) (LOUT (L), L=1, 7)
100 CONTINUE
101 WRITE (IVDO, 7) TIMET, NCYC, ITER, DT
WRITE (IVDO, 5)
102 CONTINUE
103 CONTINUE
RETURN
5 FORMAT ('1')
7 FORMAT (1H, 5HTIME=, 1PE12.4, 3H, , 14HCYCLE NUMBER =, I5, 3H, ,
1 28H PRESSURE ITERATION NUMBER =, I4, 3H, , 4HDT =, E12.4)
10 FORMAT ('1', 7 ('X', 17X))
20 FORMAT ('1', 7 (5HXXXXX, 1X, F7.3, 1X, 4HXXXXX))
30 FORMAT ('1', 7 (1HX, 5X, ' (', I2, ', ', I2, ') ', 5X))
40 FORMAT ('1', 7 (1HX, 3X, F7.3, 1X, ' F', 4X))
50 FORMAT ('1', 3X, 7 (4X, I2, 5X, F7.3))
60 FORMAT ('1', 7 (1HX, 2X, ' TKE=', 1PE10.3, 1X))
70 FORMAT ('1', 7 (1HX, 2X, ' TNU=', 1PE10.3, 1X))

```

0469 RGBM001A
 0470 RGBM060A
 0471 RGBM060A
 0472 RGBM060A
 0473
 0474
 0475
 0476
 0477
 0478
 0479
 0480
 0481
 0482
 0483
 0484
 0485
 0486
 0487
 0488
 0489
 0490
 0491
 0492
 0493
 0494
 0495
 0496
 0497
 0498
 0499
 0500
 0501
 0502
 0503
 0504

RGBM001A
 RGBM060A
 RGBM060A

```

80 FORMAT ( ' ', 7(1HX,2X,'CHI=',1PE10.3,1X))
85 FORMAT ( ' ', 7(1HX,2X,'VAP=',1PE10.3,1X))
90 FORMAT ( ' ', 7(1HX,2X,'LIQ=',1PE10.3,1X))
END
SUBROUTINE VSET
INTEGER BUFL,CF,CF1,CFB,CFC,CFI,CFL,CFR,CFS,CFT,CQF,ERF,TD,VNTP,
1 VTP
REAL NU,LIQ,LIQO,LIQI,LOUT
DIMENSION CF(1),CQ(1),QCON(1),P(1),RX(1),RZ(1),TQ(1),TS(1),U(1),
1 W(1),ER(1),FFX3(102),FFY3(102),PBTIM(2),UO(1),WO(1),TQO(1),
2 TSO(1),SIE(1),SIEC(1),CHI(1),CHIO(1)
A,VAP(1),VAPO(1),LIQ(1),LIQO(1)
3 TYMF(25),FN(25),TYMT1(25),T1N(25),TYMT2(25),T2N(25),
4 COFBA(25),COFBB(25),COFBC(25),COFTA(25),COFTB(25),COFTC(25),
5 COFRA(25),COFRB(25),COFRC(25),COFLA(25),COFLB(25),COFLC(25),
6 OFOBA(25),OFOBB(25),OFOBC(25),
7 OFOBA(25),OFOBB(25),OFOBR(25),TAU(10),USL(32),USLOB(20),
8 USROB(20),USTOB(20),USBOB(20)
9 COFBD(25),COFBE(25),COFTD(25),COFTE(25),COFTF(25),COFBF(25),
*COFRD(25),COFRE(25),COFLD(25),COFLE(25),COFRF(25),COPLF(25),
AOFBTD(25),OFOBTE(25),OFOBRD(25),OFOBRE(25),
R OFOBT(25),OFOBRF(25),
CTYMF3(25),TYMT4(25),TYMT5(25),T3N(25),T4N(25),T5N(25),
* IICFR(1),IICFL(1),IICFT(1),IICFB(1)
* ,ZERO1(1165),ZERO2(608),ZERO3(16),ZERO4(3)
DIMENSION ZSIE(22),ZTQ(22),ZTS(22),ZVP(22),ZLQ(22),ZAP(22),WSP(22)
DIMENSION TRSTRT(5),WZSIE(100),WZTQ(100),WZTS(100)
A,WZVP(100),WZLQ(100),WZAP(100),WZSP(100)
COMMON/VRCOM/A(14000)
COMMON/RGB/RLAMB,CHII,GAMX,NRSTRT,TRSTRT,ZSIE,ZTQ,ZTS,WZSIE,WZTQ,
AWZTS,NPROF,WZVP,WZLQ,ZVP,ZLQ,GAML,GAMV,VAPI,LIQI
B,WSP,WZSP,BKGND,DWZS
COMMON/VRCON/ALP,ALP0,ALX,ALZ,B0,BETA,BUFL,CPI(9),CFS(9),CYL,
1 DT,DX,DZ,EM6,EPS,ERF,FSLIP,GAM,GAM1,GX,GZ,HDX,HDZ,I,I1,I2,I2K2,
2 IBP1,IBP2,IBR,IDATIN,IDIAG,IKP2,IOBS,IRSTRT,ITAPW,ITER,IVDI,
3 IVDO,K,K1,K2,K2NC,KBP1,KBP2,KBR,KNC,KWB,KWL,KWR,KWT,LABEL(20),

```

```

RGBM001A 0505
R3BM060A 0506
RGBM060A 0507
0508
0509
0510
0511
0512
0513
0514
0515
0516
0517
0518
0519
0520
0521
0522
0523
0524
0525
0526
0527
0528
0529
0530
0531
0532
0533
0534
0535
0536
0537
0538
0539
0540

```

```

4 LPR,NCYC,NCYCB,NPRT,NU,NWPC,RDT,RDX,RDZ,RDZS,RIBKB,ROI,TD,TFIN,
5 TIMET,TIOSUM,TPL,FPLT,TPR,TPRT,TQI,TSI,TTD,TWTD,UI,WI
6 ,JSR(32),UST(22),USB(22),USO(10),FFX3,FFY3
7 ,AW,BW,CW,EPSB,UBLI,UBRI,WBBI,WBTI,WEPS,WOBI,NTPAS,TGAM,CSUBP,
8 TO,SIEI,IDG,KDG,TI,MAT,RHO,AT,TMU,TK,TYMF,FN,TYMT1,T1N,TYMT2,
9 T2N,PPRAN,NRESEX,NFLOW,NT1,NT2,TSTEP,KDERBC,UOBI,COFBA,COFBR,
* COFBC,COFTA,COFTE,COFTC,COFRA,COFRB,COFRC,COFLA,COFLB,COFLC,
* OFOBTA,OFOBTB,OFOBTC,OFOBRA,OFOBRB,OFOBRF,TAU,NTAU,USL,
1 USLOB,USROB,USTOB,USBOB,UMAX,WMAX
* ,CSUBPO,EPSO,RDXDZS,FLENGH,TQJET,TSJET
COMMON /FLMCON/ DROU,DROU0,I PRFM
COMMON /VRMAT3/ AI,BI,CI,AR,BR,CR,AMU,BMU,CMU,AK,BK,CK,ACP,BCP,CCP
1 ,VMIN
COMMON/PROP/SIGN
COMMON/EXTRA/NT3,NT4,NT5,TYMT3,TYMT4,TYMT5,T3N,T4N,T5N,COFBD,
1COFBE,COFBF,COFTD,COFTE,COFTF,COFRD,COFRE,COFRF,COFLD,COFLE,
2COFLF,OFOBTD,OFOBTE,OFOBTF,OFOBRD,OFOBRE,OFOBRF,IRESET,
3 NCYCLS,TADD,NIV,IOBRAN
COMMON/INDEX/NWPCL,K2NCL
COMMON/LARGE/DIFFCO(2400)
EQUI VALENCE (A(1),CF), (A(2),U), (A(3),W), (A(4),P), (A(5),TQ),
1 (A(6),TS), (A(7),ER,CQ), (A(8),UO), (A(9),WO), (A(10),TQO),
2 (A(11),TSO), (A(12),SIE), (A(13),SIEO), (A(14),RX), (A(15),RZ),
3 (A(16),IICFR), (A(17),IICFL), (A(18),IICFT), (A(19),IICFB),
A (A(20),CHI), (A(21),CHIO),
B (A(22),VAP), (A(23),VAPO), (A(24),LIQ), (A(25),LIQO),
4 (ZERO1(1),ALP), (ZERO2(1),NT3), (ZERO3(1),AI), (ZERO4(1),DROU)
C NOTE. END - END OF NON-EXECUTABLE STATEMENTS .
C
C
C
C NOTE. VSET IS RESPONSIBLE FOR MESH, PARTICLE AND FILM INITIALIZATION .
C
C
C IDATIN=0
C IF( IBR.EQ.0 ) CALL TAPREA
C NOTE. READS,WRITES PRIMARY INPUT DATA .
C READ(IVDI,1) LABEL

```

RGBMN01A
RGBMN60A

```

READ (IVDI,2) DT,TPRT,TPLT,TWTD,TFIN,ITAPW,NPRT,IDIAG,LPR,IOBS 0577
1 ,IDG,KDG 0578
WRITE (IVDO,50) IBR,KBR,IPRPM,NCYCLS,TADD,IRESET 0579
WRITE (IVDO,1) LABEL 0580
WRITE (IVDO,51) DT,TPRT,TPLT,TWTD,TFIN,ITAPW,NPRT,IDIAG,LPR,IOBS 0581
1 ,IDG,KDG 0582
RDT=1./DT 0583
IF ( IPRPM.LT.1 ) TPLT=2.*TFIN 0584
TPL=TPLT 0585
TPR=TPRT 0586
TTD=TWTD 0587
IF ( IDATIN.LT.1 ) GO TO 100 0588
TIMET=TIMET+TADD 0589
TWTD=TIMET 0590
TPRT=TWTD 0591
TPLT=TPRT 0592
CALL MESHMK 0593
IF (IPRPM.LT.1) GO TO 500 0594
CALL FLNGEN 0595
CALL FILMCO 0596
GO TO 500 0597
C NOTE. INITIALIZES CONSTANTS . 0598
100 TIMET=0.0 0599
IRSTRT=0 0600
TD=0 0601
NCYC=0 0602
NCYCB=0 0603
EM6=1.E-6 0604
IRP1=IBR + 1 0605
KBP1=KBR+1 0606
IBP2=IBR +2 0607
KBP2=KBR+2 0608
I2K2=IBP2*KBP2*NWPC 0609
KNC=KBR*NWPC 0610
K2NC=KBP2*NWPC 0611
VRS12001 0612
VRS12002
VRS12014
VRS12402
VRS12404
VRS12406
VRS12408
VRS12412
PAGE 17

```

```

K2NCL = KBP2 * NWPCL
IKP2=IBR*K2NC
IKM =I2K2 + 2*K2NC
RIBKB=1./FLOAT(IBR*KBR)
C NOTE. GENERATES BOTH MESH AND FILM REGIONS , RESPECTIVELY .
CALL MESHMK
IF( IPRFM.LT.1 ) GO TO 2000
CALL PLMGEN
CALL FILMCO
2000 WRITE(IVDO,60)
500 K2NCL=KBP2*NWPCL
WRITE(IVDO,70)
WRITE(IVDO,80)
I1=2
K1=2
I2=IBP1
K2 = KBP1
KKL = 0
KK = 0
DO 511 I=I1,I2
KK = KK + K2NC
KKL = KKL + K2NCL
LWPC = 1
LWPCL = 1
DO 510 K=K1,K2
LWPC = LWPC + NWPCL
LWPCL = LWPCL + NWPCL
IK = KK + LWPC
IKL = KKL + LWPCL
IPK = IK + K2NC
IMK = IK - K2NC
IKP = JK + NWPCL
IKM = IK - NWPCL
CPC = CF(IK)
CFR = CF(IPK)
CFL = CP(IMK)

```

VRS12420

0613
0614
0615
0616
0617
0618
0619
0620
0621
0622
0623
0624
0625
0626
0627
0628
0629
0630
0631
0632
0633
0634
0635
0636
0637
0638
0639
0640
0641
0642
0643
0644
0645
0646
0647
0648


```

0649 CPT = CF (IKP)
0650 CFB = CF (IKM)
0651 IF (CFC.NE.1) GO TO 510
0652 IF (CFR.NE.1) DIFFCO ( IKL ) = 0.0
0653 IF (CFL.NE.1) DIFFCO (IKL+2) = 0.0
0654 IF (CPT.NE.1) DIFFCO ( IKL+1) = 0.0
0655 IF (CFB.NE.1) DIFFCO ( IKL+3) = 0.0
0656 DCR = DIFFCO (IKL)
0657 DCT = DIFFCO (IKL+1)
0658 DCL = DIFFCO (IKL+2)
0659 DCB = DIFFCO (IKL+3)
0660 WRITE (I VDO, 75) I, K, IK, IKL, CFC, CFR, CPT, CFL, CFB, DCR, DCT, DCL, DCB
0661
0662
0663
0664
0665
0666
0667
0668
0669
0670
0671
0672
0673
0674
0675
0676
0677
0678
0679
0680
0681
0682
0683
0684

```

```

510 CONTINUE
511 CONTINUE
520 RETURN
C ***** FORMATS ***** FORMATS ***** .
1 FORMAT (20A4)
2 FORMAT (5F8.3, 5I2, 2I3)
50 FORMAT (1H, 4X, 4HIBR=, I5, /, 5X, 4HKBR=, I5, /, 3X, 6HIPRFM=, I2, /, 5X,
1 8HNCYCLST=, I10, /, 5X, 5HTADD=, E12.5, 5X, 7HIRESET=, I5)
51 FORMAT (1H, 5X, 3HDT=, 1PE12.5/4X, 5HTPRT=, E12.5/4X, 5HTPLT=, E12.5/
1 4X, 5HTWTD=, E12.5/4X, 5HTPIN=, E12.5/3X, 6HITAPW=, I2/4X, 5HNPRT=, I2/
2 3X, 6HIDIAG=, I2/5X, 4H1PR=, I2/4X, 5HI OBS=, I2/5X, 4HIDG=, I3/5X, 4HKDG=,
3 I3)
52 FORMAT (1H, 104H *** ERROR 001 - MESH ARRAY A () IS DIMENSIONED TOO
1SMALL FOR MESH PARAMETERS, I.E. I BR AND KBR . ***)
60 FORMAT (1H, 63H NOTE. COMPLETION OF VSET - VARR II SET UP G
1ENERATION .)
70 FORMAT (1H1)
75 FORMAT (1H, 9I6, 4F6.1)
80 FORMAT (1H, 5X, 1H, 5X, 1HK, 4X, 2HIK, 3X, 3HIKL, 3X, 3HCPC, 3X, 3HCPR, 3X,
1 3HCPT, 3X, 3HCFL, 3X, 3HCFB, 3X, 3HDCR, 3X, 3HDCT, 3X, 3HDCL, 3X, 3HDCB)
END
SUBROUTINE MESHMK
INTEGER BUFL, CF, CF1, CFB, CFC, CFI, CFL, CFR, CFS, CFT, CQF, ERF, TD, VNTP,
1 VTP
VRS999999

```

```

REAL NU, LIQ, LIQO, LIQI, LOUT
DIMENSION CF(1), CQ(1), QCON(1), P(1), RX(1), RZ(1), TQ(1), TS(1), U(1),
1 W(1), ER(1), FFX3(102), FFX3(102), PBTIM(2), UC(1), WO(1), TQO(1),
2 TSO(1), SIE(1), SIE(1), SIE(1), CHI(1), CHIO(1)
A, VAP(1), VAPO(1), LIQ(1), LIQO(1)
3 , TYMP(25), FN(25), TYMT1(25), T1N(25), TYMT2(25), T2N(25),
4 COFBA(25), COFBB(25), COFBC(25), COFTA(25), COFTB(25), COFTC(25),
5 COFRA(25), COFRB(25), COFRC(25), COFLA(25), COFLB(25), COFLC(25),
6 COFTA(25), COFTB(25), COFTC(25),
7 OFOBRA(25), OFOBRB(25), OFOBR(25), TAU(10), USL(32), USLOB(20),
8 USROB(20), USTOB(20), USBOB(20)
9 , COFBD(25), COFBE(25), COFTD(25), COFTE(25), COFTF(25), COFBF(25),
* COFRD(25), COFRE(25), COFLD(25), COFLE(25), COFRP(25), COFLP(25),
A OFOBD(25), OFOBTE(25), OFOBRD(25), OFOBRE(25),
B OFOBTF(25), OFOBRF(25),
C TYMT3(25), TYMT4(25), TYMT5(25), T3N(25), T4N(25), T5N(25),
* IICPR(1), IICFL(1), IICFT(1), IICPB(1)
* , ZERO1(1165), ZERO2(608), ZERO3(16), ZERO4(3)
DIMENSION ZSIE(22), ZTQ(22), ZTS(22), ZVP(22), ZLQ(22), ZAP(22), WSP(22)
DIMENSION TRSTRT(5), WZSIE(100), WZTQ(100), WZTS(100)
A, WZVP(100), WZLQ(100), WZAP(100), WWSP(100)
COMMON /VRCON/A(14000)
COMMON /RGB/RIAMB, CHII, GAMX, NRSTRT, TRSTRT, ZSIE, ZTQ, ZTS, WZSIE, WZTQ,
AWZTS, NPROP, WZVP, WZLQ, ZVP, ZLQ, GAML, GAMV, VA PI, LIQI
B, WSP, WWSP, BKGND, DWNDS
COMMON /VRCON/ ALP, ALP0, ALX, ALZ, B0, BETA, BUFL, CPI(9), CFS(9), CYL,
1 DT, DX, DZ, EM6, EPS, ERF, FSLIP, GAM, GAM1, GX, GZ, HDX, HDZ, I, I1, I2, I2K2,
2 IBP1, IBP2, IBR, IDATIN, IDIAG, IKP2, IOBS, IRSTRT, ITAPW, ITER, IVDI,
3 IVDO, K, K1, K2, K2NC, KBP1, KBP2, KBR, KNC, KWB, KWL, KWR, KWT, LABEL(20),
4 LPR, NCYC, NCYCB, NPRT, NU, NNPC, RDT, RDX, RDZ, RDZS, RIBKB, ROI, TD, TFIN,
5 TIMET, TIOSUM, TPL, TPLT, TPR, TPRT, TOI, TSI, TTD, TWT, UI, WI
* , USR(32), UST(22), USB(22), USO(10), FFX3, FFX3
6 , AW, BW, CW, EPSB, UBUI, UBRI, WBI, WBTI, WEPS, WBI, NTPAS, TGAM, CSUBP,
7 TQ, SIEI, IDG, KDG, TI, MAT, RHO0, AT, TMU, TK, TYMP, FN, TYMT1, T1N, TYMT2,
8 T2N, RPRAN, NRESEX, NFLOW, NT1, NT2, TSTEP, KDERBC, UOBI, COFBA, COFBB,
9 COFBC, COFTA, COFTB, COFTC, COFRA, COFRB, COFRC, COFLA, COFLB, COFLC,

```

RGBMN6 0A

RGBMN01A
RGBMN60A

RGBVM62A
RGBVM55A
RGBVM62A
RGBMN60A
R3BVM55A
RGBMN60A
RGBMN6 0B

0685
0686
0687
0688
0689
0690
0691
0692
0693
0694
0695
0696
0697
0698
0699
0700
0701
0702
0703
0704
0705
0706
0707
0708
0709
0710
0711
0712
0713
0714
0715
0716
0717
0718
0719
0720

```

* OFOBT A, OFOBT B, OFOBT C, OFOBR A, OFOBR B, OFOBR C, TAU, NTAU, USL,
1 USLOB, USROB, USTOB, USBOB, UMAX, WMAX
* ,CSUBPO, EPSO, RDXDZS, RLENGH , TQJET, TSJET
COMMON /FLMCON/ DROU, DROUO, IPRFM
COMMON /VRMAT3/ AI, BI, CI, AR, BR, CR, AMU, BMU, CMU, AK, BK, CK, ACP, BCP, CCP
1
COMMON/PROP/SIGN
COMMON/EXTRA/NT3, NT4, NT5, TYMT3, TYMT4, TYMT5, T3N, T4N, T5N, COFBD,
1COFBE, COFBE, COFTD, COFTE, COFTF, COFRD, COFRE, COFRF, COFLD, COFLE,
2COPLF, OFOBT D, OFOBT E, OFOBT F, OFOBR D, OFOBR E, OFOBR F, IRESET,
*NCYCLS, TADD, NIV, IOBRAN
COMMON/INDEX/NWPC, K2NCL
COMMON/LARGE/DIFFCO(2400)
EQUIVALENCE (A(1), CF), (A(2), U), (A(3), W), (A(4), P), (A(5), TQ),
1 (A(6), TS), (A(7), ER, CO), (A(8), UO), (A(9), WO), (A(10), TQO),
2 (A(11), TSO), (A(12), SIE), (A(13), SIEO), (A(14), RX), (A(15), RZ),
3 (A(16), IICFR), (A(17), IICFL), (A(18), IICFT), (A(19), IICFB),
A (A(20), CHI), (A(21), CHIO),
B (A(22), VAP), (A(23), VAPO), (A(24), LIQ), (A(25), LIQO),
4 (ZFRO1(1), ALP), (ZFRO2(1), NT3), (ZFRO3(1), AI), (ZFRO4(1), DROU)
C NOTE. END - END OF NON-EXECUTABLE STATEMENTS .
C
C NOTE. MESHK IS RESPONSIBLE FOR GENERATION OF MESH SUBREGIONS .
C NOTE. READS, WRITES PRIMARY MESH INPUT DATA .
READ (IVDI, 1) DX, DZ, GX, GZ, ALX, ALZ, CYL, BO, EPS, VMIN
READ (IVDI, 2) KWR, KWL, KWT, KWB, FSLIP, ALP, GAM, ALPO, GAM1, NU, TQJET,
* TSJET
READ (IVDI, 7) AM, BW, CW, WEPS, KDERBC, UBRI, UBLI, WBTI, WBTI, WBTI, WBTI
READ (IVDI, 8) WOB, UOBI, CSUBPO
READ (IVDI, 10) TGAM, TO, TI, TSTEP, MAT, NRESEX
READ (IVDI, 1) AI, BI, CI, AR, BR, CR, AMU, BMU, CMU
READ (IVDI, 1) AK, BK, CK, ACP, BCP, CCP, SIGN
READ (IVDI, 11) NFLOW, NT1, NT2, NT3, NT4, NT5, NTAU
WRITE (IVDO, 61) NFLOW, NT1, NT2, NT3, NT4, NT5, NTAU
IF (NFLOW.GT.0) GO TO 190
NIV=1.0

```

RGBMN01A
RGBMN60A

MESH 6

```

190 NFLOW = NFLOW
    CONTINUE
    READ (IVDI, 12)
    READ (IVDI, 12)
    READ (IVDI, 12)
    IF (NT3.EQ.0) GO TO 195
    READ (IVDI, 12)
    IF (NT4.EQ.0) GO TO 195
    READ (IVDI, 12)
    IF (NT5.EQ.0) GO TO 195
    READ (IVDI, 12)
195 CONTINUE
    IF ( NTAU.LT.1 ) GO TO 200
    READ (IVDI, 12) ( TAU(I), I=1, NTAU )
    C NOTE. READ COEFFICIENTS A, B, AND C FOR THE BOTTOM EXTERIOR BOUNDARY .
200 READ (IVDI, 13) I, COFA, COFB, COFC, COFD, COFE, COFF
    IF ( I.LT.1 ) GO TO 210
    COFBA(I) = COFA
    COFBB(I) = COFB
    COFBC(I) = COFC
    COFBD(I) = COFD
    COFBE(I) = COFE
    COFBF(I) = COFF
    WRITE (IVDO, 64) I, COFBA(I), COFBB(I), COFBC(I), COFBD(I), COFBE(I),
1 COFBF(I)
    GO TO 200
    C NOTE. READ COEFFICIENTS A, B, AND C FOR THE TOP EXTERIOR BOUNDARY .
210 READ (IVDI, 13) I, COFA, COFB, COFC, COFD, COFE, COFF
    IF ( I.LT.1 ) GO TO 220
    COFTA(I) = COFA
    COFTB(I) = COFB
    COFTC(I) = COFC
    COFTD(I) = COFD
    COFTE(I) = COFE
    COFTF(I) = COFF
    WRITE (IVDO, 64) I, COFTA(I), COFTB(I), COFTC(I), COFTD(I), COFTE(I),
0757
0758
0759
0760
0761
0762
0763
0764
0765
0766
0767
0768
0769
0770
0771
0772
0773
0774
0775
0776
0777
0778
0779
0780
0781
0782
0783
0784
0785
0786
0787
0788
0789
0790
0791
0792

```

```

1 COPTF(I)
GO TO 210
C NOTE. READ COEFFICIENTS A, B, AND C FOR THE RIGHT EXTERIOR BOUNDARY .
220 READ (IVDI, 13) I, COFA, COFB, COFC, COFD, COFE, COFF
IF ( I. LT. 1 ) GO TO 230
COFRA (I) =COFA
COFRB (I) =COFB
COFRC (I) =COFC
COFRD (I) =COFD
COFRE (I) =COFE
COFRF (I) =COFF
WRITE (IVDO, 64) I, COFRA (I), COFRB (I), COFRC (I), COFRD (I), COFRE (I),
1 COFRF (I)
GO TO 220
C NOTE. READ COEFFICIENTS A, B, AND C FOR THE LEFT EXTERIOR BOUNDARY .
230 READ (IVDI, 13) I, COFA, COFB, COFC, COFD, COFE, COFF
IF ( I. LT. 1 ) GO TO 240
COFLA (I) =COFA
COFLB (I) =COFB
COFLC (I) =COFC
COFLD (I) =COFD
COFLE (I) =COFE
COFLF (I) =COFF
WRITE (IVDO, 64) I, COFLA (I), COFLB (I), COFLC (I), COFLD (I), COFLE (I),
1 COFLF (I)
GO TO 230
C NOTE. READ COEFFICIENTS A, B, AND C FOR THE TOP INTERIOR OBSTACLE .
240 READ (IVDI, 13) I, COFA, COFB, COFC, COFD, COFE, COFF
IF ( I. LT. 1 ) GO TO 250
OFOTBTA (I) =COFA
OFOTB (I) =COFB
OFOTC (I) =COFC
OFOTD (I) =COFD
OFOTE (I) =COFE
OFOTF (I) =COFF
WRITE (IVDO, 64) I, OFOTBTA (I), OFOTB (I), OFOTC (I), OFOTD (I), OFOTE (I),

```

0793
0794
0795
0796
0797
0798
0799
0800
0801
0802
0803
0804
0805
0806
0807
0808
0809
0810
0811
0812
0813
0814
0815
0816
0817
0818
0819
0820
0821
0822
0823
0824
0825
0826
0827
0828

```

0829 1OFOBTE (I), OFOBTFF (I)
0830 GO TO 240
0831 C NOTE. READ COEFFICIENTS A, B, AND C FOR THE RIGHT INTERIOR OBSTACLE .
0832 250 READ (IVDI, 13) I, COFA, COFB, COFC, COFD, COFE, COFF
0833 IF ( I.LT. 1 ) GO TO 310
0834 OFOBRA (I) =COFA
0835 OFOBRB (I) =COFB
0836 OFOBRC (I) =COFC
0837 OFOBRD (I) =COFD
0838 OFOBRE (I) =COFE
0839 OFOBRF (I) =COFF
0840 WRITE (IVDO, 64) I, OFOBRA (I), OFOBRB (I), OFOBRC (I), OFOBRD (I),
0841 1OFOBRE (I), OFOBRF (I)
0842 GO TO 250
0843 310 READ (IVDI, 14) I, K, RXC, RZC
0844 WRITE (IVDO, 65) I, K, RXC, RZC
0845 IF ( I.LT. 1 ) GO TO 320
0846 IK = (K-1) *NWPC + (I-1) *K2NC + 1
0847 RX (IK) =RXC
0848 RZ (IK) =RZC
0849 GO TO 310
0850 320 CONTINUE
0851 WRITE (IVDO, 50) DX, DZ, GX, GZ, ALX, ALZ, CYL, B0, EPS, VMIN MESH 8
0852 WRITE (IVDO, 51) KWR, KWL, KWT, KWB, FSLIP, ALP, GAM, ALPO, GAM1, NU, TQJET,
0853 * TSJET
0854 WRITE (IVDO, 59) AM, BW, CW, WEPS, KDERBC, UBRI, UBLI, WBTI, WBTI
0855 WRITE (IVDO, 58) WOB, UOBI, CSUBPO
0856 WRITE (IVDO, 60) TGAM, TO, TI, TSTEP, MAT, NRESEX
0857 WRITE (IVDO, 52) AI, BI, CI, AP, BR, CR, AMU, BMU, CMU
0858 WRITE (IVDO, 53) AK, BK, CK, ACP, BCP, CCP, SIGN
0859 WRITE (IVDO, 61) NPLOW, NT1, NT2, NTAU
0860 WRITE (IVDO, 57) ( TAU (I), I =1, NTAU )
0861 NMAX =AMAX0 ( NPLOW, NT1, NT2 )
0862 WRITE (IVDO, 62)
0863 DO 319 I =1, NMAX
0864 WRITE (IVDO, 63) I, TYMF (I), FN (I), TYMT1 (I), T1N (I), TYMT2 (I), T2N (I)

```

```

319 CONTINUE
      NMAX=AMAX0(NT3,NT4,NT5)
      DO 321 I=1,NMAX
        WRITE(IVDO,66) TYMT3(I),T3N(I),TYMT4(I),T4N(I),TYMT5(I),T5N(I)
      CONTINUE
321  C NOTE. GENERATION OF MESH CELL SIZES .
      RDX=1./DX
      RDZ=1./DZ
      HDX=.5*DZ
      HDZ=.5*DZ
      RDZS=1./(DZ*DZ)
      BETA=.5*B0/(RDX*RDX + RDZ*RDZ)
      IF ( KDERBC.GT.0 ) FSLIP=1.0
      IF ( CYL.GT.1.E-6 ) KWL=1
      EPSB=4.*NU/AMIN1 ( DX,DZ )
      NTPAS=1
      IF ( ALX.LT.EM6 .OR. ALZ.LT.EM6 ) NTPAS=2
      RDZDS=1./ ( RDX*RDX + RDZ*RDZ )
      X1=FLOAT( IBER ) *DX
      Z1=FLOAT( KBR ) *DZ
      RLENGH=1./AMAX1( X1,Z1 )
      EPS0=EPS
      TR=TI + 459.7
      C NOTE. CALCULATION OF SPECIFIC MATERIAL FOR SIE INITIAL AND RHO0 .
      GO TO( 400,420,440,460 ),MAT
      C NOTE. COMPUTATION FOR SODIUM MATERIAL .
400  SIEII=0.38935*TR - 0.553E-4*TR**2 + 0.1137E-7*TR**3 - 29.02
      RHOII=59.566 - 7.9504E-3*TI - .2872E-6*TI**2 + 0.06035E-9*TI**3
      RHOO=59.566 - 7.9504E-3*T0 - 0.2872E-6*T0**2 + 0.06035E-9*T0**3
      AT=397.17/TR + 1.0203
      TMU=(10.0**AT/3600.)/TR**0.4925
      NU=TMU/RHOII
      TK=0.015085 - 5.2167E-6*TI + 5.809E-10*TI**2
      CSUBP=0.38935 - 1.106E-4*TI + 0.3411E-7*TI**2
      RPRAN=TK/( CSUBP*TMU )
      GO TO 500

```

```

VRS12004
VRS12006
VRS12018
VRS12020

VRS12022

```

```

C NOTE. COMPUTATION FOR WATER MATERIAL .
420 SIEI=1.0004*TI - 32.013
RHOII=62.742 - 0.372E-2*TI - 0.44E-4*TI**2
RHO = 62.742 - 0.372E-2*TC - 0.44E-4*TC**2
BT=446.0/( TI+207.0 ) - 5.0
TMU=1.622*10.**BT
NU=TMU/RHOII
TK=8.369E-5 + 2.368E-7*TI - 5.89E-10*TI**2
CSUBP=1.0004
RPRAN=TK/( CSUBP*TMU )
GO TO 500

440 SIEI= AI*TI*TI + BI*TI + CI
RHOII= AR*TI*TI + BR*TI + CR
RHO = AR*TO*TO + BR*TO + CR
TMU = AMU*TI*TI + BMU*TI + CMU
TK = AK*TI*TI + BK*TI + CK
CSURP= ACP*TI*TI + BCP*TI + CCP
NU=TMU/RHOII
RPRAN=TK/( CSUBP*TMU )
GO TO 500

460 CONTINUE
NU=TMU/RHOII
RPRAN=TK/( CSUBP*TMU )
C NOTE. NL=NUMBER OF LEFT MOST CELL , NR=NUMBER OF RIGHT MOST CELL ,
C NOTE. GENERATION OF INTERIOR MESH CELLS , I.E. FLUID AND OBSTACLE .
500 IF (IDATIN.GT.0.AND.IRESET.EQ.0) GO TO 590
READ(IVDI,5) NL,NR,NB,NT,ICELTY
WRITE(IVDO,54) NL,NR,NB,NT,ICELTY
IF( NL.EQ.0 ) GO TO 700
READ(IVDI,6) SIEI,TQI,TSI,UI,WI,CHII,VAPI,LIQI
WRITE(IVDO,55) SIEI,TQI,TSI,UI,WI,CHII,VAPI,LIQI
I1=NL
I2=NR
K1=NB
K2=NT
KK=1 + ( I1-2 ) * K2NC

```

RGBMK60A
RGBMK60A


```

DO 589 I=I1,I2
KK=KK + K2NC
LWPC=(K1-2)*NWPC
DO 579 K=K1,K2
LWPC=LWPC + NWPC
IK=KK + LWPC
CF(IK)=ICELTY
C NOTE. FOR OBSTACLES WITH TAU FACTORS - SET SIEI = OBSTACLE TEMPERA -
C NOTE. TURE IN F DEGREES .
SIE(IK)=SIEI
IF( ICELTY.GE.30 .AND. NTAU.GT.0 ) P(IK)=SIEI
TQ(IK)=TQI
TS(IK)=TSI
U(IK)=UI
W(IK)=WI
CHI(IK)=CHII
VAP(IK)=VAPI
LIQ(IK)=LIQI
SIEO(IK)=SIEO(IK)
TQO(IK)=TQO(IK)
TSO(IK)=TSO(IK)
UO(IK)=UO(IK)
WO(IK)=WO(IK)
CHIO(IK)=CHIO(IK)
VAPO(IK)=VAPO(IK)
LIQO(IK)=LIQO(IK)
578 CONTINUE
579 CONTINUE
589 CONTINUE
GO TO 500
590 CONTINUE
C NOTE. GENERATION OF EXTERIOR BOUNDRY MESH CELLS .
700 I1=1
TSMAX=-1.0E+20
TMAX=TSMAX
WMAX=TMAX

```

RGBMK01A

RGBMK02A
RGBMK60A
RGBMK60A

R3BMK02A
R3BMK60A
R3BMK60A

```

UMAX=WMAX
TSMIN=+1.0E+20
TMIN=TSMIN
WMIN=TMIN
UMIN=WMIN
TQMAX=-1.E+20
I2=IBP2
K1=1
K2=KBP2
KK=1 + (I1-2)*K2NC
DO 789 I=I1, I2
KK=KK + K2NC
LWPC=(K1-2)*NWPC
DO 779 K=K1, K2
LWPC=LWPC + NWPC
IK=KK + LWPC
UMAX=AMAX1( UMAX, U( IK ) )
WMAX=AMAX1( WMAX, W( IK ) )
UMIN=AMIN1( UMIN, U( IK ) )
WMIN=AMIN1( WMIN, W( IK ) )
TSMAX=AMAX1( TSMAX, TS( IK ) )
TSMIN=AMIN1( TSMIN, TS( IK ) )
TQMAX=AMAX1( TQMAX, TQ( IK ) )
CFC= CF( IK )
IF( K.EQ.K1 .AND. CFC.LT.11 ) CF( IK )=10
IF( K.EQ.K2 .AND. CFC.LT.11 ) CF( IK )=10
IF( I.EQ.I1 .AND. CFC.LT.11 ) CF( IK )=10
IF( I.EQ.I2 .AND. CFC.LT.11 ) CF( IK )=10
IF( I.EQ.I1 .AND. K.EQ.K1 ) CF( IK )=2
IF( I.EQ.I1 .AND. K.EQ.K2 ) CF( IK )=2
IF( I.EQ.I2 .AND. K.EQ.K1 ) CF( IK )=2
IF( I.EQ.I2 .AND. K.EQ.K2 ) CF( IK )=2
IF( CFC.LT.20 .OR. ICBS.EQ.0 ) GO TO 770
C NOTE. FLAGS CELLS SURROUNDING THE OBSTACLE CELL.
CFR=CF( IK+K2NC )
CFL=CF( IK-K2NC )

```

```

0973
0974
0975
0976
0977
0978
0979
0980
0981
0982
0983
0984
0985
0986
0987
0988
0989
0990
0991
0992
0993
0994
0995
0996
0997
0998
0999
1000
1001
1002
1003
1004
1005
1006
1007
1008

```

```

CFT=CF (IK+NWPC)
CFB=CF (IK-NWPC)
IICFR (IK) =1
IICFL (IK) =1
IICFT (IK) =1
IICFB (IK) =1
IF (CPR.NE.1) IICFR (IK) =0
IF (CPL.NE.1) IICFL (IK) =0
IF (CPT.NE.1) IICFT (IK) =0
IF (CFB.NE.1) IICFB (IK) =0
770 CONTINUE
779 CONTINUE
789 CONTINUE
RETURN
C ***** FORMATS ***** FORMATS ***** .
1 FORMAT (10F8.3)
2 FORMAT (4I2,8F8.3)
5 FORMAT (4I5,I2)
6 FORMAT (8F8.3)
7 FORMAT (4F8.3,I2,4F8.3)
8 FORMAT (3F8.3)
10 FORMAT (4F8.3,2I2)
11 FORMAT (7X,I3,5 (5X,I3) ,7X,I3)
12 FORMAT (8F8.3)
13 FORMAT (3X,I3,2X,6F8.3)
14 FORMAT (2 (3X,I3) ,2 (5X,F8.3) )
50 FORMAT (1H ,5X,3HDX=,1PE12.5/6X,3HDZ=,E12.5/6X,3HGX=,E12.5/
1 6X,3HGZ=,E12.5/5X,4HALX=,E12.5/5X,4HALZ=,E12.5/5X,4HCYL=,E12.5/
2 6X,3HB0=,E12.5/5X,4H EPS=,E12.5/4X,5HVIN=,E12.5)
51 FORMAT (1H ,4X,4HKWR=,I2/5X,4HKWL=,I2/5X,4HKWT=,I2/5X,4HKWB=,I2/
1 3X,6HFSLIP=,1PE12.5/5X,4HALP=,E12.5/5X,4HGAM=,E12.5/4X,5HALP0=,
2E12.5/4X,5HGAM1=,E12.5/6X,3HNU=,E12.5/3X,6HTQJET=,E12.5/3X,
36HTSJET=,E12.5)
52 FORMAT (1H ,5X,3HAI=,1PE12.5/6X,3HBI=,E12.5/6X,3HCI=,E12.5/
1 6X,3HAR=,E12.5/6X,3HBR=,E12.5/6X,3HCR=,E12.5/5X,4HAMU=,E12.5/
2 5X,4HBMU=,E12.5/5X,4HCMU=,E12.5)

```

RGBMK60A

53 FORMAT (1H ,5X,3HAK=,1PE12.5/6X,3HBK=,E12.5/6X,3HCK=,E12.5/5X,
14HACP=,E12.5/5X,4HBCP=,E12.5/5X,4HCCP=,E12.5/5X,5HSIGN=,E12.5)
54 FORMAT (1H ,3HNL ,I5,3HNR ,I5,3HNB ,I5,3HNT ,I5,8HICELTYP ,I2)
55 FORMAT (1H ,3X,5HSIEI=,1PE12.5/5X,4HTQI=,E12.5/5X,4HTSI=,E12.5/
16X,3HUI=,E12.5/6X,3HWI=,E12.5/5X,4HCHI=,E12.5/5X,4HVAP=,E12.5/5X,4RGBMK60A
2HLIQ=,E12.5)
57 FORMAT (1H ,20H TAU FOR OBSTACLES =,7 (2X,1PE12.5))
58 FORMAT (1H ,3X,5HWOBI=,1PE12.5/4X,5HUOBI=,E12.5/1X,8HCSUBPOB=,
1 E12.5)
59 FORMAT (1H ,5X,3HAW=,1PE12.5/6X,3HBW=,E12.5/6X,3HCW=,E12.5/
1 4X,5HWEPS=,E12.5/2X,7HKDERBC=,I2/4X,5HUBRI=,E12.5/4X,5HUBLI=,
2 E12.5/4X,5HWBTI=,E12.5/4X,5HWBBI=,E12.5)
60 FORMAT (1H ,3X,5HTGAM=,1PE12.5/6X,3HTO=,E12.5/6X,3HTI=,E12.5/
1 3X,6HTSTEP=,E12.5/5X,4HMAT=,I2/1X,8HNRESEXP=,I2)
61 FORMAT (1H ,7H NFLOW ,I3,5H NT1 ,I3,5H NT2 ,I3,5H NT3 ,I3,5H NT4 ,
1 I3,5H NT5 ,I3,6H NTAU ,I3)
62 FORMAT (1H ,3X,1HI,9X,4HTYMF,12X,2HPN,11X,5HTYMT1,11X,3HT1N,11X,
1 5HTYMT2,11X,3HT2N)
63 FORMAT (1H ,2X,I3,2X,6 (2X,1PE11.4,2X))
64 FORMAT (1H ,3H I ,I3,2X,6P8.3)
65 FORMAT (1H ,3H I ,I3,3H K ,I3,5H RXC ,F8.3,5H RZC ,F8.3)
66 FORMAT (1H ,///,22X,6 (2X,1PE11.4,2X))
END
SUBROUTINE VM
INTEGER BUFL,CF,CF1,CFB,CFC,CFI,CFL,CFR,CFS,CFT,CQF,ERF,TD,VNTP,
1 VTP
REAL NU,LIQ,LIQO,LIQI,LIQJ,LIQK,LIQL,LIQM,LIQO,LIQOC,LIQCC
REAL LIQL,LIQR,LIQT,LIQB,LIQC,LIQCO
DIMENSION EFRAC (5),RLAM (5),ELAM (5)
DIMENSION CF (1),CQ (1),QCON (1),P (1),RX (1),RZ (1),TO (1),TS (1),U (1),
1 W (1),ER (1),PFX3 (102),FFY3 (102),PBTIM (2),UO (1),WO (1),TOO (1),
2 TSO (1),SIE (1),SIEJ (1),SIEK (1),SIEO (1)
A,VAP (1),VAPO (1),LIQ (1),LIQO (1)
3 ,TYNF (25),FN (25),TYMT1 (25),T1N (25),TYMT2 (25),T2N (25),
4 COFBA (25),COFBB (25),COFBC (25),COFTA (25),COFTB (25),COFTC (25),
5 COFRA (25),COFRB (25),COFRC (25),COFLA (25),COFLB (25),COFLC (25),

1045
1046
1047
1048
1049
1050
1051
1052
1053
1054
1055
1056
1057
1058
1059
1060
1061
1062
1063
1064
1065
1066
1067
1068
1069
1070
1071
1072
1073
1074
1075
1076
1077
1078
1079
1080

RGBHM60A
RGBVM60A
RGBVM56A

RGBHM01A
RGBHM60A

6 OFOBTA(25),OFOTB(25),OFOTC(25),
7 OFOBRA(25),OFORRB(25),OFORC(25),TAU(10),USL(32),USLOB(20),
8 USROB(20),USTOB(20),USBOB(20)
9 ,COFBD(25),COFBE(25),COFTD(25),COFTE(25),COFTF(25),COFBF(25),
*COFRD(25),COFRE(25),COFLD(25),COFLE(25),COFRF(25),COFLF(25),
AOFOTD(25),OFOTTE(25),OFOTRD(25),OFOTRE(25),
B OFOTTF(25),OFOTRF(25),
CTYMF3(25),TYMT4(25),TYMT5(25),T3N(25),T4N(25),T5N(25),
* IICFR(1),IICFL(1),IICFT(1),IICFB(1)
* ,ZERO1(1165),ZERO2(608),ZERO3(16),ZERO4(3)
DIMENSION ZSIE(22),ZTQ(22),ZTS(22),ZVP(22),ZLQ(22),ZAP(22),WSP(22) RGBVM62A
DIMENSION TRSRT(5),ZSIE(100),WZTQ(100),WZTS(100) RGBVM55A
A,WZVP(100),WZLQ(100),WZAP(100),WWSP(100) RGBVM62A
COMMON/VRCON/A(14000) RGBMN60A
COMMON/RGB/RLAMB,CHII,GAMX,NRSTRT,TRSTRT,ZSIE,ZTQ,ZTS,WZSIE,WZTQ, RGBVM55A
AWZTS,NPROF,WZVP,WZLQ,ZVP,ZLQ,GAML,GAMV,VAPI,LIQI RGBMN60A
B,WSP,WWSP,BKGND,DWINDS RGBMN60B
COMMON/VRCON/ALP,ALP0,ALX,ALZ,B0,BETA,BUFL,CFI(9),CFS(9),CYL,
1 DT,DX,DZ,EM6,EPS,ERF,FSLIP,GAM,GAM1,GX,GZ,HDX,HDZ,I,I1,I2,I2K2,
2 IBP1,IBP2,IBR,IDATIN,IDIAG,IKP2,IOBS,IRSTRT,ITAPW,ITER,IVDI,
3 IVDO,K,K1,K2,K2NC,KBP1,KBP2,KBR,KNC,KWB,KWL,KWR,KWT,LABEL(20),
4 LPR,NCYC,NCYCB,NPRT,NU,NWPC,RDT,RDX,RDZ,EDZS,RIBKB,ROI,TD,TFIN,
5 TIMEI,TIOSUM,TPL,IPLT,TPR,TPRT,TQI,TSI,TTD,TWTD,UI,WI
* ,USR(32),UST(22),USB(22),USO(10),FFX3,FFY3
6 ,AW,RW,CW,EPSEB,UBLI,UBRI,WBBI,WBTI,WEPS,WOB1,NTPAS,TGAM,CSUBP,
7 T0,SIEI,IDG,KDG,TI,MAT,RHO0,AT,TMU,TK,TYMP,PN,TYMT1,T1N,TYMT2,
8 F2N,RPRAN,NRESEX,NFLOW,NT1,NT2,TSTEP,KDERBC,UOBI,COFBA,COFBB,
9 COFBC,COFTA,COFTB,COFTC,COFRA,COFRB,COFRC,COFLA,COFLB,COFIC,
* OFOBTA,OFOTB,OFOTC,OFOTD,OFOTTE,OFOTRD,OFOTRE,OFOTRF,OFOTR,OFOTR,OFOTR,OFOTR,
1 USLOB,USROB,USTOB,USBOB,UMAX,WMAX
* ,CSUBPO,EPS0,RDXDZS,RLENGH,TQJET,TSJET
COMMON/FLMCON/ DROU,DROU0,I PRFM
COMMON /VRMAT3/ AI,BI,CI,AR,BR,CR,AMU,BMU,CMU,AK,BK,CK,ACP,BCP,CCP
1 ,VMIN
COMMON/PROP/SIGN
COMMON/EXTRA/NT3,NT4,NT5,TYMT3,TYMT4,TYMT5,T3N,T4N,T5N,COFBD,


```

READ (IVDI,56) (WZSIE(K),WZTQ(K),WZTS(K),WZVP(K),WZLQ(K),WZAP(K),WWRGBVM62A
ASP(K),K=1,NPROF)
1153
1154 RGBVM62A
1155 RGBVM62A
1156 WWRITE(IVDO,59) (WZSIE(K),WZTQ(K),WZTS(K),WZVP(K),WZLQ(K),WZAP(K),WWRGBVM62A
1157 RGBVM62A
1158 RGBVM62A
1159 RGBVM55A
1160 RGBVM55A
1161 RGBVM70A
1162 RGBVM62A
1163 RGBVM60A
1164 RGBVM60A
1165 RGBVM55A
1166 RGBVM55A
1167 RGBVM55A
1168 RGBVM70A
1169 RGBVM62A
1170 RGBVM60A
1171 RGBVM60A
1172 RGBVM55A
1173 RGBVM55A
1174 RGBVM55A
1175 RGBVM70A
1176 RGBVM62A
1177 RGBVM60A
1178 RGBVM60A
1179 RGBVM55A
1180 RGBVM55A
1181 RGBVM55A
1182
1183
1184
1185
1186
1187
1188

C TRANSFER OF PROFILES BEFORE ANY RESTART CASES
DO 99 K=2,KBP1
WSP(K)=WVSP(K-1)
ZAP(K)=WZAP(K-1)
ZVP(K)=WZVP(K-1)
ZLQ(K)=WZLQ(K-1)
ZSIE(K)=WZSIE(K-1)
ZTQ(K)=WZTQ(K-1)
ZTS(K)=WZTS(K-1)
99 WSP(1)=0.0
ZAP(1)=0.0
ZVP(1)=ZVP(2)
ZLQ(1)=ZLQ(2)
ZSIE(1)=ZSIE(2)
ZTQ(1)=ZTQ(2)
ZTS(1)=ZTS(2)
WSP(KBP2)=0.0
ZAP(KBP2)=0.0
ZVP(KBP2)=ZVP(KBP1)
ZLQ(KBP2)=ZLQ(KBP1)
ZSIE(KBP2)=ZSIE(KBP1)
ZTQ(KBP2)=ZTQ(KBP1)
ZTS(KBP2)=ZTS(KBP1)

C NOTE. CALCULATION OF CONSTANTS AND PREASSIGNED BRANCHES .
IF(IRSTRT.EQ.0) GO TO 100
CALL VRPRT
IF( IDROU.GT.0 ) DROU=DROU*AMIN1(DX,DZ)/AMAX1(UMAX,WMAX,EM6)
IF( IPRFM.GT.0 ) CALL VRPFM
IRSTRT=?
100 ITER=0

```

```

ICALI=1
X1=AMAX1( UMAX, WMAX )
VELOLD=X1
EPS=EPS0*X1**RLENGTH
IF( X1.LT.VMIN ) EPS=EPS0*VMIN*RLENGTH
IF( EPS0.LT.EM6 ) EPS=ABS( EPS0 )
ASSIGN 2000 TO KBC
C NOTE. COMPUTATION OF FNTAU, T1NTAU AND T2NTAU .
FNTAU=SI( TYMP, FN, TIMET, NFLOW )
T1NTAU=SI( TYMT1, T1N, TIMET, NT1 )
IF(NT2.EQ.0) GO TO 107
T2NTAU=SI( TYMT2, T2N, TIMET, NT2 )
IF(NT3.EQ.0) GO TO 107
T3NTAU=SI( TYMT3, T3N, TIMET, NT3 )
IF(NT4.EQ.0) GO TO 107
T4NTAU=SI( TYMT4, T4N, TIMET, NT4 )
IF(NT5.EQ.0) GO TO 107
T5NTAU=SI( TYMT5, T5N, TIMET, NT5 )
107 CONTINUE
C NOTE. ZERO OUT THE CQ(IK) ARRAY FOR TAU FACTORS IN SIE EQUATION .
I1=2
I2=IBP1
K1=2
K2=KBP1
KK=1
ITAU CN=0
DO 109 I=I1, I2
KK=KK + K2NC
LWPC=0
DO 109 K=K1, K2
LWPC=LWPC + NWPC
IK=KK + LWPC
CQ(IK)=0.0
109 CONTINUE
C NOTE. CALCULATION OF DIAGNOSTIC CONSTANTS .

```



```

1225 ASSIGN 12500 TO KDAGTU
1226 C NOTE. PREASSIGN BRANCHES FOR RESISTANCE EQUATIONS , I.E. RX AND RZ .
1227   RXC=0.0
1228   RZC=0.0
1229   ASSIGN 2300 TO KRXRZ
1230   IF( NWPC.GT.13 ) ASSIGN 2250 TO KRXRZ
1231 C NOTE. PREASSIGN BRANCHES FOR PLANE - CYL=0.0 - OR CYLINDRICAL
1232 C NOTE. - CYL=1.0 - COORDINATES .
1233   FCU=0.0
1234   PCW=0.0
1235   RL=1.0
1236   RC=RL
1237   RR=RC
1238   DR=DX
1239   RRL=1.0
1240   RRC=RRL
1241   RRR=RRC
1242   RRRC=1.0
1243   RRP=RRRC
1244   RDR=RDZ
1245   RDRS=1./ ( DR*DR )
1246   RDRM=RDR
1247   RDRP=RDRM
1248   RDZM=RDZ
1249   RDZP=RDZM
1250   ASSIGN 2400 TO KCLU
1251   ASSIGN 2500 TO KCLW
1252   ASSIGN 2220 TO KRU
1253   IF( CYL.LT.EM6 ) GO TO 120
1254   ASSIGN 2370 TO KCLU
1255   ASSIGN 2470 TO KCLW
1256   ASSIGN 2215 TO KRU
1257   120 ASSIGN 13000 TO KDIAG
1258   IF( IDIAG.LT.1 ) GO TO 200
1259   ASSIGN 12200 TO KDIA3
1260   IF( IDIAG.GT.1 ) ASSIGN 12500 TO KDIAG

```

```

VM212002
VM212004

```

```

VM215002

```

```

VM215006
VM215010
VM215014
VM215016
VM215018

```

```

200 TSUM=0.0
   TIOSUM=0.0
C NOTE. COMPUTATION OF BOUNDARY CONDITIONS .
C
1000 LWPC=1 - NWPC
      IF( KDERBC.LT.1 ) GO TO 1100
C
C NOTE. COMPUTATION OF RIGHT AND LEFT BOUNDARY CONDITIONS .
1100 LWPC=1 - NWPC
      I1=1
      I2=IBP2
      K1=1
      K2=KBP2
      NDERR=0
      NDERL=0
      NCOFR=0
      NCOFL=0
      DO 1289 K=K1,K2
      LWPC=LWPC+NWPC
      IMK=LWPC
      CFL= CF (IMK)
      ICFL=CFL
      IPK=IMK + IKP2
      IPPK=IPK + K2NC
      IMKT=IMK + K2NC
      IPKT=IPK
      CFR= CF(IPPK)
      ICFR=CFR
      IF( CFL.NE.2 ) GO TO 1105
      IF( K.EQ.K2 ) GO TO 1103
      IMKT=IMK + K2NC + NWPC
      IPKT=IPK + NWPC
      CFL= CF (IMK+NWPC)
      CFR= CF (IPPK+NWPC)
      GO TO 1105

```

VM111002

```

1103  IMKT=IMK + K2NC - NWPC
      IPKT=IPK - NWPC
      CFL= CF(IMK-NWPC)
      CFR= CF(IPPK-NWPC)
      1105  W(IMK)=W(IMKT)
           W(IPPK)=W(IPK)
C NOTE. COMPUTATION OF REFLECTIVE BOUNDARY CONDITIONS ON TQ AND TS .
      SIE(IMK)=SIE(IMKT)
      SIE(IPPK)=ZSIE(K)
      TQ(IMK)=TQ(IMKT)
      TQ(IPPK)=ZTQ(K)
      TS(IMK)=TS(IMKT)
      TS(IPPK)=ZTS(K)
      CHI(IMK)=CHI(IMKT)
      CHI(IPPK)=0.0
      IF(U(IPKT).GT.0.0) CHI(IPPK)=CHI(IPKT)
      VAP(IMK)=VAP(IMKT)
      VAP(IPPK)=ZVP(K)
      LIQ(IMK)=LIQ(IMKT)
      LIQ(IPPK)=ZLQ(K)
      GO TO ( 1120,1130,1140,1150 ),KWL
C NOTE. COMPUTATION OF RIGID LEFT WALL BOUNDARY CONDITION .
1120  U(IMK)=0.0
      GO TO 1180
C NOTE. COMPUTATION OF CONTINUATIVE LEFT WALL BOUNDARY CONDITION .
1130  IF( IITER.GT.0 ) GO TO 1180
      U(IMK)=U(IMK+K2NC)
      W(IMK) = -W(IMK+K2NC)
      W(IMK-NWPC) = -W(IMK+K2NC-NWPC)
      GO TO 1180
C NOTE. COMPUTATION OF PERIODIC LEFT WALL BOUNDARY CONDITION .
1140  U(IMK)=U(IPK)
      GO TO 1180
C NOTE. VARIABLE BOUNDARY OPTION AT LEFT WALL .
1150  NCFL=CFL - 9
      GO TO ( 1152,1130,1155,1160 ),NCFL

```

```

1297
1298
1299
1300
1301
1302
1303
1304
1305
1306
1307
1308
1309
1310
1311
1312
1313
1314
1315
1316
1317
1318
1319
1320
1321
1322
1323
1324
1325
1326
1327
1328
1329
1330
1331
1332

```

```

      RGBVM5 1A
      RGBVM0 2A

      RGBVM5 1A

      RGBVM5 1A

      RGBVM5 1A
      RGBVM5 2A
      RGBVM5 2A
      RGBVM5 2A
      RGBVM6 0A
      RGBVM6 0A
      RGBVM6 0A
      RGBVM6 0A

      VM114002

      VM115004

```

```

1333 C NOTE. RIGID BOUNDARY SECTION AT LEFT WALL .
1334 1152 NRIGID=KDERBC + 1
1335 GO TO( 1120,1153 ),NRIGID
1336 C NOTE. DERIVED BOUNDARY CONDITION AT LEFT WALL .
1337 1153 WC=W(IMKT)
1338 IF( K.EQ.1 ) GO TO 1120
1339 IF( K.GE.(KBR+1) ) GO TO 1120
1340 ICF1=CF(IMKT)
1341 IF( ICF1.GE.30 ) GO TO 1120
1342 QC=TQ(IMKT)
1343 SC=TS(IMKT)
1344 NDERL=NDERL + 1
1345 WSA=USL(NDERL)
1346 QW=5.*WSA*WSA
1347 W(IMK) = -WC
1348 SW = WSA * WSA * HDX/WC
1349 TQ(IMK)=2.*QW - QC
1350 TS(IMK)=2.*SW - SC
1351 GO TO 1120
1352 C NOTE. CONSTANT INFLOW AT LEFT WALL .
1353 1155 U(IMK)=UBLI
1354 GO TO 1180
1355 C NOTE. VARIABLE OR FUNCTIONAL INFLOW AT LEFT WALL .
1356 1160 IF( ICF1.EQ.2 ) GO TO 1180
1357 NCOPL=NCOPL + 1
1358 TI=COPLB(NCOPL)*T1NTAU + COPLC(NCOPL)*T2NTAU
1359 1+COPLD(NCOPL)*T3NTAU+COFLE(NCOPL)*T4NTAU+COPLF(NCOPL)*T5NTAU
1360 ASSIGN 1162 TO KIRORC
1361 SIEK=SIE(IMKT)
1362 GO TO 1500
1363 1162 AREA=3.14159265*FLOAT(2*K-3)*DZ*DZ
1364 IF( CYL.LT.1.0 ) AREA=K=DZ
1365 FLK=COPLA(NCOPL)*FNNTAU
1366 UBAR=PLK/RHOD
1367 U(IMK)=UBAR/AREAK
1368 IF(NIV.EQ.1) U(IMK)=FLK

```

RGBVM01A

```

SIE(IMK)=SIEII
TS(IMK)=TS(IPK)
TQ(IMK)=TQ(IPK)
1180 GO TO( 1220,1230,1240,1250 ),KWR
C NOTE. COMPUTATION OF RIGID RIGHT WALL BOUNDARY CONDITION .
1220 U(IPK)=0.0
      GO TO 1280
C NOTE. COMPUTATION OF CONTINUATIVE RIGHT WALL BOUNDARY CONDITION .
1230 IF( ITER.GT.C ) GO TO 1280
      U(IPPK)=U(IPK-K2NC)
      W(IPPK-NWPC)=W(IPK-NWPC)
      GO TO 1280
C NOTE. COMPUTATION OF PERIODIC RIGHT WALL BOUNDARY CONDITION .
1240 U(IPPK)=U(IMK+K2NC)
      W(IPPK)=W(IMK+K2NC)
      GO TO 1280
C NOTE. VARIABLE BOUNDARY OPTION AT RIGHT WALL .
1250 NCFR=CFR - 9
      GO TO( 1252,1230,1255,1260 ),NCFR
C NOTE. RIGID BOUNDARY SECTION AT RIGHT WALL .
1252 NRIGID=KDERBC + 1
      GO TO( 1220,1253 ),NRIGID
C NOTE. DERIVED BOUNDARY CONDITION AT RIGHT WALL .
1253 WC=W(IPKT)
      IF (K.GF.(KBR+1)) GO TO 1220
      IF ( K.EQ.1 ) GO TO 1220
      ICF2=CF(IPKT)
      IF (ICF2.GE.30) GO TO 1220
      QC=TQ(IPKT)
      SC=TS(IPKT)
      NDERR=NDERR + 1
      WSA=USR(NDERR)
      QW=5.*WSA*WSA
      SW = WSA * WSA * HDX/WC
      W(IPPK) = -WC
      TQ(IPPK)=2.*QW-QC

```

```

RGBVM02A 1369
RGBVM02A 1370
RGBVM02A 1371
1372
1373
1374
1375
1376
1377
1378
1379
1380
1381
1382
1383
1384
1385
1386
1387
1388
1389
1390
1391
1392
1393
1394
1395
1396
1397
1398
1399
1400
1401
1402
1403
1404

```

```

RGBVM02A
RGBVM02A
RGBVM02A

VM124002

RGBVM02A
VM125004

```

```

1405 TS(IPPK)=2.*SW-SC
1406 GO TO 1220
1407 C NOTE. CONSTANT INFLOW AT RIGHT WALL .
1408 1255 U(IPK)=UERI
1409 GO TO 1280
1410 C NOTE. VARIABLE OR FUNCTIONAL INFLOW AT RIGHT WALL .
1411 1260 IF( ICFR.EQ.2 ) GO TO 1280
1412 NCOFR=NCOFR + 1
1413 TI=COFRB(NCOFR)*T1NTAU + COFRC(NCOFR)*T2NTAU
1414 1+COPRD(NCOFR)*T3NTAU+COPRE(NCOFR)*T4NTAU+COPRF(NCOFR)*T5NTAU
1415 ASSIGN 1262 TO KIROBC
1416 SIEK=SIE(IPKT)
1417 GO TO 1500
1418
1419 1262 AREAK = 3.14159265 * 2 * IBR * DR * DZ
1420 IF( CYL.LT.1.0 ) AREAK=DZ
1421 FLK=COFRA(NCOFR)*FNNTAU
1422 UBAR=FLK/RHOII
1423 U(IPK)=UBAR/AREAK
1424 IF(NIV.EQ.1) U(IPK)=FLK
1425 SIEC=SIE(IPKT)
1426 SIEW=SIEI
1427 SIE(IPPK)=(2*SIEW+(ALX-1.0)*SIEC)/(1.0+ALX)
1428 QC = TQ(IPKT)
1429 QW = TQJET * U(IPK)*U(IPK)
1430 SC = TS(IPKT)
1431 SW = TSJET * U(IPK) * DZ
1432 SW=ABS(SW)
1433 QW=AMAX1(QW,1.0E-5)
1434 SW=AMAX1(SW,NU)
1435 TQ(IPPK)=(2*QW+(ALX-1.0)*QC)/(1.0+ALX)
1436 TS(IPPK)=(2*SW+(ALX-1.0)*SC)/(1.0+ALX)
1437 1280 CONTINUE
1438 1289 CONTINUE
1439 C NOTE. COMPUTATION OF TOP AND BOTTOM BOUNDARY CONDITIONS .
1440 NDERB=0
      NDERT=0

```

R3BVM01A

VM128000
 VH128900

1441
1442
1443
1444
1445
1446
1447
1448
1449
1450
1451
1452
1453
1454
1455
1456
1457
1458
1459
1460
1461
1462
1463
1464
1465
1466
1467
1468
1469
1470
1471
1472
1473
1474
1475
1476

VM131002

RGBVM50A
RGBVM51A

RGBVM52A
RGBVM52A

PAGE 41

```
NCOPB=0
NCOFT=0
KK=1 - K2NC
DO 1489 I=I1,I2
KK=KK+K2NC
IKM=KK
CFB= CP (IKM)
ICFB=CFB
IKP=IKM + KNC
IKPP=IKP + NWPC
CFT= CF (IKPP)
ICFT=CFT
IKMT=IKM + NWPC
IKPT=IKP
IF ( CFB.NE.2 ) GO TO 1305
IF ( I.EQ.I2 ) GO TO 1303
IKMT=IKM + K2NC + NWPC
IKPT=IKP + K2NC
CFB= CP (IKM+K2NC)
CFT= CP (IKPP+K2NC)
GO TO 1305
1303 IKMT=IKM - K2NC + NWPC
IKPT=IKP - K2NC
CFB= CP (IKM-K2NC)
CFT= CP (IKPP-K2NC)
1305 U (IKM) =-U (IKMT)
U (IKPP) =U (IKP)
C NOTE. COMPUTATION OF REFLECTIVE BOUNDARY CONDITIONS ON TQ AND TS .
SIE (IKM) =SIE (IKMT)
SIE (IKPP) =SIE (IKPT)
TQ (IKM) =TQ (IKMT)
TQ (IKPP) =TQ (IKPT)
TS (IKM) =TS (IKMT)
TS (IKPP) =TS (IKPT)
CHI (IKM) =CHI (IKMT)
CHI (IKPP) =0.0
```

```

IF(W(IKPT).GT.0.0) CHI(IKPP)=CHI(IKPT)
VAP(IKM)=VAP(IKMT)
VAP(IKPP)=VAP(IKPT)
LIQ(IKM)=LIQ(IKMT)
LIQ(IKPP)=LIQ(IKPT)
GO TO( 1320,1330,1340,1350 ),KWT
C NOTE. COMPUTATION OF RIGID TOP WALL BOUNDARY CONDITION .
1320 W(IKP)=0.0
GO TO 1380
C NOTE. COMPUTATION OF CONTINUATIVE TOP WALL BOUNDARY CONDITION .
1330 IF( I TER.GT.0 ) GO TO 1380
W(IKPP)=W(IKP-NWPC)
U(IKPP-K2NC)=U(IKP-K2NC)
GO TO 1380
C NOTE. COMPUTATION OF PERIODIC TOP WALL BOUNDARY CONDITION .
1340 W(IKPP)=W(IKM+NWPC)
U(IKPP)=U(IKM+NWPC)
GO TO 1380
C NOTE. VARIABLE BOUNDARY OPTION AT TOP WALL .
1350 NCPT=CFT - 9
GO TO( 1352,1330,1355,1360 ),NCPT
C NOTE. RIGID BOUNDARY SECTION AT TOP WALL .
1352 NRIGID=KDERBC + 1
GO TO( 1320,1353 ),NRIGID
C NOTE. DERIVED BOUNDARY CONDITION AT TOP WALL .
1353 UCT=U(IKP)
IF( I.EQ.1 ) GO TO 1320
IF( I.GE.(IBR+1) ) GO TO 1320
ICP3=CF(IKP)
IF( ICF3.GE.30 ) GO TO 1320
QCT=TQ(IKP)
SCT=TS(IKP)
NDERT=NDERT + 1
USAT=UST(NDERT)
QWT=5.*USAT*USAT
1356 SWT = USAT * USAT * EDZ /UCT

```

```

RGBVM52A
RGBVM60A
RGBVM60A
RGBVM60A
RGBVM60A
VM134002
RGBVM51A
VM135004

```

```

1477
1478
1479
1480
1481
1482
1483
1484
1485
1486
1487
1488
1489
1490
1491
1492
1493
1494
1495
1496
1497
1498
1499
1500
1501
1502
1503
1504
1505
1506
1507
1508
1509
1510
1511
1512

```



```

1513 U(IKPP) = -UCT
1514 TQ(IKPP) = 2.*QWT - QCT
1515 TS(IKPP) = 2.*SWT - SCT
1516 GO TO 1320
1517
1518 C.NOTE CONSTANT INFLOW AT TOP WALL .
1519 1355 W(IKP) = WBTI
1520 GO TO 1380
1521
1522 C.NOTE. VARIABLE OR FUNCTIONAL INFLOW AT TOP WALL .
1523 1360 IF( ICFT.EQ.2 ) GO TO 1380
1524 NCOFT = NCOFT + 1
1525 TI = COFTB(NCOFT) * TINTAU + COFTC(NCOFT) * T2NTAU
1526 1 + COFTD(NCOFT) * T3NTAU + COFTE(NCOFT) * T4NTAU + COFTF(NCOFT) * T5NTAU
1527 ASSIGN 1362 TO KIROBC
1528 SIEC = SIE(IKPT)
1529 GO TO 1500
1530
1531 1362 AREA I = 3.14159265 * FLOAT(2 * I - 3) * DR * DR
1532 IF( CYL.LT.1.0 ) AREA I = DX
1533 FLI = COFTA(NCOFT) * FNNTAU
1534 WBAR = FLI / RH0II
1535 W(IKP) = WBAR / AREA I
1536 IP(NIV.EQ.1) W(IKP) = FLI
1537 SIEC = SIE(IKP)
1538 SIFW = SIFII
1539 SIE(IKPP) = (2 * SIEW + (ALZ - 1.0) * SIEC) / (1.0 + ALZ)
1540 QCT = TQ(IKP)
1541 QWT = TQJET * W(IKP) * W(IKP)
1542 SCT = TS(IKP)
1543 SWT = TSJET * W(IKP) * DR
1544 SWT = ABS(SWT)
1545 QWT = AMAX1(QWT, 1.0E-5)
1546 SWT = AMAX1(SWT, NU)
1547 TQ(IKPP) = (2 * QWT + (ALZ - 1.0) * QCT) / (1.0 + ALZ)
1548 TS(IKPP) = (2 * SWT + (ALZ - 1.0) * SCT) / (1.0 + ALZ)
1549 GO TO( 1420, 1430, 1440, 1450 ), KWB
1550 C.NOTE. COMPUTATION OF RIGID BOTTOM WALL BOUNDARY CONDITION .
1551 1420 W(IKM) = 0.0

```

RGB/03/78

RGBVM01A

```

1549 GO TO 1480
1550 C NOTE. COMPUTATION OF CONTINUATIVE BOTTOM WALL BOUNDARY CONDITION .
1551 1430 IF( I.TER.GT.0 ) GO TO 1480
1552 W(IKM)=W(IKM+NWPC)
1553 U(IKM)=-U(IKM+NWPC)
1554 U(IKM-K2NC)=-U(IKM+NWPC-K2NC)
1555 GO TO 1480
1556
1557 VM 145004
1558
1559 C NOTE. COMPUTATION OF PERIODIC BOTTOM WALL BOUNDARY CONDITION .
1560 1440 W(IKM)=W(IKP)
1561 GO TO 1480
1562 C NOTE. VARIABLE BOUNDARY OPTION AT BOTTOM WALL .
1563 1450 NCFB=CFB - 9
1564 GO TO( 1452,1430,1455,1460 ),NCFB
1565 C NOTE. RIGID BOUNDARY SECTION AT BOTTOM WALL .
1566 1452 NRIGID=KDERBC + 1
1567 GO TO( 1420,1453 ),NRIGID
1568 C NOTE. DERIVED BOUNDARY CONDITION AT BOTTOM .
1569 1453 IK=IKM + NWPC
1570 IP( I.EQ.1 ) GO TO 1420
1571 IF( I.GE.(IBP+1) ) GO TO 1420
1572 ICF4=CF(IK)
1573 IP( ICF4.GE.30) GO TO 1420
1574 UCB=U(IK)
1575 QCB=TQ(IK)
1576 SCB=TS(IK)
1577 NDERB=NDERB + 1
1578 USAB=USB(NDERB)
1579 QWB=5.*USAB*USAB
1580 SWB=USAB*USAB*HDZ/UCB
1581 U(IKM)=-UCB
1582 TQ(IKM)=2.*QWB - QCB
1583 TS(IKM)=2.*SWB - SCB
1584 GO TO 1420
1585
1586 C NOTE. CONSTANT INFLOW AT BOTTOM WALL .
1587 1455 W(IKM)=WBBI
1588 GO TO 1480

```

```

1585 C NOTE. VARIABLE OR FUNCTIONAL INFLOW AT BOTTOM WALL .
1586 1460 IP( ICFB.EQ.2 ) GO TO 1480
1587 NCOFB=NCOFB + 1
1588 TI=COFBB(NCOFB) *T1NTAU + COFBC(NCOFB) *T2NTAU
1589 1+COFBD(NCOFB) *T3NTAU+COFBE(NCOFB) *T4NTAU+COFBF(NCOFB) *T5NTAU
1590 ASSIGN 1462 TO KIROBC
1591 SIEX=SIE(IKMT)
1592 GO TO 1500
1593 1462 AREAI=3.14159265*FLOAT(2*I-3) *DR*DR
1594 IF( CYL.LT.1.0 ) AREAI=DX
1595 FLI=COFBA(NCOFB) *FNNTAU
1596 WBAR=FLI/RHOII
1597 W(IKM)=WBAR/AREAI
1598 IF(NIV.EQ.1) W(IKM)=FLI
1599 SIEC=SIE(IK )
1600 SIEW=SIEII
1601 SIE(IKM)=(2*SIEW+(ALZ-1.0)*SIEC)/(1.0+ALZ)
1602 QCB=TQ(IK)
1603 QWB=TQJET*W(IKM)*W(IKM)
1604 SCB=TS(IK)
1605 SWB=TSJET*W(IKM)*DR
1606 QWB=AMAX1(QWB,1.0E-5)
1607 SWB=AMAX1(SWB,NU)
1608 TQ(IKM)=(2*QWB+(ALZ-1.0)*QCB)/(1.0+ALZ)
1609 TS(IKM)=(2*SWB+(ALZ-1.0)*SCB)/(1.0+ALZ)
1610 1480 CONTINUE
1611 1489 CONTINUE
1612 GO TO 1700
1613 C NOTE. COMPUTATION OF SIE AND RHO FOR VARIABLE OR FUNCTIONAL INFLOW
1614 C NOTE. AT A BOUNDARY WALL .
1615 1500 TR=TI + 459.7
1616 GO TO( 1510,1520,1530,1540 ),NAT
1617 C NOTE. COMPUTATION FOR SODIUM MATERIAL .
1618 1510 SIEII=0.38935*TR - 0.553E-4*TR*TR + 0.1137E-7*TR*TR*TR-29.02
1619 RHOII=59.566 - 7.9504E-3*TI - .2872E-6*TI*TI + 0.06035E-9*TI*TI*TI
1620 AT=397.17/TR + 1.0203

```

RGBVH0 1A

VN148000
VN148900

```

1621 TMU=(10.0*AT/3600.)/TR**0.4925
1622 TK=0.015085 - 5.2167E-6*TI + 5.809E-10*TI*TI
1623 TEMP =-385.27 + 2.6602*SIEX + 5.9894E-04*SIEX*SIEX +
1624 1 1.5575E-06*SIEX*SIEX*SIEX-2.9048E-09*SIEX*SIEX*SIEX*SIEX+
1625 2 1.15427E-12*SIEX*SIEX*SIEX*SIEX*SIEX*SIEX
1626 IP( ICSUBP.GT.0 ) TI=TEMP
1627 CSUBP=0.38935 - 1.106E-4*TI + 0.3411E-7*TI*TI
1628 GO TO 1550
1629
1630 C NOTE. COMPUTATION FOR WATER MATERIAL .
1631 1520 SIEII=1.0004*TI - 32.013
1632 RHOII=62.742 - 0.372E-2*TI - 0.44E-4*TI*TI
1633 BT=446.0/( TI+207.0 ) - 5.0
1634 TMU=1.622*10.**BT
1635 TK=8.369E-5 + 2.368E-7*TI - 5.89E-10*TI*TI
1636 TEMP=0.9996*SIEX + 32.0002
1637 CSUBP=1.0004
1638 GO TO 1550
1639
1640 1530 SIEII= AI*TI*TI + BI*TI + CI
1641 RHOII= AR*TI*TI + BR*TI + CR
1642 TMU = AMU*TI*TI + BMU*TI + CMU
1643 TK = AK*TI*TI + BK*TI + CK
1644 CIT=CI-SIEX
1645 TEMP=SI( AI,BI,CIT,-1 )
1646 CSUBP= ACP*TI*TI + BCP*TI + CCP
1647 GO TO 1550
1648 CONTINUE
1649 NU=TMU/RHOII
1650 RPRAN=TK/( CSUBP*TMU )
1651 GO TO KIROBC,( 1162,1262,1362,1462,1605,1615,1625,1635,1736,1756 )
1652
1653 C NOTE. COMPUTATION OF THE TAU FACTOR FOR USE IN THE SIE EQUATION .
1654
1655 C
1656 C NOTE. FLUID CELL TO THE LEFT OF THE IK OBSTACLE .
1657 ICSUBP=0
1658 IP( ITAUCN.GT.1 .OR. NTAU.LT.1 ) GO TO 1714
1659 ASSIGN 1695 TO KIROBC

```

```

1657 SIEX=SIIE (IMK)
1658 ICSUBP=1
1659 GO TO 1500
1660 NTAU=CFC - 29
1661 RTAU=1./TAU(NTAU)
1662 P (IK)=1./(1.+DT*RTAU)*( P(IK) + DT*RTAU*TEMP )
1663 CQ(IMK)=CSUBPO*RTAU*( TEMP-P (IK) )
1664 ICSUBP=0
1665 GO TO 1714
1666
1667 C NOTE. FLUID CELL TO THE BOTTOM OF THE IK OBSTACLE .
1668 1610 ICSUBP=0
1669 IF( ITAUCN.GT.1 .OR. NTAU.LT.1 ) GO TO 1724
1670 ASSIGN 1615 TO KIROBC
1671 SIEX=SIIE (IKM)
1672 ICSUBP=1
1673 GO TO 1500
1674 NTAU=CFC - 29
1675 RTAU=1./TAU(NTAU)
1676 P (IK)=1./(1.+DT*RTAU)*( P(IK) + DT*RTAU*TEMP )
1677 CQ (IKM)=CSUBPO*RTAU*( TEMP-P (IK) )
1678 ICSUBP=0
1679 GO TO 1724
1680
1681 C NOTE. FLUID CELL TO THE TOP OF THE IK OBSTACLE .
1682 1620 ICSUBP=0
1683 IF( ITAUCN.GT.1 .OR. NTAU.LT.1 ) GO TO 1744
1684 ASSIGN 1625 TO KIROBC
1685 SIEX=SIIF (IKP)
1686 ICSUBP=1
1687 GO TO 1500
1688 NTAU=CFC - 29
1689 RTAU=1./TAU(NTAU)
1690 CQ (IKP)=CSUBPO*RTAU*( TI-P (IK) )
1691 ICSUBP=0
1692 GO TO 1744
1693
1694 C NOTE. FLUID CELL TO THE RIGHT OF THE IK OBSTACLE .
1695 1630 ICSUBP=0

```

R3BVM03A

```

1693 IP ( ITAUCN.GT.1 .OR. NTAU.LT.1 ) GO TO 1764
1694 ASSIGN 1635 TO KIROBC
1695 SIEX=SIIE(IPK)
1696 ICSUBP=1
1697 GO TO 1500
1698 NTAU=CFC - 29
1699 RTAU=1./TAU(NTAU)
1700 P(IK)=1./(1.+DT*RTAU)*( P(IK) + DT*RTAU*TEMP )
1701 CQ(IPK)=CSUBPO*RTAU*( TEMP-P(IK) )
1702 ICSUBP=0
1703 GO TO 1764
1704
1705
1706
1707
1708
1709
1710
1711
1712
1713
1714
1715
1716
1717
1718
1719
1720
1721
1722
1723
1724
1725
1726
1727
1728

```

C
C NOTE . COMPUTATION OF OBSTACLE SUBREGIONS BOUNDARY CONDITIONS .
C

```

1700 KK=1
    ITAUCN=ITAUCN + 1
    I1=2
    I2=IBP1
    K1=2
    K2=KBP1
    IF( IOBS.EQ.0 ) GO TO 1990
    NDERR=0
    NDERL=0
    NDERB=0
    NDERT=0
    NCOPT=0
    NCOFR=0
    DO 1789 I=I1,I2
    KK=KK + K2NC
    LWPC=0
    DO 1779 K=K1,K2
    LWPC=LWPC + NWPC
    IK=KK + LWPC
    IMK=IK - K2NC
    IKM=IK - NWPC
    IKP=IK + NWPC

```

```

IPK=IK + K2NC
ICFC=CP(IK)
CFC=ICFC
IP( CFC.EQ.1 ) GO TO 1778
CPT=IICPT(IK)+1
CFB=IICFB(IK)+1
CFR=IICFR(IK)+1
CPL=IICPL(IK)+1
IF( CFT.GT.1 ) GO TO 1710
IP( CFB.GT.1 ) GO TO 1710
IF( CFR.GT.1 ) GO TO 1710
IF( CPL.GT.1 ) GO TO 1710
U(IK)=0.0
U(IMK)=0.0
W(IK)=0.0
W(IMK)=0.0
TS(IK)=0.0
TQ(IK)=0.0
SIE(IK)=0.0
GO TO 1770
C NOTE. OBSTACLE BOUNDARY CONDITION AT THE LEFT FACE .
1710 GO TO( 1720,1600 ),CPL
C NOTE. NON-FLUID CELL TO THE LEFT OF THE IK OBSTACLE .
1712 U(IMK)=0.0
GO TO 1720
C NOTE. FLUID CELL TO THE LEFT OF THE IK OBSTACLE .
1714 U(IMK)=0.0
NRIGID=KDERBC + 1
GO TO ( 1715,1716 ),NRIGID
C NOTE. RIGID BOUNDARY AT THE LEFT FACE .
1715 W(IK)=PSLIP*W(IMK)
SIE(IK)=SIE(IMK)
TQ(IK)=TQ(IMK)
TS(IK)=TS(IMK)
GO TO 1720
C NOTE. DERIVED BOUNDARY CONDITION AT THE LEFT FACE .

```

```

1729
1730
1731
1732
1733
1734
1735
1736
1737
1738
1739
1740
1741
1742
1743
1744
1745
1746
1747
1748
1749
1750
1751
1752
1753
1754
1755
1756
1757
1758
1759
1760
1761
1762
1763
1764

```

```

1716 WC=W (IKM)
1765
1766 QC=TQ(IKM)
1767 SC=TS (IKM)
1768 NDERL=NDERL + 1
1769 WSA=USLOB(NDERL)
1770 QWT=5.*WSA*WSA
1771 SW=WSA*WSA*HDX/WC
1772 W(IK)=-WC
1773 TQ(IK)=2.*QW - QC
1774 TS(IK)=2.*SW - SC
1775 GO TO 1712
1776
1777 C NOTE. OBSTACLE BOUNDARY CONDITION AT THE BOTTOM FACE .
1778
1779 1720 GO TO( 1730,1610 ),CFB
1780
1781 C NOTE. NON-FLUID CELL TO THE BOTTOM OF THE IK OBSTACLE .
1782
1783 1722 W(IKM)=0.0
1784 GO TO 1730
1785
1786 C NOTE. FLUID CELL TO THE BOTTOM OF THE IK OBSTACLE .
1787
1788 1724 W(IKM)=0.0
1789 NRIGID=KDERBC + 1
1790 GO TO( 1725,1726 ),NRIGID
1791
1792 C NOTE. RIGID BOUNDARY AT THE BOTTOM FACE .
1793
1794 1725 U(IK)=FSLIP*U(IKM)
1795 SIE(IK)=SIE(IKM)
1796 TQ(IK)=TQ(IKM)
1797 TS(IK)=TS(IKM)
1798 GO TO 1730
1799
1800 C NOTE. DERIVED BOUNDARY CONDITION AT THE BOTTOM FACE .
1801
1802 1726 UCT=U(IKM)
1803 QCT=TQ(IKM)
1804 SCT=TS(IKM)
1805 NDERB=NDERB + 1
1806 USAT=USBOB(NDERB)
1807 QWT=5.*USAT*USAT
1808 SWT=USAT*USAT*HDZ/UCT
1809 U(IK)=-UCT
1810 TQ(IK)=2.*QWT - QCT

```



```

1801 TS (IK) = 2.*SWT - SCT
1802 GO TO 1722
1803 C NOTE. OBSTACLE BOUNDARY CONDITION AT THE TOP FACE .
1804 1730 IF ( CFC.GE.30 ) GO TO 1740
1805 C NOTE. VARIABLE BOUNDARY OPTION AT THE TOP FACE .
1806 NCOFT=CFC - 21
1807 GO TO ( 1732,1734,1740,1740,1740 ), NCOFT
1808 C NOTF. CONSTANT INFLOW AT THE TOP FACE .
1809 1732 W (IK) = WBI
1810 GO TO 1745
1811 C NOTE. VARIABLE OR FUNCTIONAL INFLOW AT THE TOP FACE .
1812 1734 NCOFT=NCOFT + 1
1813 TI=OFOBFB(NCOFT) *T1NTAU + OFOBTB(NCOFT) *T2NTAU
1814 1+OFOBTD(NCOFT) *T3NTAU+OFOBTE(NCOFT) *T4NTAU+OFOBTF(NCOFT) *T5NTAU
1815 ASSIGN 1736 TO KIROBC
1816 SIEX=SIE (IKP)
1817 GO TO 1500
1818 1736 AREA1=3.14159265*FLOAT(2*I-3) *DR*DR
1819 IF ( CYL.LT.1.0 ) AREA1=DX
1820 FLI=OFOBTA(NCOFT) *FNNTAU
1821 WBAR=FLI/RHOII
1822 W (IK) = WBAR/AREA1
1823 IF (NIV.EQ.1) W (IK) =FLI
1824 SIEC=SIE (IKP )
1825 SIEW=SIEII
1826 SIE (IK ) =(2*SIEW+ (ALZ-1.0) * SIEC) / (1.0+ALZ)
1827 QCT = TQ (IKP)
1828 QWT = TQJET * W (IK) *W (IK)
1829 SCT = TS (IKP)
1830 SWT = TSJET * W (IK) * DR
1831 QWT=AMAX1 (QWT,1.0E-5)
1832 SWT=AMAX1 (SWT,NU)
1833 TQ (IK ) =(2*QWT+ (ALZ-1.0) *QCT) / (1.0+ALZ)
1834 TS (IK ) =(2*SWT+ (ALZ-1.0) *SCT) / (1.0+ALZ)
1835 U (IK) =FSLIP*U (IKP)
1836 GO TO 1750

```

RGBVM0 1A

```

1837 C NOTE. OBSTACLE BOUNDARY CONDITION AT THE TOP FACE .
1838 1740 GO TO( 1750,1620 ),CFT
1839 C NOTE. NON-FLUID CELL TO THE TOP OF THE IK OBSTACLE .
1840 1742 W(IK)=0.0
1841 GO TO 1750
1842 C NOTE. FLUID CELL TO THE TOP OF THE IK OBSTACLE .
1843 1744 W(IK)=0.0
1844 NRIGID=KDERBC + 1
1845 GO TO( 1745,1746 ),NRIGID
1846 C NOTE. RIGID BOUNDARY AT THE TOP FACE .
1847 1745 U(IK)=-U(IKP)
1848 SIE(IK)=SIE(IKP)
1849 TQ(IK)=TQ(IKP)
1850 TS(IK)=TS(IKP)
1851 GO TO 1750
1852 C NOTE. DERIVED BOUNDARY CONDITION AT THE TOP FACE .
1853 1746 UCT=U(IKP)
1854 QCT=TQ(IKP)
1855 SCT=TS(IKP)
1856 NDERT=NDERT + 1
1857 USAT=USTOB(NDERT)
1858 QWT=5.*USAT*USAT
1859 SWT = USAT * USAT * HDZ/UCT
1860 U(IK) = -UCT
1861 TQ(IK)=2.*QWT - QCT
1862 TS(IK)=2.*SWT - SCT
1863 GO TO 1742
1864 C NOTE. OBSTACLE BOUNDARY CONDITION AT THE RIGHT FACE .
1865 1750 IF( CFC.GE.30 ) GO TO 1760
1866 C NOTE. VARIABLE BOUNDARY OPTION AT THE RIGHT FACE .
1867 NCFR=CFC - 21
1868 GO TO( 1776,1776,1776,1752,1754 ),NCFR
1869 C NOTE. CONSTANT INFLOW AT THE RIGHT FACE .
1870 1752 U(IK)=UOBI
1871 GO TO 1765
1872 C NOTE. VARIABLE OR FUNCTIONAL INFLOW AT THE RIGHT FACE .

```

RGBVM50A

```

1754 NCOFR=NCOFR + 1
      TI=OPOBRB(NCOFR)*T1NTAU + OPOBRC(NCOFR)*T2NTAU
      1+OPOBRD(NCOFR)*T3NTAU+OPOBRE(NCOFR)*T4NTAU+OPOBRF(NCOFR)*T5NTAU
      ASSIGN 1756 TO KIROBC
      SJEX=SIE(IPK)
      GO TO 1500
1756 AREAK = 3.14159265 * 2*(I-1) * DR * DZ
      IF ( CYL.LT.1.0 ) AREAK=DZ
      FLK=OPOBRA(NCOFR)*FNTAU
      UBAR=FLK/RHOII
      U(IK)=UBAR/AREAK
      IF(NIV.EQ.1) U(IK)=FLK
      SIEC=SIE(IPK)
      SIEW=SI E I
      SIE(IK) =(2*SIEW+(ALX-1.0)*SIEC)/(1.0+ALX)
      QC = TQ(IPK)
      QW = TQJET * U(IK)*U(IK)
      SC = TS(IPK)
      SW = TSJET * U(IK) * DZ
      QW=AMAX1(QW,1.0E-5)
      SW=AMAX1(SW,NU)
      TQ(IK) =(2*QW+(ALX-1.0)*QC)/(1.0+ALX)
      TS(IK) =(2*SW+(ALX-1.0)*SC)/(1.0+ALX)
      W(IK)=FSLIP*W(IPK)
      GO TO 1770
C NOTE. OBSTACLE BOUNDARY CONDITION AT THE RIGHT FACE .
1760 GO TO( 1770,1630 ),CPR
C NOTE. NON-FLUID CELL TO THE RIGHT OF THE IK OBSTACLE .
1762 U(IK)=0.0
      GO TO 1770
C NOTE. FLUID CELL TO THE RIGHT OF THE IK OBSTACLE .
1764 U(IK)=0.0
      NRIGID=KDERBC + 1
      GO TO( 1765,1766 ),NRIGID
C NOTE. RIGID BOUNDARY AT THE RIGHT FACE .
1765 W(IK)=FSLIP*W(IPK)

```

RGBVM01A

```

SIE(IK)=SIE(IPK)
TQ(IK)=TQ(IPK)
TS(IK)=TS(IPK)
GO TO 1770
C NOTE. DERIVED BOUNDARY CONDITION AT THE RIGHT FACE .
1766 WC=#(IPK)
QC=TQ(IPK)
SC=TS(IPK)
NDERR=NDERR + 1
WSA=USROB(NDERR)
QW=5.*WSA*WSA
SW = WSA * WSA * HDX/WC
W(IK) = -WC
TQ(IK)=2.*QW - QC
TS(IK)=2.*SW - SC
GO TO 1762
1770 IF( CFT.EQ.2 .AND. CFC.GE.30 ) W(IK)=0.0
1776 IF( CFR.EQ.2 .AND. CFC.LT.25 ) U(IK)=0.0
1778 CONTINUE
1779 CONTINUE
1789 CONTINUE
1990 GO TO KBC, ( 2000,2990,4100,5000,5060 )
C
C NOTE. CHECKS FOR INITIAL CYCLES PRINTS , I.E. NPRT=0 NO PRINT,
C NOTE. NPRT=1 CYCLE 0 PRINT AND NPRT=2 CYCLE 0,1 PRINTS .
C
2000 IF( NCYC.LT.NPRT ) GO TO 2010
GO TO 2030
2010 CALL VRPRT
IF( IPRFM.GT.0 ) CALL VRFLM
C NOTE. CALL TO THE VARIABLE RESTANCE SUBROUTINE .
C NOTE. BEGIN THE N PASS PHASE OF THE TILDE EQUATION SECTION .
2030 DO 2999 NTE=1,NTPAS
IF( NWPC.GT.11 ) CALL VREQ
C
C NOTE. U AND W TILDE VELOCITY EQUATIONS SECTION .

```

VH200004

C
C NOTE. TRANSFERS VELOCITIES TO STORAGE ARRAY (AT TIME=N) .

```
K1=1
K2=KBP2
LWPC=1 - NWPC
DO 2109 K=K1,K2
LWPC=LWPC+NWPC
IK=LWPC
IKS=I2K2 + IK
SIE(IKS)=SIE(IK)
U(IKS)=U(IK)
W(IKS)=W(IK)
TQ(IKS)=TQ(IK)
TS(IKS)=TS(IK)
CHI(IKS)=CHI(IK)
VAP(IKS)=VAP(IK)
LIQ(IKS)=LIQ(IK)
CONTINUE
I1=2
I2=IBP1
K1=2
K2=KBP2
KK=0
KKL = 0
DO 2989 I=I1,I2
KK=KK+K2NC
KKL = KKL + K2NCL
LWPCL = 1
LWPC=1
IKMS=I2K2 + 1
SIE(1)=SIE(IKMS)
U(1)=U(IKMS)
W(1)=W(IKMS)
TQ(1)=TQ(IKMS)
TS(1)=TS(IKMS)
CHI(1)=CHI(IKMS)
```

2109

1945		
1946		
1947		
1948		
1949		
1950		
1951	VM210008	
1952		
1953		
1954		
1955		
1956		
1957		
1958		
1959	R3BVM52A	
1960	RGBVM60A	
1961	RGBVM60A	
1962	VM210900	
1963		
1964		
1965		
1966		
1967		
1968		
1969		
1970	VM221002	
1971		
1972		
1973		
1974		
1975		
1976		
1977		
1978		
1979		
1980	RGBVM52A	

```

VAP(1)=VAP(IKMS)
LIQ(1)=LIQ(IKMS)
SIE(IKMS)=SIE(KK+1)
U(IKMS)=U(KK+1)
W(IKMS)=W(KK+1)
TQ(IKMS)=TQ(KK+1)
TS(IKMS)=TS(KK+1)
CHI(IKMS)=CHI(KK+1)
VAP(IKMS)=VAP(KK+1)
LIQ(IKMS)=LIQ(KK+1)
GO TO KRU, ( 2215,2220 )
C NOTE. COMPUTATION OF RADIUS CONSTANTS IN THE I DIRECTION .
2215 RR=FLOAT(I-1)*DX
RC=RR-HDX
RL=RR-DX
RRR=1./RR
REC=1./RC
RRC1=RR + HDX
RRC=1./RRC1
RRP=RR + DR
2220 DO 2979 K=K1,K2
C NOTE. COMPUTATION OF CELL INDICES .
LWPC=LWPC+NWPC
IK=KK + LWPC
LWPCL = LWPCL + NWPCL
IKL = KKL + LWPCL
DCR = DIFFCO(IKL)
DCT = DIFFCO(IKL+1)
DCL = DIFFCO(IKL+2)
DCB = DIFFCO(IKL+3)
C NOTE. BYPASS OBSTACLE CELLS .
CFC=CF(IK)
IPK=IK + K2NC
IKP=IK + NWPC
IMKS=I2K2 + LWPC
IKMS=IMKS - NWPCL

```

```

1981 RGBVM60A
1982 RGBVM60A
1983
1984
1985
1986
1987
1988 RGBVM52A
1989 RGBVM60A
1990 RGBVM60A
1991 VM221012
1992
1993
1994
1995
1996
1997
1998
1999
2000
2001
2002
2003
2004
2005
2006
2007
2008
2009
2010
2011
2012
2013
2014
2015
2016

```

VM222002

UR=U (IPK)
 UC=U (IK)
 UL=U (IMKS)
 WT=W (IKP)
 WC=W (IK)
 WB=W (IKMS)
 PC=P (IK)
 PR=P (IPK)
 PT=P (IKP)
 SIEC=SIE (IK)
 SIER=SIE (IPK)
 SIET=SIE (IKP)
 SIEL=SIE (IMKS)
 SIEB=SIE (IKMS)
 SIECO=SIEO (IK)
 UCO=UO (IK)
 WCO=WO (IK)

C NOTE . COMPUTATION OF TQ AND TS CONSTANTS .

TQC=TQ (IK)
 TOR=TQ (IPK)
 TOT=TQ (IKP)
 TOL=TQ (IMKS)
 TOB=TQ (IKMS)
 TQCO=TQO (IK)
 TSC=TS (IK)
 TSR=TS (IPK)
 TST=TS (IKP)
 TSL=TS (IMKS)
 TSB=TS (IKMS)
 TSCO=TSO (IK)
 CHIC=CHI (IK)
 CHIR=CHI (IPK)
 CHIT=CHI (IKP)
 CHIL=CHI (IMKS)
 CHIB=CHI (IKMS)
 CHICO=CHIO (IK)

2017
 2018
 2019
 2020
 2021
 2022
 2023
 2024
 2025
 2026
 2027
 2028
 2029
 2030
 2031
 2032
 2033
 2034
 2035
 2036
 2037
 2038
 2039
 2040
 2041
 2042
 2043
 2044
 2045
 2046
 2047
 2048
 2049
 2050
 2051
 2052

RGBVM5 2A
 RGBVM52A
 RGBVM5 2A
 RGBVM52A
 RGBVM52A
 RGBVM52A


```

2089 DURL=RDR*RRC*TSC*( RR*UC - RL*UL )
2090 DUR=RDR*( DURR - DURL )
2091 DUZ=RDZ*( TSTR*(U(IK?) -UC)*RDZP - TSBRR*(UC-U (IKMS))*RDZM )
2092 FUT=DUR + DUZ
2093 GO TO KCLU,( 2370,2400 )
2094 C NOTE. COMPUTATION OF THE U TILDE CYLINDRICAL FLUX TERM .
2095 2370 FCU=.5*RRR*( URA*URA + ULA*ULA + .5*ALX*URAA*(UC-UR)
2096 + .5*ALX*ULAA*(UL-UC) )
2097 C NOTE. COMPUTATION OF W TILDE FLUXES .
2098 2400 UTA=.5*(UC+U(IKP))
2099 UTAA=ABS(UTA)
2100 ULT=.5*(UL+U (IKMS+NWPC))
2101 ULTA=ABS(ULT)
2102 WTA=.5*( WC+WT )
2103 WTA=ABS ( WTA )
2104 WBA=.5*( WB+WC )
2105 WBA=ABS ( WBA )
2106 FWX=.5*RDZ*( UTA*(WC+W(IPK)) + ALX*UTAA*(WC-W(IPK))
2107 - ULT*(W(IKMS)+WC) - ALX*ULTA*(W(IKMS)-WC) )
2108 FWZ=.5*RDZ*( WTA*(WC+WT) + ALZ*WTA*(WC-WT)
2109 - WBA*(WB+WC) - ALZ*WBA*(WB-WC) )
2110 C NOTE. CALCULATION OF THE W TILDE DIFFUSION TERMS .
2111 DWRR=RDRP*RR*TSTR*(W(IPK)-WC)
2112 DWRL=RDRM*RRL*TSTL*(WC-W(IKMS))
2113 DWR=RRC*RDR*( DWRR - DWRL )
2114 DWZ=RDZP*( TST*(WT-WC)*RDZ - TSC*(WC-WB)*RDZ )
2115 FWT=DWR + DWZ
2116 GO TO KCLW,( 2470,2500 )
2117 C NOTE. COMPUTATION OF THE W TILDE CYLINDRICAL FLUX TERM .
2118 2470 FCW=.25*RRC*( UTA*(WC+W(IPK)) + ULT*(W(IKMS)+WC)
2119 + ALX*UTAA*(WC-W(IPK)) + ALX*ULTA*(W(IKMS)-WC) )
2120 C NOTE. COMPUTATION OF BOTH Q AND SIGMA TURBULANCE QUANTITIES .
2121 2500 TQRA=.5*(TQC+TQR)
2122 IF( ICALI.EQ.1 ) GO TO 2591
2123 TQLA=.5*(TQC+TQL)
2124 TQTA=.5*( TQC+TOT)

```

VH237002

VH240002

VH240006

VH240012

VH240014

```

2125      TQBA = .5 * (TQC + TQB)
2126      TSRA = .5 * (TSC + TSR)
2127      TSLA = .5 * (TSC + TSL)
2128      TSTA = .5 * (TSC + TST)
2129      TSBA = .5 * (TSC + TSB)
2130
2131      C NOTE. CALCULATION OF THE SIJ TERM, I.E. THE SOURCE TERM.
2132      SIJ = RDRS * (WC - UL) ** 2 + RDZS * (WC - WB) ** 2 + .25 * CYL * (RRC * (UC + UL) ** 2 +
2133      1      0.03125 * (RDZ * ( U (IKP) + U (IMKS + NWPC) - U (IKMS) - U (1) )
2134      + RDR * ( W (IPK) + W (IPK - NWPC) - W (IMKS) - W (1) ) ) ** 2
2135
2136      C NOTE. CALCULATION OF THE Q EQUATION CONVECTION TERMS.
2137      CQR = -.5 * RRC * PDR * ( RR * ( UC * (TQC + TQR) + ALX * ABS(UC) * (TQC - TQR) )
2138      1      - RL * ( UL * (TQL + TQC) + ALX * ABS(UL) * (TQL - TQC) ) )
2139      CQZ = -.5 * RDZ * (WC * (TQC + TQT) + ALZ * ABS(WC) * (TQC - TQT)
2140      1      - WB * (TQB + TQC) - ALZ * ABS(WB) * (TQB - TQC) )
2141
2142      C NOTE. CALCULATION OF THE Q EQUATION DIFFUSION TERM.
2143      DQRR = RRC * RDR * ( RR * TSRA * (TQR - TQC) ) * DCR
2144      DQRL = RRC * RDR * ( RL * TSLA * ( TQC - TQL ) ) * DCL
2145      DQR = RDR * ( DQRR - DQRL)
2146      DQZT = RDZ * ( TSTA * ( TQT - TQC ) ) * DCT
2147      DQZB = RDZ * ( TSBA * ( TQC - TQB ) ) * DCB
2148      DQZ = RDZ * ( DQZT - DQZB)
2149
2150      C NOTE. CALCULATION OF THE Q EQUATION DECAY TERM.
2151      DQ = 4 * ALP * TQC / ( TSC + 1.E-20 )
2152
2153      C NOTE. CALCULATION OF THE NEW Q AT TIME N+1.
2154      TQ(IK) = (1. / (1. + DT * DQ) ) * ( TQCO + DT * (CQR + CQZ + 2. * TSC * SIJ +
2155      1      GAM * (DQR + DQZ) ) )
2156
2157      C NOTE. COMPUTATION OF SIGMA QUANTITIES.
2158
2159      C NOTE. CALCULATION OF THE SIGMA EQUATION CONVECTION TERMS.
2160      CSR = -.5 * RRC * RDR * ( RR * ( UC * (TSC + TSR) + ALX * ABS(UC) * (TSC - TSR) )
2161      1      - RL * ( UL * (TSL + TSC) + ALX * ABS(UL) * (TSL - TSC) ) )
2162      CSZ = -.5 * RDZ * ( WC * (TSC + TST) + ALZ * ABS(WC) * (TSC - TST)
2163      1      - WB * (TSB + TSC) - ALZ * ABS(WB) * (TSB - TSC) )
2164
2165      C NOTE. CALCULATION OF THE SIGMA EQUATION DIFFUSION TERM.
2166      IF( I.LT.I2 ) GO TO 2502
2167      IFLGS = 0
2168      IFLGQ = 0

```

```

2161 IF ( TQR.LT.0.0 ) IFL3Q=1
2162 IF ( TSR.LT.0.0 ) IFLGS=1
2163 IFLG1=IFLGQ+IFLGS
2164 IF ( IFLG1.EQ.2 ) TQR=-TQR
2165 IF ( K.GT.K1 ) GO TO 2504
2166 IFLGS=0
2167 IFLGQ=0
2168 IF ( TQB.LT.0.0 ) IFL3Q=1
2169 IF ( TSB.LT.0.0 ) IFLGS=1
2170 IFLG1=IFLGQ + IFLGS
2171 IF ( IFLG1.EQ.2 ) TQB=-TQB
2172 IF ( K.LT.KBP1 ) GO TO 2506
2173 IFLGS=0
2174 IFLGQ=0
2175 IF ( TQT.LT.0.0 ) IFL3Q=1
2176 IF ( TST.LT.0.0 ) IFLGS=1
2177 IFLG1=IFLGQ + IFLGS
2178 IF ( IFLG1.EQ.2 ) TQT=-TQT
2179 IF ( I.GT.I1 ) GO TO 2508
2180 IFLGS=0
2181 IFLGQ=0
2182 IF ( TQL.LT.0.0 ) IFLGQ=1
2183 IF ( TSL.LT.0.0 ) IFLGS=1
2184 IFLG1=IFLGQ + IFLGS
2185 IF ( IFLG1.EQ.2 ) TQL=-TQL
2186 CONTINUE
2187 DSR = RRC * RDR * ( RR * TQRA * ( TQR/TSR - TQC/TSC ) ) * DCR
2188 DSRL = REC * RDR * ( RL * TQLA * ( TQC/TSC - TQL/TSL ) ) * DCL
2189 DSR = RDR * ( DSRR - DSRL)
2190 DSZT = RDZ * ( TQTA * ( TQT/TST - TQC/TSC ) ) * DCT
2191 DSZB = RDZ * ( TQBA * ( TQC/TSC - TQB/TSB ) ) * DCB
2192 DSZ = RDZ * ( DSZT - DSZB)
2193 DIJ=GAM*TSC/TQC*( DQR+DQZ ) - GAM1*TSC*TSC/TQC*TQC*( DSR+DSZ)
2194 DIJ=GAM*TSC/TQC*( DQR+DQZ ) - GAM1*TSC*TSC*TSC/TQC**2*( DSR+DSZ)
2195 DS=4.*ALP0*TQC/( TSC+1.E-20 )
2196 DS=ALP*TQC/(TSC+1.E-20)

```

RGBVM000
 RGBVM000
 HWG04/78
 HWG04/78

```

C NOTE. CALCULATION OF THE NEW SIGMA AT N+1 .
TS (IK) = (1. / (1. + DT * DS)) * ( TSCO + DT * (CSR + CSZ + TSC * TSC / TQC * SIJ + DIJ) )
IF (TQ (IK) .LT. ZTQ (K)) TQ (IK) = ZTQ (K)
IF (TS (IK) .LT. ZTS (K)) TS (IK) = ZTS (K)
C CALCULATION OF TERMS IN THE VAP TRANSPORT EQUATION
CVR = .5 * RRC * RDR * ( RR * ( UC * (VAPC + VAPR) + ALX * ABS (UC) * (VAPC - VAPR) )
1 - RL * ( UL * (VAPL + VAPC) + ALX * ABS (UL) * (VAPL - VAPC) ) )
CVZ = .5 * RDZ * ( WC * (VAPC + VAPT) + ALZ * ABS (WC) * (VAPC - VAPT)
1 - WB * (VAPB + VAPC) - ALZ * ABS (WB) * (VAPB - VAPC) )
DVR = RDR * (RR * GAMV * TSRA * DCR * (VAPR - VAPC))
DVRL = RDR * (RL * GAMV * TSLA * DCL * (VAPC - VAPL))
DVR = REC * RDR * (DVR - DVRL)
DVZT = RDZ * (GAMV * TSTA * DCT * (VAPT - VAPC))
DVZB = RDZ * (GAMV * TSBA * DCB * (VAPC - VAPB))
DVZ = RDZ * (DVZT - DVZB)
VAP (IK) = VAPCO + DT * (-CVR - CVZ + DVR + DVZ)
C CALCULATION OF TERMS IN THE LIQ TRANSPORT EQUATION
CLR = .5 * RRC * RDR * ( RR * ( UC * (LIQC + LIQR) + ALX * ABS (UC) * (LIQC - LIQR) )
1 - RL * ( UL * (LIQL + LIQC) + ALX * ABS (UL) * (LIQL - LIQC) ) )
CLZ = .5 * RDZ * ( WC * (LIQC + LIQT) + ALZ * ABS (WC) * (LIQC - LIQT)
1 - WB * (LIQB + LIQC) - ALZ * ABS (WB) * (LIQB - LIQC) )
DLRR = RDR * (RR * GAML * TSRA * DCR * (LIQR - LIQC))
DLRL = RDR * (RL * GAML * TSLA * DCL * (LIQR - LIQL))
DLR = REC * RDR * (DLRR - DLRL)
DLZT = RDZ * (GAML * TSTA * DCT * (LIQT - LIQC))
DLZB = RDZ * (GAML * TSBA * DCB * (LIQC - LIQB))
DLZ = RDZ * (DLZT - DLZB)
LIQ (IK) = LIQCO + DT * (-CLR - CLZ + DLR + DLZ)
C EQUILIBRIUM MOISTURE THERMODYNAMICS SECTION
CIT = CI - SIEC
TEMPC = SI (AI, BI, CIT, -1)
RHOC = AR * TEMPC * TEMPC + BR * TEMPC + CR
C CALCULATE THE ABSOLUTE THERMODYNAMIC TEMPERATURE (DEG C)
ABT = (TEMPC + 459.7) * (ZAP (K) / 1000.) * *.2856 / (1. + 0.61 * VAP (IK) / RHOC) / 1
A.8

```



```

DIR=RRC *RDR*(DIRR-DIRL)
DIZT=RDZ*(GAMT*TTSTA*DCT*(SIET-SIEC))
DI7B=RD7*(GAMT*TSBA*DCB*(SIEC-SIEB))
DIZ=RDZ*(DIZT-DIZB)
C CALCULATION OF DECAY HEAT (BTU/LBM*SEC)
DECHT=4.150934E10*CHI(IK)*SER/(RHOC*WMOLX)
C NOTE. COMPUTATION OF THE NEW SPECIFIC INTERNAL ENERGY AT N+1 .
SIE(IK)=SIECO + DT*( -CIP - CIZ + DIR + DIZ - CQ(IK)+DECHT)
C CALCULATION OF TERMS IN THE CHI TRANSPORT EQUATION
CXR=.5*RRC*RDR*( RR*( UC*( CHIC+CHIR) + ALX*ABS(UC) * (CHIC-CHIR) )
1 - RL*( UL*( CHIL+CHIT) + ALZ*ABS(WC) * (CHIC-CHIT)
CXZ=.5*RDZ*( WC*(CHIC+CHIT) + ALZ*ABS(WB) * (CHIB-CHIC) )
1 - WB*(CHIB+CHIC) - ALZ*ABS(WB) * (CHIB-CHIC) )
DXRR=RDR*(RR*GAMX*TSRA*DCR*(CHIR-CHIC))
DXRL=RDR*(RL*GAMX*TSLA*DCL*(CHIC-CHIL))
DXR=RRC *RDR*(DXRR-DXRL)
DXZT=RDZ*(GAMX*TTSTA*DCT*(CHIT-CHIC))
DXZB=RDZ*(GAMX*TSBA*DCB*(CHIC-CHIB))
DXZ=RDZ*(DXZT-DXZB)
CHI(IK)=CHICO*(1.0-RLAMB*DT)+DT*(-CXR-CXZ+DXR+DXZ)
GO TO 2650
C NOTE. CALCULATION OF SPECIFIC MATERIAL FOR TEMPERATURE AND
C NOTE. RELATIVE DENSITY .
2591 GO TO ( 2592,2594,2596,2598 ),MAT
C NOTE. CALCULATION OF SODIUM MATERIAL FOR TEMPERATURE AND RHO .
2592 TEMPC=-385.27 + 2.6602*SIEC + 5.9894E-04*SIEC*SIEC +
1 1.5575E-06*SIEC**3 - 2.9048E-09*SIEC**4 +
2 1.15427E-12*SIEC**5
TEMPT=-385.27 + 2.6602*SIET + 5.9894E-04*SIET*SIET +
1 1.5575E-06*SIET**3 - 2.9048E-09*SIET**4 +
2 1.15427E-12*SIET**5
TEMPR=-385.27 + 2.6602*SIER + 5.9894E-04*SIER*SIER +
1 1.5575E-06*SIER**3 - 2.9048E-09*SIER**4 +
2 1.15427E-12*SIER**5
RHOC=59.566 - 7.9504E-3*TEMPC - 0.2872E-6*TEMPC*TEMPC +
1 0.06035E-9*TEMPC*TEMPC*TEMPC

```

```

2269
2270
2271
2272
2273
2274
2275
2276
2277
2278
2279
2280
2281
2282
2283
2284
2285
2286
2287
2288
2289
2290
2291
2292
2293
2294
2295
2296
2297
2298
2299
2300
2301
2302
2303
2304

```

```

RGBVM56A
RGBVM56A
RGBVM52C
RGBVM52C
RGBVM52C
RGBVM52C
RGBVM52C
RGBVM52C
RGBVM52C
RGBVM52C
RGBVM52C
RGBVM52C
RGBVM52C
RGBVM52C
RGBVM52C
RGBVM52C
RGBVM52C
RGBVM52C
RGBVM52C
RGBVM52C
RGBVM52C
RGBVM52C
RGBVM52C
RGBVM52C

```

```

RHOT=59.566 - 7.9504E-3*TEMP - 0.2872E-6*TEMP*TEMP +
1 0.06035E-9*TEMP*TEMP*TEMP
RHOR=59.566 - 7.9504E-3*TEMP - 0.2872E-6*TEMP*TEMP +
1 0.06035E-9*TEMP*TEMP*TEMP
RHOA=0.5*( RHOC+RHOT )
RHOAX=0.5*( RHOC+RHOR )
RHOX=( RHOAX-RHO0 )/RHO0
RHOZ=( RHOA-RHO0 )/RHO0
GO TO 2600
C NOTE. CALCULATION OF WATER MATERIAL FOR TEMPERATURE AND RHO .
2594 TEMPC=0.9996*SIEC + 32.0002
TEMPT=0.9996*SIEC + 32.0002
TEMPR=0.9996*SIEC + 32.0002
RHOC=62.742 -0.372E-2*TEMPC - 0.44E-4*TEMPC*TEMPC
RHOT=62.742 -0.372E-2*TEMPT - 0.44E-4*TEMPT*TEMPT
RHOA=0.5*( RHOC+RHOT )
RHOAX=0.5*( RHOC+RHOR )
RHOZ=( RHOA-RHO0 )/RHO0
RHOR=62.742 -0.372E-2*TEMPR - 0.44E-4*TEMPR*TEMPR
RHOX=( RHOA-RHO0 )/RHO0
GO TO 2600
2596 CIT=CI - SIEC
TEMPC=SI ( AI,BI,CIT,-1 )
CIT=CI-SIEC
TEMPT=SI ( AI,BI,CIT,-1 )
CIT=CI-SIEC
TEMPR=SI ( AI,BI,CIT,-1 )
RHOC=AR*TEMPC*TEMPC + BR*TEMPC + CR
RHOT=AR*TEMPT*TEMPT + BR*TEMPT + CR
RHOR=AR*TEMPR*TEMPR + BR*TEMPR + CR
RHOA=0.5*( RHOC+RHOT )
RHOZ=( RHOA-RHO0 )/RHO0
RHOAX=0.5*( RHOC+RHOR )
RHOX=( RHOA-RHO0 )/RHO0
GO TO 2600
2598 CONTINUE

```

```

C NOTE. COMPUTATION OF FULL TILDE EQUATIONS AT TIME=N+1 .
2600 IF( ICALL.EQ.2 ) GO TO 2650
      U(IK)=(1./(1.+DT*RXCI))*( UCO + DT*( RDX*(PC-PR) + RHOX*GX
1      - FUX - FUZ - FCU + FUT ) )
      W(IK)=(1./(1.+DT*RZC))*( WCO + DT*( RDZ*(PC-PT) + RHOZ*GZ
1      - FWX - FWZ - FCW + FWT ) )

2650 IF( ICALL.EQ.1 ) GO TO 2700
C NOTE. UPDATING THE Q EQUATION WITH THE RESISTANCE FACTORS .
      RXC=RX(IK)*ABS( UO(IK) )**NRESEX
      RXL=RX(IK)*ABS( UO(IK) )**NRESEX
      RZC=RZ(IK)*ABS( WO(IK) )**NRESEX
      RZB=RZ(IK)*ABS( WO(IK) )**NRESEX
2700  U(1)=U(IKKS)
      W(1)=W(IKKS)
      TQ(1)=TQ(IKKS)
      TS(1)=TS(IKKS)
      SIE(1)=SIE(IKKS)
      CHI(1)=CHI(IKKS)
      VAP(1)=VAP(IKKS)
      LIQ(1)=LIQ(IKKS)
      SIR(IKKS)=SIBC
      U(IKKS)=UC
      W(IKKS)=WC
      TQ(IKKS)=TQC
      TS(IKKS)=TSC
      CHI(IKKS)=CHIC
      VAP(IKKS)=VAPC
      LIQ(IKKS)=LIQC
2979  CONTINUE
2989  CONTINUE
      ASSIGN 2990 TO KBC
      IF( NTE.LT.NTPAS ) GO TO 1100
2990  CONTINUE
2999  CONTINUE
      IF( ICALL.EQ.2 ) GO TO 5050
C NOTE. IMPLICIT PRESSURE ITERATION .

```

```

2341
2342
2343
2344
2345
2346
2347
2348
2349
2350
2351
2352
2353
2354
2355
2356
2357
2358
2359
2360
2361
2362
2363
2364
2365
2366
2367
2368
2369
2370
2371
2372
2373
2374
2375
2376

```

```

RGBVM52B
RGBVM60A
RGBVM60A

```

```

RGBVM52B
RGBVM60A
RGBVM60A

```



```

4050 IFC=0
      ASSIGN 4100 TO KBC
      GO TO 1100
C NOTE. BEGIN PRESSURE ITERATION AFTER SETTING BOUNDARY CONDITIONS .
4100 I1=2
      I2=IBP1
      K1=2
      K2=KBP1
      KK=1
      DO 4489 I=I1,I2
      KK=KK + K2NC
      LWPC=0
      RADD=(FLOAT(I)-1.5)*DX
      RRADD=1./RADD
      IF ( CYL.LT.EM6 ) RRADD=0.0
      DO 4479 K=K1,K2
      LWPC=LWPC + NWPC
      IK=KK + LWPC
      IMK=IK - K2NC
      IKM=IK - NWPC
      CFC=CF(IK)
      IF ( CFC.NE.1 ) GO TO 4470
      D=RDZ*(U(IK)-U(IMK)) + RDZ*(W(IK)-W(IMK)) + .5*RRADD*(U(IK)+U(IMK))
      DTP=-BETA*D
      RXC=RK(IK)*ABS( UO(IK) )**NRESEX
      RXL=RX(IMK)*ABS( UO(IMK) )**NRESEX
      RZC=RZ(IK)*ABS( WO(IK) )**NRESEX
      RZB=RZ(IMK)*ABS( WO(IMK) )**NRESEX
      U(IK)=U(IK) + RDX*DTP/(1.+DT*RXC)
      U(IMK)=U(IMK) - RDX*DTP/(1.+DT*RXL)
      W(IK)=W(IK) + RDZ*DTP/(1.+DT*RZC)
      W(IMK)=W(IMK) - RDZ*DTP/(1.+DT*RZB)
      P(IK)=P(IK) + RDT*DTP
C NOTE. CHECKS FOR CONVERGENCE OF PRESSURE FIELD .
      IF ( ABS(D).GT.EPS ) IFC=1
4470 CONTINUE

```

VM452002

VM412006
VM412008
VM412010

VM420002

```

4479 CONTINUE
4489 CONTINUE
      ITPR=ITPR + 1
      IP(ITPR.LT.1500) GO TO 4510
C NOTP. PRESSURES FAILED TO CONVERGE WITHIN 999 ITERATIONS .
      WRITE (IVDO,50)
      ERP=AMIN1(1.0,.1*NCYC)
      GO TO 4600
4510 IP( IFC.EQ.1 ) GO TO 4050
4600 ASSIGN 5000 TO KBC
      ITPRC=ITPR
      ITPR=0
      GO TO 1100
C
C NOTP. COMPUTES THE DIVERGENCE ERRORS - ER(IK) .
C
5000 ICALI=2
      GO TO 2030
5050 ASSIGN 5060 TO KBC
      GO TO 1100
5060 ITPR=ITPRC
      I1=1
      I2=IBP2
      K1=1
      K2=KBP2
      KK=1 - K2NC
      DMX=0.0
      TSMA X=-1.E+20
      TMAX=TSMAX
      WMAX=TWMAX
      UMAX=UWMAX
      TMIN=+1.E+20
      WMIN=TWMIN
      UMIN=UWMIN
      PMAX=-1.E+20
      TOMAX=PWMAX

```

VH452002

2413
2414
2415
2416
2417
2418
2419
2420
2421
2422
2423
2424
2425
2426
2427
2428
2429
2430
2431
2432
2433
2434
2435
2436
2437
2438
2439
2440
2441
2442
2443
2444
2445
2446
2447
2448

```

DO 5029 I=I1,I2
KK=KK + K2NC
LWPC=-NWPC
RRADD=1./(( FLOAT(I) - 1.5)*DX )
DO 5019 K=K1,K2
LWPC=LWPC + NWPC
IK=KK + LWPC
IMK=IK - K2NC
IKM=IK - NWPC
CPC=CF(IK)
IF( CFC.NE.1 ) GO TO 5001
ER(IK)= RDX*( U(IK)-J(IMK) ) + RDZ*( W(IK)-W(IMK) )
DMX=AMAX1( DMX, ABS(ER(IK)) )
1 + .5*CYL*RRADD*( U(IK)+U(IMK) )
5001 SIEO(IK)=SIE(IK)
TQO(IK)=TQ(IK)
TSO(IK)=TS(IK)
UO(IK)=U(IK)
WO(IK)=W(IK)
SIEO(IK)=SIE(IK)
CHIO(IK)=CHI(IK)
VAP(IK)=VAP(IK)
LIQO(IK)=LIQ(IK)
SIEC=SIE(IK)
IF( CFC.GE.30 ) GO TO 5018
GO TO( 5002,5004,5006,5008 ),MAT
C NOTE. COMPUTATION OF TEMPERATURE FOR SODIUM MATERIAL .
5002 TEMP =-385.27 + 2.6602*SIEC + 5.9894E-04*SIEC*SIEC +
1 1.5575E-06*SIEC**3 - 2.9048E-09*SIEC**4 +
2 1.15427E-12*SIEC**5
GO TO 5010
C NOTE. COMPUTATION OF TEMPERATURE FOR WATER MATERIAL .
5004 TEMP=0.9996*SIEC + 32.0002
GO TO 5010
5006 CIT=CI-SIEC
TEMP=SI( AI,BI,CIT,-1 )

```

RGBVM52B
RGBVM60A
RGBVM60A

```

5008 GO TO 5010
5010 CONTINUE
      UMAX=AMAX1 ( UMAX,U( IK ) )
      WMAX=AMAX1 ( WMAX,W( IK ) )
      TMAX=AMAX1 ( TMAX,TEMP )
      TSMAX=AMAX1 ( TSMAX,TS( IK ) )
      UMIN=AMIN1 ( UMIN,U( IK ) )
      WMIN=AMIN1 ( WMIN,W( IK ) )
      TMIN=AMIN1 ( TMIN,TEMP )
      TQMAX=AMAX1 ( TQMAX,T2( IK ) )
      PHAX=AMAX1 ( PHAX,P( IK ) )
      IF( I.EQ.IDG .AND. K.EQ.KDG ) GO TO 5012
      GO TO 5018
5012 UDG=U( IK)
      WDG=W( IK)
      TDG=TEMP
      TIM=TIMET + DT
5018 CONTINUE
5019 CONTINUE
5029 CONTINUE
      IF( ERF.LT.1 ) GO TO 10000
      CALL VRPRT
      IF( IPRFM.GT.0 ) CALL VRPLM
      RETURN
C
C NOTE. UPDATES TIME AND NUMBER OF CYCLES .
C
10000 TIMET=TIMET + DT
      NCYC=NCYC + 1
      SMSIE=0.0
      SMCHI=0.0
      FCHI=0.0
      VELCHI=0.0
C
      COMPUTE PLUME CENTER AND SIGMA (HEIGHT) FOR CHI DISTRIBUTION
      DO 11150 K=2,KBP1
      DO 11160 I=2,IBP1

```

```

RGBVH70A
RGBVH70A
RGBVH70A
RGBVH70A
RGBVH54B
RGBVH54A
RGBVH54A
PAGE
70

```

```

IK=1+NWPC*((I-1)*KBP2)+K-1)
CIT=CI-SIE(IK)
TEMPC=SI(AI,BI,CIT,-1)
RHOC=AR*TEMPC*TEMPC+BR*TEMPC+CR
SMSIE=SMSIE+(RHOC*DX*DZ*SIE(IK))
SMCHI=SMCHI+(CHI(IK)-BKGND)
FCHI=FCHI+(FLOAT(K)-1.5)*DZ*(CHI(IK)-BKGND)
VELCHI=VELCHI+WSP(K)*(CHI(IK)-BKGND)
11160 CONTINUE
11150 CONTINUE
YPLUME=FCHI/SMCHI
VELCHI=VELCHI/SMCHI
DWNDS=DWNDS+VELCHI*DT
IF(IDIAG.GT.0)WRITE(IVDO,51)TIMET,NCYC,ITER,DT,DMX
IF(IDIAG.EQ.0)GO TO 11000
IF(IDATIN.EQ.1)GO TO 11001
11000 IF(TIMET+1.0E-5.LT.TPRT)GO TO 11100
TPRT=TPRT+TPR
CALL VRPRT
GO TO 11100
11001 TPRT=TPRT+TPR
11100 IF(IPRFM.LT.1.OR.TIMET+1.0E-5.LT.TPLT)GO TO 11200
TPLT=TPLT+TPL
WRITE(IVDO,60)YPLUME,VELCHI,DWNDS
60 FORMAT(' ',15HPLOME CENTER AT,F8.2,6H FEET.,15H PLUME SPEED IS,
1P8.2,22H DOWNWIND DISTANCE IS,F6.0)
WRITE(IVDO,63)SMSIE
63 FORMAT(4H ',TOTAL ENERGY ON MESH IS ',E12.5)
WRITE(IVDO,51)TIMET,NCYC,ITER,DT,DMX
CALL VRF LM
11200 CONTINUE
C TIMING SECTION FOR RESTARTING PROGRAM ON A COARSER MESH
11300 IF(TIMET+1.0E-5.LT.TRSTRT(NRSTRT))GO TO 11400
CALL COARSE
NRSTRT=NRSTRT+1

```

```

RGBVM54A 2521
RGBVM70A 2522
RGBVM70A 2523
RGBVM70A 2524
RGBVM70A 2525
RGBVM70A 2526
RGBVM70A 2527
RGBVM70A 2528
RGBVM54A 2529
RGBVM54A 2530
RGBVM70A 2531
RGBVM70A 2532
RGBVM70A 2533
RGBVM54A 2534
RGBVM54A 2535
RGBVM54A 2536
RGBVM54A 2537
RGBVM54A 2538
RGBVM54A 2539
RGBVM54A 2540
RGBVM54A 2541
RGBVM54A 2542
RGBVM54A 2543
RGBVM54A 2544
RGBVM54B 2545
RGBVM54A 2546
RGBVM54B 2547
RGBVM55B 2548
RGBVM55B 2549
RGBVM55B 2550
RGBVM55B 2551
RGBVM55A 2552
RGBVM55A 2553
RGBVM55A 2554
RGBVM55A 2555
RGBVM55A 2556

```



```

IF ( VEL.GT.EM6 ) DT=ISTEP*ALENG/VEL
DTDIF=TSSTEP*RDZDZS/TSMAX
VELNEW=AMAX1 ( UMAX,WMAX )
TAUDT=0.20*VELNEW/( VELNEW-VELOLD+EM6 )
TAUDT=ABS( TAUDT )
DT=AMIN1 ( DT,DTDIF,TAUDT )
RDT=1./DT
13010 IDATIN=0
IF( TIME+1.0E-5 .LT. TFIN ) GO TO 100
RETURN
C *** * FORMATS ***** FORMATS ***** FORMATS *****
50 FORMAT(1H,75H *** ERROR 004 - PRESSURES FAILED TO CONVERGE WITHIN
1 1500 ITERATIONS . ***)
51 FORMAT(1H,5HTIME=,1PE12.4,3H , , 14HCYCLE NUMBER =,I5,3H , ,
1 28H PRESSURE ITERATION NUMBER =,I4,3H , , 4HDT =,E12.4,3H , ,
2 16HMAX DIVERGENCE =,E12.4)
52 FORMAT(1H,5X,62H THE FOLLOWING DIAGNOSTICS OCCUR AFTER TIME HAS B
1EEN UPDATED .)
54 FORMAT(1H,5X,2HI=,I3,3H K=,I3,4H U=,1PE12.5,4H W=,E12.5,
1 4H T=,E12.5,3H * ,6H UMAX=,E12.5,6H UMIN=,E12.5/6H WMAX=,E12.5,
2 6H WMIN=,E12.5,17X,7H TMAX=,E12.5,7H THIN=,E12.5,7H TSMAX=,
3 E12.5/7H EPS=,E12.5)
55 FORMAT(1H,5X,10HTIME/CYC =,1PE10.3,10H TOT TIME=,E10.3,
1 10HI/O T/CYC=,E10.3,10H TOT I/O =,E10.3)
END

```

VH999991

2593
2594
2595
2596
2597
2598
2599
2600
2601
2602
2603
2604
2605
2606
2607
2608
2609
2610
2611
2612
2613
2614
2615
2616
2617




```

*****
*
* TO SET ELEMENTS OF REAL OR INTEGER ARRAYS TO ZERO. A1,A2,...
* ARE ARRAY NAMES AND N1,N2,... ARE INTEGER VALUES OR
* EXPRESSIONS GIVING THE ARRAY SIZES.
** I.E. - CALL ERASE(C,26*31,N,7*31,E,254)
*
*****
ERASE START 0
      SAVE (14,12),,*
      BALR 12,0
      USING *,12
      SR 0,0
      SR 2,2          PARAMETER LIST INDEX=0
      L 6,=F'4'
E1    L 3,0(2,1)     LOAD 3 WITH ARRAY ADDRESS
      L 4,4(2,1)     LOAD 4 WITH ADDRESS OF ARRAY LENGTH
      L 7,0(4)       LOAD 7 WITH ARRAY LENGTH-1 TIMES 4
      SLA 7,2
      SR 7,6
      SR 5,5
E2    ST 0,0(5,3)    STORE ZERO
      BXLE 5,6,E2
      LTR 4,4        TEST FOR LAST ARGUMENT IN LIST
      BM RETN
      A 2,=F'8'
      B E1          PICK UP NEXT ARGUMENT PAIR
RETN  RETURN (14,12),T
      END
      INTEGER BUFL,CF,CF1,CFB,CFC,CPI,CPL,CFR,CFS,CPT,CQF,ERF,TD,VNTP,
1     VTP
      REAL NU,LIQ,LIQO,LIQI,LOUT
      DIMENSION CF(1),CQ(1),QCON(1),P(1),RX(1),RZ(1),TQ(1),TS(1),U(1),
1     W(1),ER(1),FFX3(102),FFY3(102),PBTIN(2),UO(1),WO(1),TQO(1),
2     TSO(1),SIE(1),SIED(1),CHI(1),CHIO(1)
      A,VAP(1),VAPO(1),LIQ(1),LIQO(1)

```

```

ERAS0010 0001
* ERAS0020 0002
* ERAS0030 0003
* ERAS0040 0004
* ERAS0050 0005
** ERAS0060 0006
* ERAS0070 0007
*****
ERAS0080 0008
ERAS0090 0009
ERAS0100 0010
ERAS0110 0011
ERAS0120 0012
ERAS0130 0013
ERAS0140 0014
ERAS0150 0015
ERAS0160 0016
ERAS0170 0017
ERAS0180 0018
ERAS0190 0019
ERAS0200 0020
ERAS0210 0021
ERAS0220 0022
ERAS0230 0023
ERAS0240 0024
ERAS0250 0025
ERAS0260 0026
ERAS0270 0027
ERAS0280 0028
ERAS0290 0029
RGBMN6 0A 0032
RGBMN0 1A 0035
RGBMN6 0A 0036

```

0037 3 TYMF (25) ,FN (25) ,TYMT1 (25) ,T1N (25) ,TYMT2 (25) ,T2N (25) ,
 0038 4 COFA (25) ,COFBA (25) ,COFBB (25) ,COFBC (25) ,COFLA (25) ,COFLB (25) ,COFLC (25) ,
 0039 5 COFA (25) ,COFBA (25) ,COFBB (25) ,COFBC (25) ,COFLA (25) ,COFLB (25) ,COFLC (25) ,
 0040 6 OFOFTA (25) ,OFOFTB (25) ,OFOFTC (25) ,
 0041 7 OFOBRA (25) ,OFOBBA (25) ,OFOBBC (25) ,TAU (10) ,USL (32) ,USLOB (20) ,
 0042 8 USROB (20) ,USTOB (20) ,USBOB (20) ,
 0043 9 COFBD (25) ,COFBE (25) ,COFTD (25) ,COFTE (25) ,COFTF (25) ,COFBE (25) ,
 0044 *COFRD (25) ,COFRE (25) ,COFLD (25) ,COFLE (25) ,COFRF (25) ,COFLF (25) ,
 0045 AOFBTD (25) ,OFORTE (25) ,OFORBD (25) ,OFORBE (25) ,
 0046 B OFORTE (25) ,OFORBE (25) ,
 0047 CTYMT3 (25) ,TYMT4 (25) ,TYMT5 (25) ,T3N (25) ,T4N (25) ,T5N (25) ,
 0048 * IICFR (1) ,IICFL (1) ,IICFB (1) ,
 0049 * ZER01 (1165) ,ZER02 (608) ,ZER03 (16) ,ZER04 (3) ,
 0050 DIMENSION ZSIE (22) ,ZTQ (22) ,ZVF (22) ,ZLQ (22) ,ZAF (22) ,WSP (22) RGBWM62A
 0051 DIMENSION TRSIRT (5) ,ZSIR (100) ,WZTQ (100) ,WZTS (100) RGBWM55A
 0052 A ,WZVF (100) ,WZLQ (100) ,WZAF (100) ,WZSP (100) RGBWM62A
 0053 COMMON/VRCOM/A (14000) RGBMN60A
 0054 COMMON/RGB/RLAMB,CHI, GAMX, NRSTRT, TRSIRT, ZSIE, ZTQ, ZTS, WZSIE, WZTQ, RGBWM55A
 0055 WZTS, NPROF, WZVF, WZLQ, ZVF, ZLQ, GAML, GAMV, VAPI, LIQI RGBMN60A
 0056 B, WSP, WZSP, BKND, DWZS RGBMN60B
 0057 COMMON /VRCON /ALP,ALPO,ALX,ALZ,B0,BETA,BURL,CFI (9) ,CFS (9) ,CYL,
 1 DT,DX,DZ,EM6,EPS,ERF,FSLIP,GAM,GAM1,GX,GZ,HDX,HDZ,I,1,12,12K2,
 2 IBP1,IBP2,IBR, IDALIN, IDIAG, IKP2, IOBS, IRSTRT, I TAPW, I TER, I VDI,
 3 I VDO, K, K1, K2, K2NC, KBP1, KBP2, KBR, KNC, KWB, KWL, KWR, KWT, LABEL (20) ,
 4 LPR, NCYC, NCYCB, NPRT, NU, NWPC, RDT, RDX, RDZ, RDZS, RIBKB, ROI, TD, TFIN,
 5 TIMET, TIOSUM, TPL, TPLT, TPR, TPRT, TQI, TSI, TTD, TWD, UI, WI
 * USR (32) ,UST (22) ,USB (22) ,USO (10) ,FFX3, FFX3
 6 ,AW,BW,CM,EPSS,UBLI,UBRI,WBBI,WBTI,WBPS,WOBI,NTPAS,TGAM,CSUBB,
 7 TO,SI,HI,IDG,KDG,TL,MAT,RHOO,AT,TMU,TK,TYMF, FN,TYMT1,T1N,TYMT2,
 8 T2N,RRBAN,NRESK,NFLOW,NT1,NT2,TSTRP,KDERBC,UOBI,COFBA,COFBB,
 9 COFBC,COFLA,COFLB,COFLC,COFRA,COFRC,COFLA,COFLB,COFLC,
 * OFOFTA,OFOFTB,OFOFTC,OFORBA,OFORBB,OFORBC,TAU,NTAU,USL,
 1 USLOB,USROB,USTOB,USBOB,UMAX,WMAX
 * CSUBO,EPSS,RDX,DZS,RLNGH ,TQJFT,TSJBT
 COMMON /FLMCON /DROU,DROU,IBRFM
 COMMON /VRMAT3 /AI,BI,CI,AR,BR,CR,AMU,BMU,CMU,AK,BK,CK,ACP,BCP,CCP

```

0001 ERAS0010
0002 ERAS0020
0003 ERAS0030
0004 ERAS0040
0005 ERAS0050
0006 ERAS0060
0007 ERAS0070
0008 ERAS0080
0009 ERAS0090
0010 ERAS0100
0011 ERAS0110
0012 ERAS0120
0013 ERAS0130
0014 ERAS0140
0015 ERAS0150
0016 ERAS0160
0017 ERAS0170
0018 ERAS0180
0019 ERAS0190
0020 ERAS0200
0021 ERAS0210
0022 ERAS0220
0023 ERAS0230
0024 ERAS0240
0025 ERAS0250
0026 ERAS0260
0027 ERAS0270
0028 ERAS0280
0029 ERAS0290
0030
0031
0032 RGBMN6 0A
0033
0034
0035 RGBMN0 1A
0036 RGBMN6 0A
1 PAGE

```

* TO SET ELEMENTS OF REAL OR INTEGER ARRAYS TO ZERO. A1,A2,...
* ARE ARRAY NAMES AND N1,N2,... ARE INTEGER VALUES OR
* EXPRESSIONS GIVING THE ARRAY SIZES.
** I.E. - CALL ERASE(C,26*31,N,7*31,E,254)
*

ERASE START 0
SAVE (14,12),*
BALR 12,0
DSING *,12
SR 0,0
SR 2,2
L 6,=F'4'
L 3,0(2,1)
L 4,4(2,1)
L 7,0(4)
SLA 7,2
SR 7,6
SR 5,5
ST 0,0(5,3)
BXLE 5,6,E2
LTR 4,4
BM RETN
A 2,=F'8'
B E1
RETN RETURN (14,12),T
END
INTEGER BUFL,CF,CF1,CFB,CFC,CFL,CFR,CFS,CFT,CQF,ERF,TD,VNTP,
1 VTP
REAL NU,LIQ,LIQO,LIQI,LOUT
DIMENSION CF(1),CQ(1),QCON(1),P(1),RX(1),RZ(1),TQ(1),TS(1),U(1),
1 W(1),ER(1),FFX3(102),FFY3(102),PBTIM(2),DO(1),WO(1),TQO(1),
2 TSO(1),SIE(1),SIEO(1),CHI(1),CHIO(1)
A,VAP(1),VAPO(1),LIQ(1),LIQO(1)

3 , TYMF (25), FN (25), TYMT1 (25), T1N (25), TYMT2 (25), T2N (25),
 4 COFBA (25), COFBB (25), COFBC (25), COFTA (25), COFTB (25), COFTC (25),
 5 COFRA (25), COFRB (25), COFRC (25), COFLA (25), COFLB (25), COFLC (25),
 6 OFOFTA (25), OFOFTB (25), OFOFTC (25),
 7 OFOBRA (25), OFOBRB (25), OFOBR C (25), TAU (10), USL (32), USLOB (20),
 8 USROB (20), USTOB (20), USBOB (20)
 9, COFBD (25), COFBE (25), COFTD (25), COFTE (25), COFTF (25), COFBF (25),
 *COFRD (25), COFRE (25), COFLD (25), COFLE (25), COFRF (25), COFLF (25),
 AOFOTD (25), OFOOTE (25), OFOORD (25), OFOORE (25),
 B OFOTF (25), OFOBRF (25),
 C TYMT3 (25), TYMT4 (25), TYMT5 (25), T3N (25), T4N (25), T5N (25),
 * IICFR (1), IICFL (1), IICFT (1), IICFB (1)
 * , ZERO1 (1165), ZERO2 (608), ZERO3 (16), ZERO4 (3)
 DIMENSION ZSIE (22), ZTQ (22), ZTS (22), ZVP (22), ZLQ (22), ZAP (22), WSP (22) RGBVM62A
 DIMENSION TRSIRT (5), #ZSIE (100), WZTQ (100), WZTS (100) RGBVM55A
 A, WZVP (100), WZLQ (100), WZAP (100), WWS (100) RGBVM62A
 COMMON /VR COM /A (14000) RGBMN60A
 COMMON /RGB /RLAMB, CHII, GAMX, NRSIRT, TRSIRT, ZSIE, ZTQ, ZTS, WZSIE, WZTQ, RGBVM55A
 AWZTS, NPROF, WZVP, WZLQ, ZVP, ZLQ, GAML, GAMV, VAPI, LIQI RGBMN60A
 B, WSP, WWS, BKGND, DWNDS RGBMN60B
 COMMON /VR CON / ALP, ALPO, ALX, ALZ, B0, BETA, BUFL, CFI (9), CFS (9), CYL,
 1 DT, DX, DZ, EM6, EPS, ERF, FSLIP, GAM, GAM1, GX, GZ, HDX, HDZ, I, I1, I2, I2K2,
 2 IBP1, IBP2, IBR, IDAFIN, IDIAG, IKP2, IOBS, IRSIRT, I TAPW, I TER, IVDI,
 3 I VDO, K, K1, K2, K2NC, KBP1, KBP2, KBR, KNC, KWB, KWL, KWR, KWT, LABEL (20),
 4 LPR, NCYC, NCYCB, NPRT, NU, NWPC, RDT, RDX, RDZ, RDZS, RIBKB, ROI, TD, TFIN,
 5 TIMET, TIOSUM, TPL, TPLT, TPR, TPRT, TQI, TSI, TTD, TWT, UI, WI
 * ,USR (32), UST (22), USB (22), USO (10), PFX3, FFF3
 6 ,AW,BH,CW,EP SB,UBLI,UBRI,WBBI,WBTI,WEPS,W0BI,NTPAS,I GAM,CSUBP,
 7 TO,SI EI, I DG, KDG, TI, MAT, RHOO, AT, TMU, TK, TYMF, FN, TYMT1, T1N, TYMT2,
 8 T2N, RPRAN, NRESEK, NFLOW, NT1, NT2, TSTEP, KDER BC, UOBI, COFBA, COFBB,
 9 COFBC, COFTA, COFTB, COFTC, COFRA, COFRB, COFRC, COFLA, COFLB, COFLC,
 * OFOFTA, OFOFTB, OFOFTC, OFOBRA, OFOBRB, OFOBR C, TAU, NTAU, USL,
 1 USLOB, USROB, USTOB, USBOB, UMAX, WMAX
 * ,CSUBPO, EPS0, RDX DZS, RLENGTH, TQJET, TSJET
 COMMON /FLM CON / DROU, DROU0, IPRPH
 COMMON /VR MAT3 / AI, BI, CI, AR, BR, CR, AMU, BMU, CMU, AK, BK, CK, ACP, BCP, CCP